# EPIGENETIC REGULATION OF CYTOSOLIC PHOSPHOLIPASE A$_2$

## TAN SIEW HON, CHARLENE
### *(B. Sc. (Hons), NUS)*

## A THESIS SUBMITTED
## FOR THE DEGREE OF MASTER OF SCIENCE

## DEPARTMENT OF ANATOMY
## YONG LOO LIN SCHOOL OF MEDICINE
## NATIONAL UNIVERSITY OF SINGAPORE

## 2015

# DECLARATION

I hereby declare that this thesis is my original work and it has been written by me in its entirety. I have duly acknowledged all the sources of information which have been used in the thesis.

This thesis has also not been submitted for any degree in any university previously.

_____

Tan Siew Hon Charlene

14 October 2015

## ACKNOWLEDGEMENTS

I take this opportunity with pride and utmost gratitude to thank the people who have made the materialisation of this thesis possible. First and foremost, I extend my deepest appreciation to my two supervisors, **Associate Professor Ng Yee Kong** and **Associate Professor Ong Wei Yi** (Department of Anatomy, Yong Loo Lin School of Medicine, National University of Singapore) for their unwavering support and patient guidance throughout the course of my study. Their dedication to their work and passion in what they do has showed me what it truly means to be a teacher and scientist. I also wish to thank **Professor Bay Boon Huat** (Department of Anatomy, Yong Loo Lin School of Medicine, National University of Singapore), for providing me with an opportunity to do my postgraduate studies in the department.

Special thanks to **Dr Lena Ho Wai Mun** (Institute of Medical Biology, A*Star) for her plentiful help and advice given, as well as time sacrificed to help in my work. I am also indebted to **Rifkhana** (Department of Physiology, National University of Singapore) and **Annie Hsu** (Department of Pharmacology, National University of Singapore) for their practical assistance whenever help was needed.

I wish to express my deepest thanks to my colleagues, mentors and mentees both past and present, whom I now consider friends; **Chew Wee Siong, Loke Sau Yeen, Yap Mei Yi Alicia, Ee Sze Min, Ng Pei Ern Mary, Tan Wee Shan Joey, Shalini d/o Suku Maran, Chian Vee Nee, Tan Hui Ru Laura, Ho Fung-Yih Christabel, Tong**

**Jie Xin and Heng Swan Ser** for the many laughter, tears and joy we have shared throughout the past years.

Last but not least, I wish to thank my family, **Henry, Christina, Herman and Charmaine**, for always believing in me; as well as my beloved, **Wensley**, for being an endless source of spiritual and mental support. Last but not least, I give all glory and honor to my **Lord Jesus Christ**, for giving me the faith to press on through difficult times, and without whom none of this would have been possible.

# TABLE OF CONTENTS

## SUMMARY

The group IVA cytosolic phospholipase $A_2$ (cPLA$_2\alpha$ or PLA2G4A) contributes to chronic neurodegeneration via the generation of arachidonic acid and proinflammatory eicosanoids. While much is known about regulation of cPLA$_2$ by post-translational modifications such as phosphorylation, little is known about its epigenetic regulation. In the first part of the study, treatments with histone deacetylase (HDAC) inhibitors trichostatin A (TSA), valproic acid (VPA), tubacin and especially the class I HDAC inhibitor, MS-275, were found to increase cPLA$_2\alpha$ mRNA expression in SH-SY5Y human neuroblastoma cells. Co-treatment of the histone acetyltransferase (HAT) inhibitor, anacardic acid, modulated upregulation of cPLA$_2\alpha$ induced by TSA. Specific involvement of class I HDACs and the Tip60 HAT in cPLA$_2\alpha$ regulation was further shown, where a Tip60-specific HAT inhibitor, NU9056, modulated the upregulation of cPLA$_2\alpha$ induced by MS-275. In addition, co-treatment of the histone methyltransferase (HMT) inhibitor, 5'-deoxy-5'-methylthioadenosine (MTA), with TSA suppressed TSA-induced cPLA$_2\alpha$ upregulation. The above changes in cPLA$_2\alpha$ mRNA expression were corroborated at the protein level by Western blots and immunocytochemistry. Chromatin immunoprecipitation (ChIP) showed that TSA increased binding of trimethylated H3K4 to the proximal promoter region of the cPLA$_2\alpha$ gene. Cell injury after TSA treatment as indicated by lactate dehydrogenase (LDH) release was modulated by anacardic acid, and a role of cPLA$_2$ in mediating TSA-induced injury was shown after co-incubation with the cPLA$_2$ selective inhibitor, arachidonyl trifluoromethyl ketone (AACOCF$_3$). In the second part of the study, a similar

suppression of TSA-induced cPLA$_2\alpha$ expression was observed after co-incubation of cells with leaf extracts of *Clinacanthus nutans* Lindau (*C. nutans*), commonly referred to as 'Sabah Snake Grass', with TSA. HAT inhibitory properties of *C. nutans* were detected via HAT activity assay. Similar to anacardic acid, *C. nutans* also abrogated TSA-induced cell injury, indicating its cytoprotective potential. Together, these findings provide hope for epigenetic regulation of cPLA$_2$, and the potential of phytochemicals to affect this process, to be a potential target for therapy for chronic inflammation.

## LIST OF TABLES

# LIST OF FIGURES

## LIST OF ABBREVIATIONS

| | |
|---|---|
| AA | Anacardic acid |
| AACOCF$_3$ | Arachidonyl trifluoromethyl ketone |
| AD | Alzheimer's disease |
| AFU | Arbitrary fluorescence units |
| ALS | Amyotrophic lateral sclerosis |
| ANOVA | Analysis of variance |
| APP | Amyloid precursor protein |
| ATCC | American type culture collection |
| ATP | Adenosine triphosphate |
| BSA | Bovine-serum albumin |
| CCM | Curcumin |
| cDNA | Complementary DNA |
| ChIP | Chromatin immunoprecipitation |
| CNS | Central nervous system |
| COX | Cyclooxygenase |
| cPLA$_2$ | Cytosolic phospholipase A$_2$ |
| DALY | Disability-adjusted life year |
| DHA | Docosahexanoic acid |
| DMEM | Dulbecco's modified eagle's medium |
| DMSO | Dimethyl sulfoxide |
| EGCG | Epigallocatechin-3-gallate |
| FBS | Fetal bovine serum |
| GAPDH | Glyceraldehyde-3-phosphate dehydrogenase |

| | |
|---|---|
| IL-6 | Interleukin-6 |
| IL-8 | Interleukin-8 |
| IL-1α | Interleukin-1-alpha |
| IL-1ß | Interleukin-1-beta |
| LDH | Lactate dehydrogenase |
| LOX | Lipoxygenase |
| Lp-PLA$_2$ | Lipoprotein-associated phospholipase A$_2$ |
| LSD1 | Lysine specific demethylase 1 |
| LTP | Long-term potentiation |
| HAT | Histone acetyltransferase |
| HD | Huntington's disease |
| HDAC | Histone deacetylase |
| HKMT | Histone lysine methyltransferase |
| HMT | Histone methyltransferase |
| iPLA$_2$ | Calcium-independent phospholipase A$_2$ |
| MTA | 5'-deoxy-5'-methylthioadenosine |
| NF-kB | Nuclear factor-kappa B |
| NSAIDs | Non-steroidal anti-inflammatory drugs |
| PAF | Platelet activating factor |
| PBS | Phosphate buffered saline |
| PD | Parkinson's disease |
| PLA$_2$ | Phospholipase A$_2$ |
| PKC | Protein kinase C |
| PRMT | Protein arginine methyltransferase |

| | |
|---|---|
| PS1 | Presenilin 1 |
| PS2 | Presenilin 2 |
| RIPA | Radioimmunoprecipitation assay |
| ROS | Reactive oxygen species |
| SAHA | Suberoylanilide hydroxamic acid |
| SIRT | Sirtuin |
| sPLA$_2$ | Secretory phosholipase A$_2$ |
| SRE | Sterol regulatory element |
| SREBP | Sterol regulatory element binding protein |
| TBST | Tris-buffered saline with 0.1% Tween-20 |
| TNFα | Tumor necrosis factor-alpha |
| TSA | Trichostatin A |
| TSS | Transcriptional start site |
| VPA | Valproic acid |

## PUBLICATIONS

Various parts of this study have been published in international refereed journals:

1. **Tan Charlene SH**, Ong WY (2015). Epigenetic regulation of cytosolic phospholipase $A_2$ in SH-SY5Y human neuroblastoma cells. Molecular Neurobiology.

# SECTION I

# INTRODUCTION

## 1.0    Neurodegeneration

## 1.1    Epidemiology

'Neurodegeneration' is a broad term referring to "any pathological condition primarily affecting neurons" (Przedborski et al., 2003). A few hundred types of neurodegenerative diseases exist, classified based on their clinical features and areas of lesion (Przedborski et al., 2003). Neurodegeneration is one of the leading contributors to disease burden worldwide, affecting both developing and developed countries (Kalaria et al., 2008, Lee, 2009). Global health estimates reveal Alzheimer's disease (AD) as the most prevalent neurological disease, followed by Parkinson's disease (PD) and multiple sclerosis (WHO, 2012). According to the Global Health Education Consortium (Lee, 2009), global neurological disease burden is projected to increase 12% from 2005 to 2030, with a 62% increase in disability-adjusted life years (DALYs[1]) for neurodegenerative diseases, in contrast to a 20% increase in DALYs for cerebrovascular diseases (WHO, 2006). An estimated figure of up to 16 million Americans and 115.4 million individuals worldwide will suffer from AD by 2050 (Hebert et al., 2003, International, 2010). In Singapore, this figure is expected to hit 187,000, which contributes approximately 5% of the total population (Economics, 2006). There is thus a growing need for effective mitigation of these debilitating diseases.

---

[1] Disability-adjusted life year: "a measure of overall disease burden, expressed as the number of years lost due to ill-health, disability or early death"

## 1.2    Acute and chronic neurodegeneration

Neurodegenerative disorders are broadly classified as acute and chronic neurodegeneration (Allan and Rothwell, 2001). Acute neurodegeneration occurs promptly after a sudden insult and lasts for a short period, usually leading to rapid cell damage and death (Allan and Rothwell, 2001). Examples of acute neurodegeneration are stroke, cerebral or subarachnoid haemorrhage, ischaemic brain damage and traumatic brain injury (Allan and Rothwell, 2001).

Chronic neurodegeneration occurs when the unfavorable stimulus persists even after the initial insult and lasts for a prolonged period of time (Frank-Cannon et al., 2009). Examples of chronic neurodegeneration are AD, PD, amyotrophic lateral sclerosis (ALS), multiple sclerosis and Huntington's disease (HD) (Streit et al., 2004, Lull and Block, 2010).

## 1.3    Hallmarks of neurodegeneration

Various types of neurodegeneration differ according to their pathological hallmarks. Acute forms of neurodegeneration such as stroke are characterized by cell death due to injury or ischemia (Allan and Rothwell, 2001). Chronic forms of neurodegeneration are typically classified by their mode of transmission, type of protein accumulation, and brain regions affected (Table 1.3). For instance, general pathological hallmarks of AD include deposition of amyloid plaques and presence of tau-containing neurofibrillary tangles in neurons, which

promote oxidative stress and neuronal death (Hsieh and Yang, 2013). Lewy bodies containing α-synuclein protein give rise to inflammation and neurotoxicity in PD (Kang et al., 2013). A summary of common neurodegenerative diseases and their corresponding clinical, pathological and anatomical hallmarks are presented in Table 1.3.

**Table 1.3** Summary of clinical, pathological and anatomical hallmarks of chronic neurodegenerative diseases [Adapted from (Soto, 2003)]

| Disease | Mode of Transmission | Protein involved | Affected brain regions |
|---|---|---|---|
| Alzheimer's disease | Sporadic (95%), Inherited (5%) | Amyloid-β, tau | Cerebral cortex, hippocampus |
| Parkinson's disease | Mostly sporadic, rarely inherited | α-synuclein | Hypothalamus, substantia nigra |
| Amyotrophic lateral sclerosis | Sporadic (90%), Inherited (10%) | Superoxide dismutase | Motor cortex, brainstem |
| Huntington's disease | Inherited (autosomal dominant) | Huntingtin | Cerebral cortex, striatum |

## 1.4    Etiology of neurodegeneration

Genetic and environmental factors promote the onset of the above-mentioned pathological hallmarks. Typical genetic factors responsible for familial or early-onset AD are genes encoding *amyloid precursor protein (APP)* (Goate et al., 1991), *presenilin 1 (PS1)* (Sherrington et al., 1995) and *presenilin 2 (PS2)* (Rogaev et al., 1995). However, these familial cases make up a small proportion (~10%) of all cases as most neurodegenerative diseases are sporadic *i.e.* non-

inherited (Tanner et al., 1999). Dysfunctions to the central nervous system (CNS) accumulate progressively over time and the disease only manifests later in life (Ritchie and Kildea, 1995). For instance, APP/PS1 mutant mice showed early dysfunctions in working memory, but amyloid burden and long-term memory loss only occurred later, indicating progressive development of the disease (Trinchese et al., 2004). Environmental factors contribute to sporadic cases of chronic neurodegeneration (Migliore and Coppedè, 2009), such as where diet-induced obesity induces accumulation of proinflammatory factors in the brain and leads to cognitive impairment (Miller and Spencer, 2014). Excessive iron accumulation with age increases tissue damage to the hippocampus and contributes to AD pathology (Grant et al., 2002, Raven et al., 2013). In contrast, moderate exercise provides anti-inflammatory and memory-enhancing effects (Cotman et al., 2007). Changes in expression of certain genes related to chronic inflammation, calcium binding and protein synthesis are also implicated in AD (Loring et al., 2001). It seems therefore that both environmental factors and gene expression changes contribute to the etiology of late-onset and sporadic neurodegeneration.

Actual mechanisms behind neurodegeneration remain highly debated. Currently, opposing schools of thought argue the relative importance of amyloid plaques and tau protein in AD (Rapoport et al., 2002, Morris et al., 2010). Much controversy exists concerning whether amyloid plaques appear early in the pathological process or at later

stages of the disease (Skaper, 2012). Still others believe that tau protein, rather than amyloid burden, correlates much better to severity of cognitive decline (Nelson et al., 2012). Furthermore, while it is traditionally thought that the tau protein occurs only in AD, and α-synuclein only in PD, recent studies show presence of the *tau protein in PD cases* (Herbert et al., 2014) and *Lewy bodies in AD cases* (Koehler et al., 2013). Therefore, much research is necessary for a clearer mechanistic understanding of the etiology of neurodegeneration.

Chronic inflammation and oxidative stress are commonly observed in neurodegenerative diseases; namely, in AD, PD, ALS and HD (Khansari et al., 2009, Hensley, 2010, Moller, 2010, Philips and Robberecht, 2011, Hirsch et al., 2012). The process involves microglial activation and production of proinflammatory mediators such as prostaglandins, nitric oxide, or cytokines that promote neuronal death (Hsieh and Yang, 2013). Microglial activity is implicated alongside tau and amyloid pathologies in neurons (Kitazawa et al., 2004), as shown by co-localisation of activated microglia, amyloid plaques and tau protein found in the neurons of brains of AD patients (Cagnin et al., 2001, Ishizawa and Dickson, 2001). Proinflammatory proteins such as C-reactive protein and interleukin-6 (IL-6) in the plasma of patients also correlate with increased risk of AD, pointing to the presence of inflammation in AD (Engelhart et al., 2004). Furthermore, non-steroidal anti-inflammatory drugs (NSAIDs) protect against AD development by

suppressing ß-amyloid formation (Vlad et al., 2008). Taken together, accumulating evidences suggest inflammation as a common characteristic of chronic neurodegenerative diseases.

## 1.5    Neuroinflammation

The term 'neuroinflammation' has been coined in recent years to describe features and pathological hallmarks present in most neurodegenerative disorders (O'Callaghan et al., 2008). Neuroinflammation is a form of inflammation unique to the CNS, characterised by activation of immune cells in the brain known as glia that release proinflammatory mediators (O'Callaghan et al., 2008). Outside of the CNS, such immune cells are known as monocytes, macrophages and neutrophils (O'Callaghan et al., 2008). Under normal conditions, inflammation in the CNS plays a neuroprotective role by aiding in clearance of foreign invaders and healing from external injury (Cappellano et al., 2013). Microglia and astroglia serve as trophic factors to facilitate neuronal repair, development and plasticity (Ridet et al., 1997, Bauer et al., 2007). They also maintain homeostasis by providing immune response to external stress and neurotoxic insults (Yang et al., 2010). This step is necessary for activation of the immune system to promote killing of foreign invaders (Lucas et al., 2010, Soehnlein and Lindbom, 2010). Under controlled conditions where the blood brain barrier is intact and leukocytes do not infiltrate, glial activity achieve their evolutionary purposes of providing neuroprotection and

recovery from injury (Streit et al., 2004). Inflammatory response shifts to an anti-inflammatory state to rescue damaged areas and facilitate clearance of debris from neurons (Varin and Gordon, 2009).

Under conditions where the proinflammatory response persists, excessive release of proinflammatory cytokines and reactive oxygen species (ROS) cause further tissue damage and neurodegeneration (Kigerl et al., 2009, Cappellano et al., 2013). These effects are evident in acute brain injuries such as stroke, traumatic brain injury and spinal cord injury (Allan and Rothwell, 2001, Patel et al., 2003, Jafarian-Tehrani, 2009). Acute neuroinflammation is generally characterized by microglial activation and overexpression of proinflammatory cytokines such as interleukin 1-alpha (IL-1α), interleukin 1-beta (IL-1ß), IL-6 and tumor necrosis factor-alpha (TNF-α) (Czerniawski and Guzowski, 2014).

Acute neuroinflammation can give rise to long-term chronic neuroinflammation, such as the long-term inflammatory effects observed after severe traumatic brain injury (Lozano et al., 2015). Chronic neuroinflammation plays a significant role in the study of CNS *disease*, as opposed to acute forms of neuroinflammation that generally play a role in CNS *injury*. In such cases, neuroinflammatory processes were reported to have begun long before neuronal death is observed, accelerating or exacerbating disease progression (Shivika et al., 2014). The term 'neuroinflammation' is thus more commonly understood and referred to in the case of chronic situations, whereby

*excessive* and *prolonged* glial activation leads to overproduction of proinflammatory cytokines and reactive oxygen species, causing neuronal degradation over time (Streit et al., 2004, O'Callaghan et al., 2008, Yang et al., 2010).

## 1.6    Role of cPLA$_2$ in neuroinflammation and neurodegeneration

Calcium-dependent cytosolic phospholipase A$_2$ (cPLA$_2$) catalyses the release of arachidonic acid from the cleavage of membrane glycerophospholipids, which contributes significantly to neuroinflammation and disease, and this is termed, the "Bazan effect" (Bazán Jr, 1970). Increased cPLA$_2$ expression is found in cases of human AD, in mice models of ALS, in mice overexpressing mutant APP, as well as in mice with age-related amyloid deposition (Clemens et al., 1996). Elevated cPLA$_2$α immunoreactivity occurs together with amyloid deposits in cortical and hippocampal neurons of AD patients (Stephenson et al., 1996, Desbene et al., 2012). Increased cPLA$_2$ immunoreactivity is also found in neuronal cultures during ischemic and excitotoxic insults (Bonventre, 1997), and in neurons of rat brains following kainic-acid induced neurotoxicity (Sandhya et al., 1998, Farooqui et al., 2000). These indicate the crucial role of cPLA$_2$ in neurodegeneration.

Oxidative stress and inflammation increases cPLA$_2$ expression in neurons and microglia (Sun et al., 2004, Sun et al., 2012). cPLA$_2$ induces neuronal death by stimulating the production of eicosanoids,

isoprostanes and the neurotoxic 4-hydroxynonenal from the catalysis of neural membrane phospholipids, leading to neurodegeneration (Ong et al., 2010). Figure 1.5 illustrates the different roles of PLA$_2$ in modulating normal brain functions and preventing neural injury (Ong et al., 2010). The cPLA$_2$ isoform is most responsible for neurodegeneration, while the calcium-independent PLA$_2$ (iPLA$_2$) isoform plays a more significant role in the prevention of neuropsychiatric diseases (Ong et al., 2010).
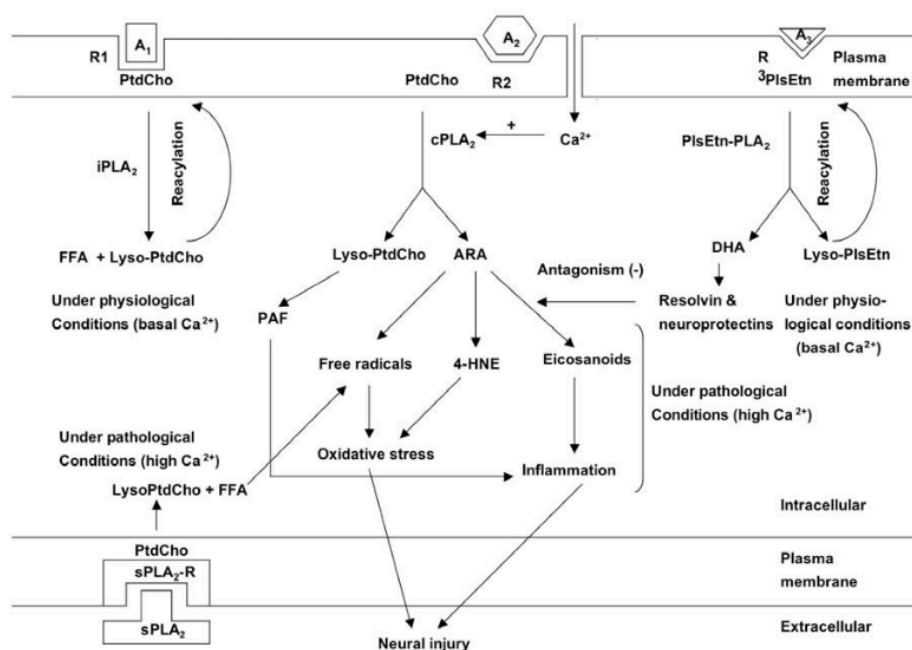


**Fig. 1.6 Diagram showing involvement of PLA$_2$ isoforms in mediating neural injury.** PlsEtn-PLA$_2$: plasmalogen selective phospholipase A$_2$; A1, A2, A3: Agonist A1, Agonist A2, Agonist A3 respectively; PtdCho: phosphatidylcholine; PlsEtn: ethanolamine plasmalogen; lyso-PtdCho: lysophosphatidylcholine; lyso-PlsEtn: lysoplasmalogen; FFA: free fatty acid; ARA: arachidonic acid; DHA: docosahexaenoic acid; 4-HNE: 4-hydroxynonenal. [Adapted from (Ong et al., 2010)]

In support of this, loss-of-function studies show that specific inhibition of cPLA$_2$ by arachidonyl trifluoromethyl ketone (AACOCF$_3$) led to neuroprotection in rat hippocampal cultures (Lu et al., 2001).

cPLA$_2$-knockout mice conferred resistance to Aβ-induced cognitive deficits and synaptic loss (Desbene et al., 2012). Antisense knockdown of cPLA$_2$ protected rat cortical neurons from Aβ-induced apoptosis by inhibiting downstream arachidonic acid-dependent pathways (Kriem et al., 2005). Together, these findings show the crucial involvement of cPLA$_2$ activity in neuroinflammation and neurodegeneration, and thus its need to be tightly regulated.

## 2.0 Phospholipases A$_2$

The phospholipase A$_2$ (PLA$_2$) superfamily of enzymes are enzymes found ubiquitously in most cells and tissues, catalyzing the hydrolysis of cellular phospholipids at the sn-2 position to release free fatty acids and lysophospholipids (Murakami et al., 1997, Winstead et al., 2000).
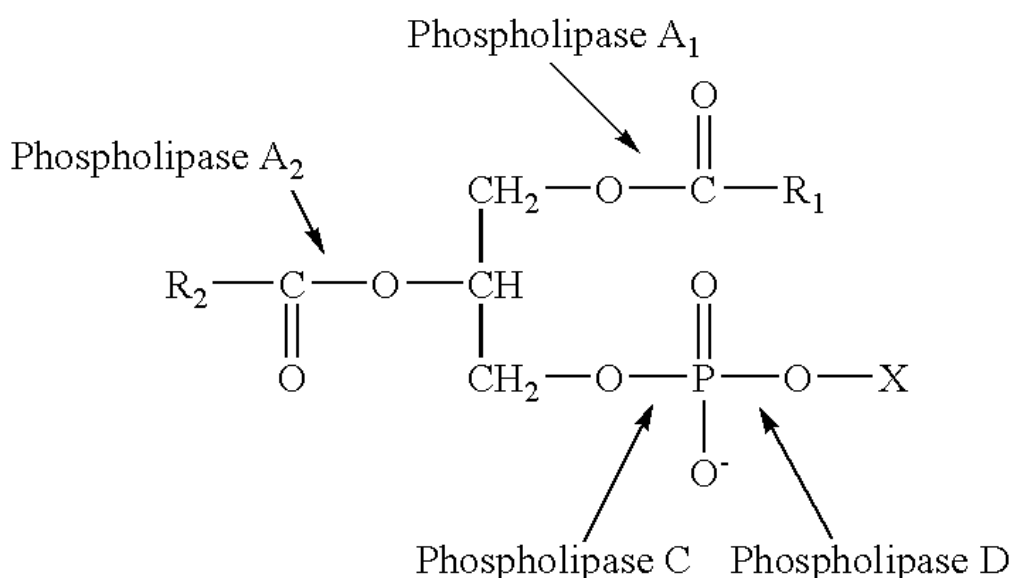
**Fig. 2.0 Illustration of different modes of action of phospholipases A$_1$, A$_2$, C and D, at different cleavage sites.** PLA$_2$ cleaves phospholipids at sn-2 position, releasing a free fatty acid and lysophospholipid. [Adapted from (Dayton et al., 2010)]

At least 19 isoforms of $PLA_2$ enzymes exist to date, differing in terms of structure, substrate specificity, calcium dependence, and localisation (Winstead et al., 2000, Murakami and Kudo, 2002). Three main families of $PLA_2$ include the secretory $PLA_2$ ($sPLA_2$), group VI calcium-independent $PLA_2$ ($iPLA_2$) and group IV calcium-dependent cytosolic $PLA_2$ ($cPLA_2$) (Murakami and Kudo, 2002).

## 2.1 Secretory phospholipase $A_2$

The secretory phospholipase $A_2$ ($sPLA_2$) gene is localised on the human chromosome 4q25 (Gelb et al., 2000). The $sPLA_2$ family of proteins has low molecular weights ranging from 14 to 17 kDa, and calcium is necessary for its function (Murakami et al., 2011). They have homologous amino acid sequences and three-dimensional structures (Gelb et al., 2000, Valentin and Lambeau, 2000), with similar calcium-binding domains and His/Asp catalytic sites maintained by disulfide bridges (Titsworth et al., 2008). There are at least ten isoforms of $sPLA_2$ named based on the patterns of disulfide bonds and their time of discovery – IB, IIA, IIC, IID, IIE, IIF, III, V, X and XII (Burke and Dennis, 2009a). Besides the catalytic domains and $Ca^{2+}$-binding domains, the $sPLA_2$-III and $sPLA_2$-XII isoforms are poorly homologous against the $sPLA_2$-I, -II, -V and -X subtypes (Murakami et al., 2011). Each $sPLA_2$ isoform produced has unique catalytic properties and localisation, thus they carry out unique pathophysiological roles in the mammalian system (Lambeau and Gelb, 2008). For instance, $sPLA_2$-III is densely

expressed in the brainstem, spinal cord and neocortex of rats and is predominantly found in the cytosol of neuronal cells (Yang et al., 2013).

Some sPLA$_2$ enzymes carry out similar functions as cPLA$_2$, generating arachidonic acid and proinflammatory eicosanoids (Lambeau and Gelb, 2008). The sPLA$_2$ releases arachidonic acid that plays important roles in neuroinflammation (Bazan, 2003, Serhan, 2004), neurotransmission (Bramham et al., 1994) and long-term potentiation (Williams et al., 1989).

## 2.2 Calcium-independent phospholipase A$_2$

The iPLA$_2$ gene is localised on the human chromosome 22q13.1 (Larsson Forsell et al., 1999). It contains a CpG island but lacks a TATA-box (Tanaka et al., 2012). It also has a putative sterol regulatory element (SRE) on the 5' flanking region of the gene, allowing the binding of sterol regulatory element binding proteins (SREBPs) for transcriptional regulation (Seashols et al., 2004). Under situations of sterol depletion, SREBPs translocate into the nucleus to bind SREs, increasing iPLA$_2$ expression (Seashols et al., 2004). On the other hand, sterol supplementation suppresses iPLA$_2$ induction, suggesting that sterols regulate iPLA$_2$ activity (Seashols et al., 2004). Alternative splicing of the iPLA$_2$ mRNA generates various isoforms with distinct tissue localisation and functions (Larsson et al., 1998). The three common isoforms of iPLA$_2$ are iPLA$_2$α, iPLA$_2$ß, and iPLA$_2$γ (Tang et al., 1997, Mancuso et al., 2000). iPLA$_2$ß, also known as group VIA

iPLA$_2$, is more well-studied and further classified into various splice variants, namely group VIA-1, VIA-2, VIA-3, ankyrin-1 and ankyrin-2 (Winstead et al., 2000).

This family of enzymes functions independently of calcium and has molecular masses ranging from 80 to 88 kDa (Farooqui and Horrocks, 2007). It contains a unique lipase consensus sequence and eight N-terminal ankyrin repeats (Farooqui and Horrocks, 2006). It has no structural similarity with cPLA$_2$ and is about five times more highly expressed (Kramer and Sharp, 1997, Ong et al., 2010). The iPLA$_2$ family is most abundant in the brain, highly expressed in the cytosol of the prefrontal cortex, striatum, hypothalamus and hippocampus of normal rats (Molloy et al., 1998, Ong et al., 2005). Dense immunolabeling of iPLA$_2$ was observed in the cerebral cortex, septum, amygdala and striatum while relatively lighter staining was observed in the thalamus, hypothalamus and subthalamic nucleus of monkey brains (Ong et al., 2005).

iPLA$_2$ is involved in the catalysis of membrane phospholipids to release docosahexanoic acid (DHA) (Balsinde et al., 1995, Strokin et al., 2003), which is anti-inflammatory and facilitates cell survival (Lukiw et al., 2005, Schwab et al., 2007). It is metabolized to docosanoids that have neuroprotective and neurotrophic properties (Marcheselli et al., 2003). It reverses effects of oxidative damage in cellular membranes (McLean et al., 1993, Ross et al., 1998), facilitates neurite outgrowth and differentiation during injury and neurodevelopmental processes

(Schaeffer et al., 2009), and prevents ischemic damage (Strokin et al., 2006). The iPLA$_2$ß isoform plays a crucial role in hippocampo-prefrontal cortical long-term potentiation (LTP) and spatial working memory in rats (Shalini et al., 2014). In line with these findings, AD patients were found to have deficient iPLA$_2$ and DHA levels, but elevated levels of cPLA$_2$ and arachidonic acid (Soderberg et al., 1991).

## 2.3    Cytosolic phospholipase A$_2$

### 2.3.1  Structure and localisation

The cPLA$_2$α gene is localised on the human chromosome 1q25, comprising at least 7 introns with a CA repeat 160 bases upstream from the transcriptional start site (TSS) (Morii et al., 1994b, Tay et al., 1994). The gene is expressed in numerous regions, but mRNA levels are most significant in the lung, kidney, spleen, heart and brain (Liscovitch, 1994). Several binding sites on the promoter regions are important for gene regulation (Cowan et al., 2004). These include the nuclear factor κB (NF-κB) binding site, glucocorticoid response element, interferon-γ-responsive element, interferon γ-activated sequence sites, and a distal regulatory sequence known as the hypoxia-inducible factor-1 binding site (Morii et al., 1994a, Wu et al., 1999, Alexandrov et al., 2006). These sites allow the binding of transcription factors such as NF-kB, NF-IL6, AP-1 and AP-2 to regulate transcription (Morii et al., 1994b).

The cPLA$_2$ family of enzymes is calcium-dependent and found intracellularly (Farooqui and Horrocks, 2007). It is an 85-kDa enzyme that possesses a unique C2 calcium-binding domain to facilitate translocation from the cytosol to the membrane, where it exerts its function (Kramer and Sharp, 1997, Malmberg et al., 2003). Both the catalytic α/β hydrolase domain and the C2 domain are necessary for appropriate functioning of the enzyme (Dessen et al., 1999, Hsu et al., 2008). The lid region and CAP region are unique to cPLA$_2$, and conformational change to the lid region is necessary for activation of the enzyme (Burke et al., 2008).
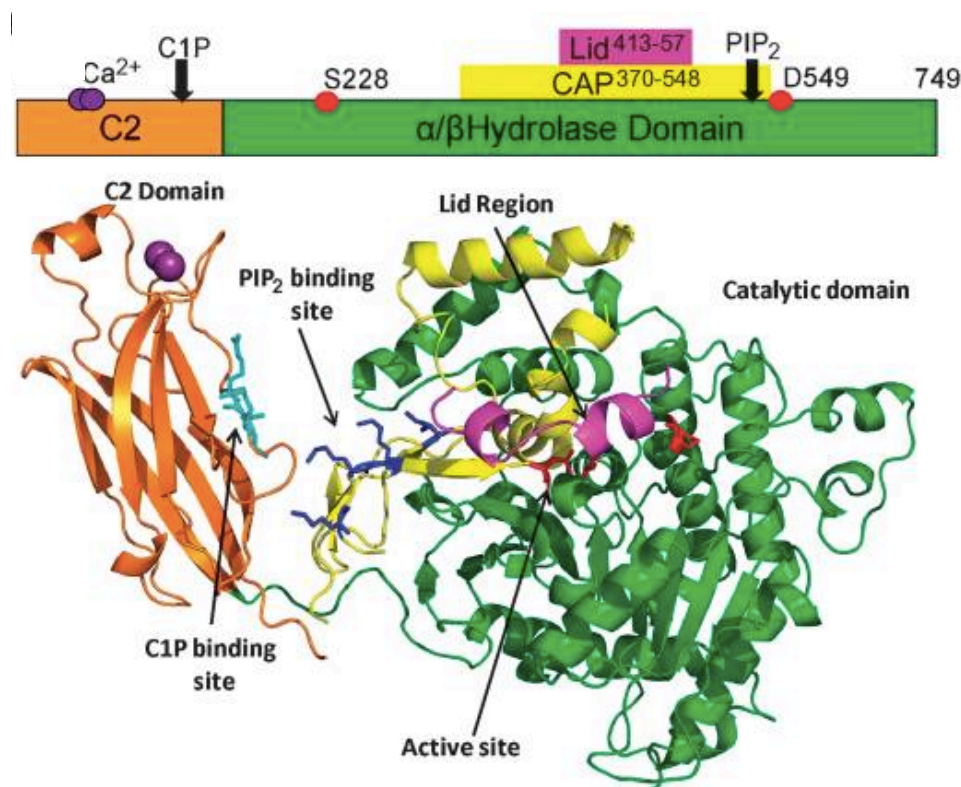


**Fig. 2.3.1 Illustration of cPLA$_2$ crystal structure.** Orange denotes the C2 Ca$^{2+}$ ion-binding domain. Purple denotes Ca$^{2+}$ ions. Green denotes catalytic domain with yellow cap region at and pink lid region. Red denotes the active site residues Serine-228, Aspartate-549 and Arginine-200. Dark blue denotes PIP2 binding site, while light blue denotes C1P binding site. [Adapted from (Burke and Dennis, 2009b)]

Three isoforms of $cPLA_2$ exist – $cPLA_2\alpha$ (85 kDa), $cPLA_2\beta$ (114 kDa) and $cPLA_2\gamma$ (61 kDa), where the function of $cPLA_2\alpha$ is most studied. They possess conserved catalytic sites, comprising a serine residue (Murakami and Kudo, 2002). These isoforms are produced by alternative splicing of the 2880-nucleotide long mRNA (Kramer and Sharp, 1997). The $cPLA_2$ mRNA and protein are expressed at very low basal levels in neurons and astrocytes (Owada et al., 1994, Ong et al., 1999, Farooqui et al., 2000). High $cPLA_2$ activity is found in the hindbrain of rats (Ong et al., 1999). It is also found in the white matter of murine fibrous astrocytes and gray matter of pial astrocytes (Lautens et al., 1998), as well as in brain astrocytes of humans (Stephenson et al., 1994).

## 2.3.2 Function of $cPLA_2$ in the brain

Cytosolic $PLA_2$ catalyses the breakdown of membrane glycerophospholipids to generate arachidonic acid and lyso-platelet activating factor (PAF) (Winstead et al., 2000, Tanaka et al., 2012). It does not require calcium for catalysis but micromolar amounts are necessary for targeting to the membrane for function (Winstead et al., 2000).Unlike $cPLA_2\alpha$, $cPLA_2\beta$ and $cPLA_2\gamma$ has phospholipase $A_1$ activity and catalyses the hydrolysis of fatty acids at the sn-1 position as well, with a lower rate of function compared to $cPLA_2\alpha$ (Murakami and Kudo, 2002). Arachidonic acid released is mainly responsible for calcium flux (Tornquist et al., 1994) and cell signaling (Piomelli, 1993).

Arachidonic acid undergoes further catalysis by lipoxygenases (LOXs) or cyclooxygenases (COXs) to generate proinflammatory eicosanoids such as leukotrienes, prostaglandins, thromboxanes, and PAF (Serhan et al., 1996).

cPLA$_2$ is involved in neural plasticity, cell growth and regeneration, generation of second messenger and neurodegeneration (Farooqui et al., 2000). In terms of neural plasticity, Ca$^{2+}$ influx activates cPLA$_2$ and generates secondary messengers such as arachidonic acid, nitric oxide and PAF (Farooqui et al., 2000). These in turn serve as retrograde messengers that initiate and maintain LTP (Farooqui et al., 2000). cPLA$_2$ is also associated with axonal growth, though the mechanism is not clear. Excessive release of proinflammatory mediators as a result of cPLA$_2$ activity, together with ROS-stimulated oxidative stress, may drive the onset of neurodegeneration (Farooqui et al., 2000). These undesirable effects of excessive cPLA$_2$ activity point to a need for cPLA$_2$ expression to be tightly regulated.

## 3.0    Epigenetics

Epigenetics is the study of heritable changes in gene function which are not a result of alterations in DNA sequence (Russo et al., 1996). DNA is packed into highly compact states known as chromatin, which comprise basic repeating units known as nucleosomes (Kornberg, 1974). Each nucleosome is an octamer of two each of histones H2A, H2B, H3 and H4, wrapped around 147 base pairs of DNA (Allis et al., 2007). Epigenetic regulation involves covalent and non-covalent alterations to the DNA itself and the proteins associated with it (Allis et al., 2007). The epigenetic pathway typically involves three steps – (1) reception of environmental signal which triggers an intracellular process, (2) initiation of epigenetic modifications within the chromatin, and (3) maintenance of the modifications (Berger et al., 2009). Environmental factors that induce epigenetic modifications include diet, physical exercise, lifestyle, pollutants and toxic insults (Berger et al., 2009).

The four main types of epigenetic modifications are histone modification, DNA methylation, nucleosome remodeling and RNA-mediated pathways (Allis et al., 2007, Portela and Esteller, 2010). DNA methylation correlates with gene silencing and involves addition of a methyl group at cytosine residues of DNA via the activity of DNA methyltransferases (Kalaria et al., 2008). Histone modifications and DNA methylation are relatively prominent and well-studied mechanisms for epigenetic regulation.

19

## 3.1 Histone modifications and chromatin structure

Histones undergo different modifications such as methylation, acetylation and phosphorylation (Jenuwein and Allis, 2001). A compact chromatin state occurs when there are high levels of attraction between positively-charged histone tails and negatively-charged DNA (Herranz and Esteller, 2007). Histone modifications thus affect chromatin structure by altering the level of attraction between the DNA and the histone tails (Herranz and Esteller, 2007).
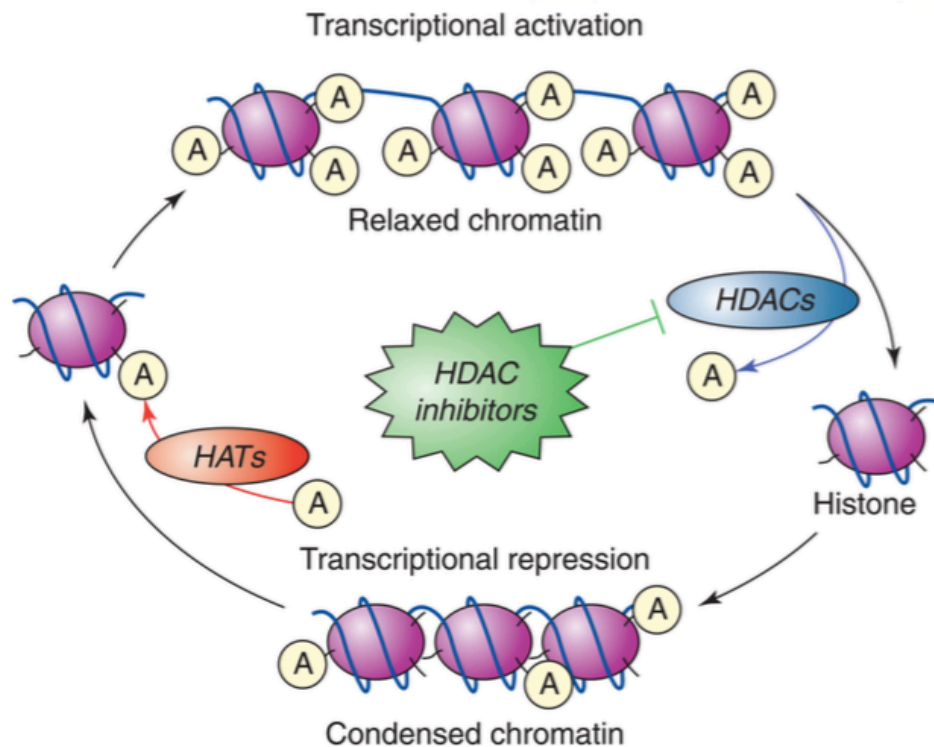


**Figure 3.1 Effect of HDACs, HATs, and respective inhibitors on regulation of chromatin conformation.** HDAC, histone deacetylase; HAT, histone acetyltransferase. [Adapted from (Chuang et al., 2009)]

Figure 3.1 provides an illustration of the effects of HDACs and HATs on regulation of chromatin conformation, via regulation of acetylation statuses of histone residues (Dhalluin et al., 1999, Winston

and Allis, 1999). Acetylations of histone lysine (K) residues lead to neutralization of the positive histones, facilitating open chromatin structure and increased gene transcription (Herranz and Esteller, 2007). Histone hyperacetylation generally gives rise to euchromatic chromatin conformation and thus more active transcription, while histone hypoacetylation facilitates a more transcriptionally inactive, heterochromatic state (Herranz and Esteller, 2007). Besides histone acetylation, histone methylations also occur and are catalysed by specific histone methyltransferases (HMTs) and histone demethylases. Selective and non-selective inhibitors of these enzymes have been developed in the study of epigenetics. Table 3.1 provides a summary of the functions of some well-known inhibitors of HDACs, HATs and HMTs, together with the histone residues affected and the corresponding effects on transcription.

**Table 3.1 HDAC, HAT and HMT inhibitor activities and respective histone modifications**

| HDAC inhibitors | HDACs inhibited | Ref | Histone residues affected | Modification | Ref |
|---|---|---|---|---|---|
| Trichostatin A (TSA) | Class I: HDAC 1, 2, 3, 8 Class IIa: HDAC 4, 9 Class IIb: HDAC 6, 10 | (Chuang et al., 2009) | H3K14, H4K8, H4K16 H3K9 H3K4 | acetylation; increase acetylation; increase trimethylation; increase | (Martinez-Diaz et al., 2010, Coffey et al., 2012) (Sike et al.) (Pufahl et al., 2012, Wu et al., 2012a) |
| Valproic Acid (VPA) | Class I, Class IIa HDACs | (Gurvich et al., 2004, Vrba et al., 2011) | H3K9 H3K14 H3K4 | acetylation; increase acetylation; increase trimethylation; increase | (Hezroni et al., 2011) (Vrba et al., 2011) (Bradbury et al., 2005, Harikrishnan et al., 2008) |
| MS-275 | HDAC 1 | (Khan et al., 2008, Kennedy et al., 2013, Beharry et al., 2014) | H3K9, H3K14 H3K4 | acetylation; increase trimethylation; increase | (Kennedy et al., 2013) (Huang et al., 2011) |
| Tubacin | HDAC 6 | (Haggarty et al., 2003) | None | - | - |

| HAT inhibitors | HATs inhibited | Ref | Histone residues affected | Modification | Ref |
|---|---|---|---|---|---|
| Anacardic Acid (AA) | p300/CBP GNAT MYST | (Balasubramanyam et al., 2003) (Cui et al., 2008) (Sun et al., 2006a) | H3K9, H3K14 | acetylation; decrease | (Cui et al., 2008) |
| NU9056 | Tip60 | (Coffey et al., 2012) | H3K14, H4K8, H4K16 | acetylation; decrease | (Coffey et al., 2012) |
| Curcumin (CCM) | p300/CBP | (Marcu et al., 2006) | H3K18, H4K16 | acetylation; increase | (Collins et al., 2013) |
| Butyrolactone-3 (MB-3) | GCN5 (GNAT family) | (Biel et al., 2004) | H3K56 | acetylation; decrease | (Malapeira et al., 2012) |

| HMT inhibitor | HMTs inhibited | Ref | Histone residues affected | Modification | Ref |
|---|---|---|---|---|---|
| 5'-deoxy-5'-methylthioadenosine (MTA) | Set1 | (Huang et al., 2006) | H3K4 | trimethylation; decrease | (Huang et al., 2006, Buro et al., 2010) |
| | | | H3K36 | trimethylation; decrease | (Buro et al., 2010) |

### 3.1.1 Histone acetyltransferases (HATs)

HATs catalyse the acetylation of histones by transferring an acetyl group from acetyl-CoA to lysine residues found on histone tails (Allis et al., 2007). HATs are typically characterized by presence of an acetyltransferase domain, and are broadly classified into five families, namely GCN5/PCAF, MYST (MOZ, YBF2/SAS3, SAS2, Tip60), TAFII 250, CBP/p300 and SRC (Marmorstein, 2001). They are classified based on sequence homology, protein structure and substrate specificity (Kuo and Allis, 1998). HATs produce acetylated histones that recruit proteins containing bromodomains (Bottomley, 2004). Abnormal function of the CBP/p300 class of HAT has been associated with cancer by affecting cell cycle regulation and apoptotic genes (Iyer et al., 2004). The GCN5/PCAF HAT is known to interact with E2F, a transcription factor that promotes S-phase cell cycle progression (Taubert et al., 2004). Both PCAF and p300 have been found to catalyse acetylation of the tumor suppressor p53 protein, in turn affecting apoptosis (Liu et al., 1999). Taken together, it is observed that HATs play crucial roles in regulation of cell proliferation and apoptosis.

Specific inhibitors of HATs have been synthesized to study the roles of HATs in histone acetylation and gene transcription (Lau et al., 2000). HATs also catalyse unique modifications on lysine substrates – for instance, p300 has a preference for the lysine 8 residue of histone H4 (H4K8), while PCAF enzymes selectively acetylates H3K14 (Schiltz et al., 1999). Table 3.1 shows a summary of the functions of some

HATs and HAT inhibitors. Thus, it is possible that HAT inhibitors can regulate gene expression.

### 3.1.2 Histone deacetylases (HDACs)

HDACs catalyse the removal of acetyl groups from lysine residules of histone tails, thereby modifying chromatin structure (Allis et al., 2007). They are classified according to their homology to yeast HDACs, namely the class I, II and IV $Zn^{2+}$-dependent enzymes and class III $Zn^{2+}$-independent enzymes (de Ruijter et al., 2003, Chuang et al., 2009). HDAC11 is the only class IV enzyme, recently identified by its distinct structure (Voelter-Mahlknecht et al., 2005). Class I HDACs comprise HDAC1, 2, 3, and 8, due to their homology to yeast RPD3 HDACs (Chuang et al., 2009, Delcuve et al., 2012b). Class II HDACs are related to yeast HDA1 HDACs and are sub-divided into class IIa and class IIb (Chuang et al., 2009, Delcuve et al., 2012b). Class IIa comprise HDAC4, 5, 7 and 9 while class IIb include HDAC6 and 10 (Chuang et al., 2009, Delcuve et al., 2012b). Class III enzymes, also known as silent information regulator-like (sirtuins or SIRT) HDACs, comprise seven subtypes and the $NAD^+$ cofactor is important for their activity (Chuang et al., 2009, Delcuve et al., 2012b). Class I HDACs are nuclear enzymes that play a role in cell proliferation and survival (Luo et al., 2009, Marks, 2010). Dimerization is necessary for HDAC activity (Luo et al., 2009), such as in the case where HDAC1 and HDAC2 form

homodimers or heterodimers based on cell type (He et al., 2005,

Yamaguchi et al., 2010).

Trichostatin A (TSA) and suberoylanilide hydroxamic acid

(SAHA) are examples of general, non-selective HDAC inhibitors that

inhibit class I, II and IV zinc-dependent HDACs (Chuang et al., 2009).

Sodium butyrate and valproic acid inhibit class I and class IIa HDACs

(Gurvich et al., 2004, Vrba et al., 2011). MS-275 is a synthetic class I

specific inhibitor (Franci et al., 2013); while bufexamac, an anti-

inflammatory drug, is a class IIb selective HDAC inhibitor (Delcuve et

al., 2012a). Tubacin is a HDAC6 inhibitor which selectively inhibits

tubulin acetylation (Haggarty et al., 2003). Table 3.1 shows a summary

of the most common HDACs and their relevant inhibitors. It is thus

possible that HDAC inhibitors of various specificities differentially

regulate gene expression.

### 3.1.3  Histone methyltransferases (HMTs)

Methylations can occur on lysine and arginine residues of

histone tails in the regulation of chromatin structure. Multiple

methylated states are possible as lysine residues can be subjected to

mono-, di- and tri-methylation, while arginine residues can be mono- or

di-methylated (Allis et al., 2007). Specific HMTs transfer methyl groups

to specific sites on histone residues (Rice and Allis, 2001). Histone

methyltransferases include two broad classes, namely, histone lysine

methyltransferases (HKMTs) and protein arginine methyltransferases

(PRMTs). HKMTs share the SET domain that contains the catalytic site allowing binding to S-adenosyl-L-methionine cofactor (Allis et al., 2007). SET proteins give rise to methylated histones that can attract binding of other proteins through the presence of chromodomains (Bottomley, 2004). Some HKMTs identified to date are MLL1, 2, 3, 4, 5, hSET1A and hSET1B (Wang and Zhu, 2008). PRMTs identified so far include PRMT1 and PRMT4, which are involved in gene activation, and PRMT5, with gene repression (Strahl and Allis, 2000).

Synthetic inhibitors of HKMTs have developed recently in the study of epigenetic regulation, one of which is 5'-deoxy-5'-methylthioadenosine (MTA), which inhibits Set1 HKMTs that facilitate H3K4 methylation (El Mansouri et al., 2011). Table 3.1 provides a description of the properties and effects of MTA on histone modification. Thus, it is possible that HMT inhibitors, such as MTA, can regulate gene expression.

### 3.1.4 Histone demethylases

Demethylation of histone residues is relatively unclear. Lysine specific demethylase 1 (LSD1) is the first demethylase that was recently discovered, which removes methyl groups selectively from H3K4me and H3K9me and is involved in transcriptional repression (Allis et al., 2007). Five other demethylases of homologous structures are later identified, which are distinct from the structure of LSD1 (Allis et al., 2007). They share a similar JmjC-domain that specifically

removes methyl groups from distinct sites on histone tails (Trewick et al., 2005, Tsukada et al., 2006). For instance, JHDM1 demethylates H3K36me1 and H3K36me3, while JHDM2A demethylates H3K9me1 and H3K9me2 (Yamane et al., 2006).

Synthetic inhibitors of LSD1 and JmjC histone demethylase inhibitors are designed but their selectivities and potencies are still under development (Lohse et al., 2011).

### 3.1.5 The 'histone code' hypothesis

Distinct patterns of covalent modifications on histone tails form 'epigenetic signatures' on the genome (Strahl and Allis, 2000). These fixed patterns of modifications forms a 'histone code' that determines the accessibility of the chromatin to binding of transcription factors (Strahl and Allis, 2000). Figure 3.1.5 show the distinct residues on which specific covalent modifications occur, and these modifications in turn determine the conformation of the chromatin and subsequent transcriptional activities.
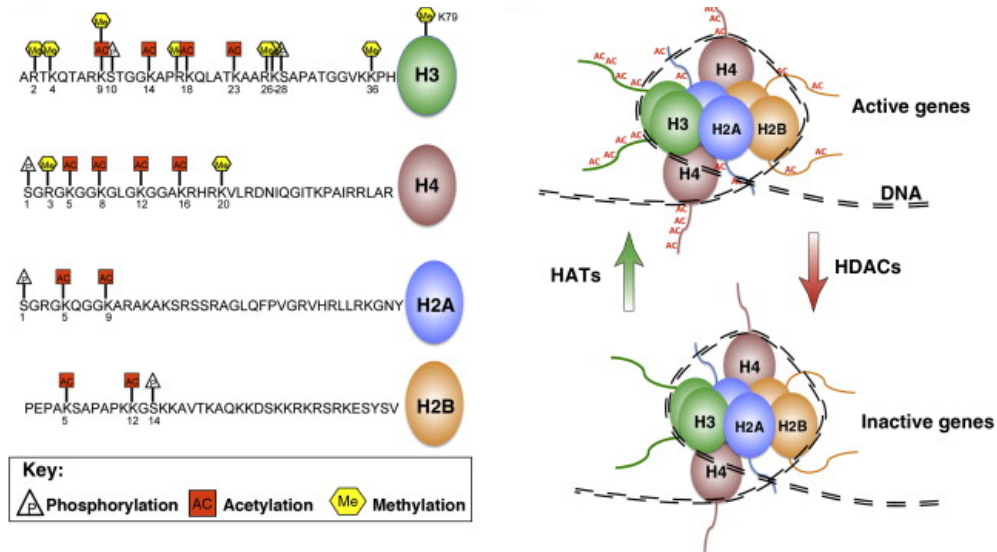
**Figure 3.1.5 Illustration of three types of histone modifications, namely phosphorylation (white), acetylation (red) and methylation (yellow) that occur on specific residues of histone tails.** HATs catalyse acetylation while HDACs catalyse deacetylation of histone tails, resulting in active and inactive genes respectively. Presence of such distinct patterns of modifications led to the 'histone code' hypothesis. [Adapted from (Fischer et al., 2010)]

Correlative studies show specific histone modifications to associate with varying transcriptional activities (Allis et al., 2007). For instance, H3K9ac is typically associated with transcriptional activation, while H3K9me, with transcriptional repression (Allis et al., 2007). Similarly, trimethylation of H3K4 is associated with open chromatin conformation and increased gene expression (Allis et al., 2007). Table 3.1.5 shows the types of histone lysine modifications associated with transcriptional activation or repression.

**Table 3.1.5  Types of histone lysine modifications** [Adapted from (Allis et al., 2007)]

|  | Role in transcription | Histone-modified sites |
| --- | --- | --- |
| Acetylation | activation | H3 (K9, K14, K18, K56) |
| Phosphorylation | activation | H3 (S10) |
| Methylation | activation | H3 (K4, K36, K79) |
|  | repression | H3 (K9, K27) H4 (K20) |

## 3.2    Epigenetics and neuroinflammation

The role of epigenetics in age-related neurodegeneration has been established in recent years (Glass et al., 2010b). In line with the age-related nature of neurodegenerative diseases such as AD and PD, it is widely accepted that epigenetic changes accumulate in individuals over the course of their lifespan, leading to disease (Glass et al., 2010b). Much research show that accumulation of stresses early in life could leave persistent and accumulating epigenetic marks in the genome, modifying behavioral function in the long run (Wilson, 2008, Khansari et al., 2009). A phenomenon known as an "age-specific epigenetic drift" has been reported in late-onset AD, where modifications in epigenetic signatures lead to gene expression and behavioral changes over time (Wang et al., 2008). Some of these involve dysregulated histone acetylation as observed in AD mouse models (Francis et al., 2009), as well as changes in DNA methylation of CpG islands of AD-related genes as observed in humans (Wilensky

et al., 2008, Wang et al., 2011). Aberrations in histone acetylation and HDAC activities have also been reported in Parkinson's disease (Kontopoulos et al., 2006).

Growing evidence show the involvement of epigenetic mechanisms in inflammation. Changes in DNA methylation levels in AD patients were associated with the expression of proinflammatory lipoprotein-associated PLA$_2$ (Lp-PLA$_2$) (Wilensky et al., 2008, Wang et al., 2011). HDAC6 and HDAC9 increase activation of anti-inflammatory T-lymphocytes by inducing the binding of transcription factor forkhead box P3 (Beier et al., 2011). Other histone modifiers, SIRT1 and SIRT6, alter the promoter-binding efficacy of the transcription factor NF-kB to inflammatory genes (Yoshizaki et al., 2010, Galli et al., 2011). Epigenetic regulation also affect transcription of the TNF-α gene, which may explain inter-individual variations in inflammatory responses (Sullivan et al., 2007). Together, these findings suggest that inflammatory responses involved in chronic neurodegeneration could be significantly influenced by epigenetic mechanisms.

## 3.3 Epigenetics and apoptosis

Apoptosis is the main process of cell death in chronic neurodegeneration (Mattson, 2000). HDAC inhibitors affect cell cycle regulation and apoptosis (Choi, 2005). For instance, TSA induces apoptosis and promotes anti-cancer activity in non-small cell lung cancer cells via reduction of cyclooxygenase-2 (COX-2) (Choi, 2005).

HDAC inhibitors such as the anti-epileptic drug, valproic acid, also confer neuroprotection (Monti et al., 2009). HAT inhibitors can have anti-cancer (Gajer et al., 2015) as well as neuroprotective properties (Durham, 2012). To date, there is little knowledge about epigenetic mechanisms behind neuronal apoptosis.

## 4.0    Nutraceuticals and phytochemicals

"Nutraceutical" is a portmanteau of two words "nutrition" and "pharmaceutical", referring to food or food products that has health-promoting and medicinal properties (Kalra, 2003). Stephen DeFelice (MD), who is the founder and chairman of the Foundation for Innovation in Medicine, Granford, NJ, coined the term (Brower, 1998). He defined nutraceutical as "a food (or part of a food) that provides medical or health benefits, including the prevention and/or treatment of a disease (Brower, 1998)." It is distinct from "functional food" as functional food supplies the body with sufficient nutrients for its survival, but nutraceuticals further prevent or treat a disease (Kalra, 2003). It is also distinct from dietary supplements as it is presented as a conventional food rather than as in a pill or tablet (Kalra, 2003). Nutraceuticals possess anti-cytotoxic effects as they generate neurotrophic factors essential for improved cell viability (Blaylock and Maroon, 2012).

Phytochemicals are chemical constituents found naturally in plants that possess health-promoting effects, and are used widely in nutraceuticals. Three major classes of plant chemicals include phenolic metabolites, terpenoids and alkaloids together with other nitrogen-containing plant constituents (Dillard and German, 2000). Phenolic metabolites originate from higher plants and are unique due to their solubility in water and many possess antioxidant properties (Bravo, 1998). Terpenoids are largely found in grains, green foods and soy-

based plants, the most studied of which are tocopherols, tocotrienols and carotenoids (Dillard and German, 2000). Other subclasses of terpenoids are phytosterols, phenolic acids, flavonoids and isoflavonoids (Dillard and German, 2000). Anacardic acid is an example of a flavonoid extract derived from cashew nuts that has anti-inflammatory properties (Sung et al., 2008). Alkaloids include glucosinolates, which are present in cruciferous vegetables, and indoles which regulate cell cycle progression and cellular apoptosis (Dillard and German, 2000).

## 4.1    Neuroprotective properties of nutraceuticals

Nutraceuticals have been identified as natural antioxidants that protect against neuronal death and neurodegeneration (Kelsey et al., 2010). Epigallocatechin 3-gallate (EGCG), the flavonoid polyphenol present in green tea, is protective against oxidative stress in rat cerebellar granular neurons (Schroeder et al., 2009) and $H_2O_2$-induced neuronal death in motor neurons (Koh et al., 2004). Quercetin, a flavonoid polyphenol in apples, increases cell viability in $H_2O_2$-induced cell death in PC12 cells (Heo and Lee, 2004). It also suppresses hippocampal neuronal cell death in rats under ischemic conditions (Pu et al., 2007). Curcumin, a yellow, non-flavonoid polyphenol found in turmeric and curry powder, decreases ROS and enhances cell survival in N2a mouse neuroblastoma cells (Dutta et al., 2009). Curcumin also protected rats from focal cerebral ischemia that is induced by blockage

of the middle cerebral artery (Yang et al., 2009). Together, these show promising effects of nutraceuticals and phytochemicals on neuroprotection, and suggests that there might be many more yet to be discovered.

## 4.2    Epigenetic properties of nutraceuticals

While it is known that nutraceuticals possess neuroprotective and antioxidant properties, little understanding exists regarding the mechanism and ways by which it exerts its function. Several nutraceuticals have been reported to possess epigenetic properties such as the regulation of SIRTs and HATs (Kelsey et al., 2010, Ghizzoni et al., 2011). Anacardic acid, a flavonoid derived from cashew nuts, is a well-known general HAT inhibitor that inhibits the p300/CBP, GCN5/PCAF and MYST family of HATs (Sung et al., 2008). Its HAT inhibitory activity gives rise to its anti-inflammatory effects in the inhibition of lipopolysaccharide-induced interleukin-8 (IL-8) expression in human alveolar epithelial cells (Yasutake et al., 2013). Plumbagin, a compound derived from the medicinal plant *Plumbago zeylanica*, inhibits the p300 HAT and downregulates NF-kB-dependent gene expression (Sandur et al., 2006, Ravindra et al., 2009). It is known to possess anti-cancer properties (Gomathinayagam et al., 2008). EGCG functions as a HAT inhibitor and is able to modify chromatin structures and via decrease in acetylation of histone tails (Choi et al., 2009, Meeran et al., 2011). Curcumin is an inhibitor of the p300 HAT which

stimulates downregulation of NF-kB-dependent expression of various

pro-inflammatory genes (Balasubramanyam et al., 2004). Thus, there

is promising evidence for epigenetic properties in nutraceuticals and

phytochemicals.

# SECTION II

# AIMS OF STUDY

Current literature shows that $cPLA_2$ plays an important role in neuroinflammation and neurodegeneration. The age-related and progressive nature of neurodegeneration suggests potential for the environment and epigenetic influences to affect the onset and progression of chronic neuroinflammation. Little is known concerning the epigenetic regulation of $cPLA_2$. Hence, the present study was carried out to test the hypothesis that significant regulation of $cPLA_2$ occurs at the epigenetic level in SH-SY5Y human neuroblastoma cells. In the first part of the study, an initial screening was performed to elucidate the effects of the general HDAC inhibitor, TSA, on mRNA expression of $PLA_2$ isoforms. More specific HDAC inhibitors were used to explore the effects of various classes of HDACs on $cPLA_2\alpha$ and $iPLA_2\beta$ expression. Co-treatments of HAT and HMT inhibitors with HDAC inhibitors were administered to study their effects on $cPLA_2$ regulation. We further explored the effects of TSA on specific histone modifications at the $cPLA_2$ promoter with chromatin immunoprecipitation. Subsequently, we investigated the effects of HAT and HMT inhibitors in cell injury induced by TSA. Co-treatment with the $cPLA_2$-selective inhibitor $AACOCF_3$ was performed to test the hypothesis that TSA induces cell injury via $cPLA_2$-related mechanisms.

Nutraceuticals and phytochemicals are found to be anti-inflammatory and neuroprotective, and many have epigenetic effects on gene expression. We next investigated the effects of the natural compound, *Clinacanthus nutans* (*C. nutans*), on $cPLA_2$ regulation in

SH-SY5Y human neuroblastoma cells. The HAT activity assay was used to test the hypothesis that *C. nutans* functions via HAT inhibitory properties. The role of *C. nutans* in modulation of cell viability was also investigated. It is hoped that our findings would provide insights into the epigenetic regulation of cPLA$_2$ and elucidate the potential for phytochemicals to affect this process, for therapy for chronic inflammation.

# SECTION III

# EXPERIMENTAL STUDY

# CHAPTER 1

# EFFECTS OF INHIBITORS OF HISTONE DEACETYLASES, HISTONE ACETYLTRANSFERASES AND HISTONE METHYLTRANSFERASES ON EPIGENETIC REGULATION OF CYTOSOLIC PHOSPHOLIPASES A$_2$

## 1.1    Introduction

Gene expression can be regulated at multiple levels, namely the regulation of chromatin conformation, transcriptional regulation, RNA processing, mRNA stability, translational regulation and post-translational modifications such as glycosylation, phosphorylation and protein degradation (Alberts et al., 2002).

Transcriptional regulation plays an important role in $cPLA_2$ expression (Cowan et al., 2004). The $cPLA_2$ gene is located on chromosome 1q25, adjacent to the COX-2 locus (Newman et al., 1997, Ghosh et al., 2006). The primary promoter region occurs between 31 to 73 positions upstream of the transcriptional start site (Cowan et al., 2004). Several binding sites at this region have been identified and proposed to be important for gene regulation (Cowan et al., 2004). Cytokines and growth factors that interact at these binding sites influence transcription of the gene (Cowan et al., 2004, Tsou et al., 2007). Glucocorticoid growth factors stimulate $cPLA_2\alpha$ expression in human amnion fibroblasts (Guo et al., 2010), and IL-1ß induces its upregulation in human rheumatoid arthritis synovial fibroblasts (Chi et al., 2011). Post-transcriptionally, the mRNA can be alternately spliced to produce $cPLA_2\alpha$, $cPLA_2$ß, $cPLA_2\gamma$, $cPLA_2\delta$, $cPLA_2\varepsilon$ and $cPLA_2\zeta$ isoforms, whereby the $cPLA_2\alpha$ isoform is most studied (Ghosh et al., 2006).

Post-translational modifications also play a role in regulation of $cPLA_2$ (Leslie, 1997). Phosphorylation of the $cPLA_2$ protein facilitates translocation from the cytosol to intracellular membranes where it carries out its function (Lin et al., 1993, Clark et al., 1995, Pavicevic et al., 2008). Treatment of

primary mouse astrocyte cultures with cytokines and ATP promotes phosphorylation of cPLA$_2$ via PKC and ERK, followed by arachidonic acid release (Xu et al., 2003). TNF-α induces cPLA$_2$ phosphorylation and arachidonic acid release via activation of the MAP kinase cascade and NF-κB (Hernandez et al., 1999). Specific phosphorylation events at the serine-515 and serine-505 residues are important for generation of arachidonic acid in vascular smooth muscle cells (Pavicevic et al., 2008).

Thus far, however, relatively little is known about epigenetic regulation of cPLA$_2$. Epigenetic modifications are typically characterized by reversible changes in gene expression following environmental stimuli (Glass et al., 2010a, Bayarsaihan, 2011) or dietary changes (Morris, 2009). Enzymes such as histone acetyltransferases (HATs), histone deacetylases (HDACs), histone methyltransferases (HMTs) and histone demethylases mediate epigenetic histone modifications and control the state of lysine residues (K) on histone tails (Allis et al., 2007). Specifically, acetylation of the lysine 9 residue of histone H3 (H3K9ac) is typically associated with activated genes (Nightingale et al., 2007, Wu et al., 2012b), and likewise, trimethylation of the lysine 4 residue of histone 3 (H3K4me3) is associated with open chromatin conformation and increased gene expression (Allis et al., 2007). HDAC inhibitors such as TSA significantly alters approximately 2% of genes (Van Lint et al., 1996), and recent studies highlighted it as a potential drug candidate, especially in the field of cancer therapy (Mariadason et al., 2000). The present study was therefore carried out to investigate possible epigenetic regulation of cPLA$_2$ in SH-SY5Y human neuroblastoma cells. The effects of

histone acetylation and methylation on $cPLA_2$ expression were explored, and possible changes in cell viability as a result of these changes, elucidated.

## 1.2    Materials and Methods

### 1.2.1    Materials

Treatments administered to SH-SY5Y cells were dimethyl sulfoxide (DMSO), trichostatin A (TSA), valproic acid (VPA), MS-275, tubacin, anacardic acid, curcumin (CCM), NU9056, C646, butyrolactone-3 (MB-3), 5'-deoxy-5'-methylthioadenosine (MTA) and arachidonyl trifluoromethyl ketone ($AACOCF_3$). DMSO, TSA, VPA, tubacin, CCM, C646 and MTA were purchased from Sigma (St. Louis, MO). MS-275 and MB-3 were purchased from Santa Cruz Biotechnology (Santa Cruz, CA). Anacardic acid was purchased from Calbiochem (San Diego, CA). NU9056 and $AACOCF_3$ were purchased from Tocris Bioscience (Bristol, UK). The stock solutions were dissolved in DMSO and further diluted in cell culture medium prior to use, except VPA whereby distilled $H_2O$ was used instead due to better solubility.

### 1.2.2    Cell culture

SH-SY5Y human neuroblastoma cells were obtained from American Type Culture Collection (ATCC, Manassas, VA). Cells were cultured in Dulbecco's Modified Eagle's Medium (DMEM) supplemented with 10% heat-inactivated fetal bovine serum (FBS) and 1% penicillin/streptomycin (Gibco-Invitrogen, Carlsbad, CA). This cell line is a suitable *in vitro* model for the study of neurodegenerative diseases such as AD because of their ability to

express mature isoforms of the tau protein (Agholme et al., 2010). They possess several characteristics similar to dopaminergic neurons, and thus are suitable as a PD models as well (Constantinescu et al., 2007). SH-SY5Y cells are generally locked in an early neuronal differentiation phase (Gilany et al., 2008, Lopes et al., 2010). SH-SY5Y cells differentiated by retinoic acid displayed increased tau phosphorylation on top of neuron-like characteristics (Jämsä et al., 2004). Retinoic acid treatment was also found to reduce HDAC1 binding to neuronal genes, bringing about changes to the epigenome (Ekici et al., 2008). Therefore, SH-SY5Y cells were not further differentiated wih retinoic acid, so that responses to treatments affecting the histones can be evaluated. The cells used were of a constant N-type origin, as inter-conversion to S-type was shown in previous literature not to occur due to their copy number variants and genetic variation (Cohen et al., 2003, Do et al., 2011). This excludes the possibility of changes in gene expression to be due to spontaneous inter-conversions between the cell types. Cells were grown in 100 mm$^2$ cell culture dishes and incubated at 37°C, 100% humidity with 95% air and 5% $CO_2$.

### 1.2.3    Cell treatments

### 1.2.3.1    Dose-dependent treatments with histone deacetylase (HDAC) inhibitors

To examine the effects of different HDAC inhibitors on $cPLA_2$ and $iPLA_2$ expression, dose-dependent treatments were administered to four groups of SH-SY5Y cells, with the first group treated with vehicle controls, and the next

three groups with increasing doses of the HDAC inhibitors. Each group consists of four biological replicates. TSA was administered in increasing doses up to the IC50 value of 0.5 $\mu$M (Muhlethaler-Mottet et al., 2008). VPA was administered up to 1000 $\mu$M as considerable epigenetic effects were observed in SH-SY5Y cells up to that dose (Jeong et al., 2003). Tubacin is known to inhibit HDAC6 at micromolar doses (Zilberman et al., 2009), while MS-275 is known to display epigenetic effects in SH-SY5Y cells at 1-10 $\mu$M (Formisano et al., 2015). Cells were incubated with respective HDAC inhibitors or vehicle for 24 hours before harvesting.

## 1.2.3.2 Dose-dependent treatment with general histone acetyltransferase (HAT) inhibitor, anacardic acid

To study the effect of the general HAT inhibitor anacardic acid on cPLA$_2$ and iPLA$_2$ expression, dose-dependent treatments of 10 $\mu$M, 20 $\mu$M and 30 $\mu$M anacardic acid were administered to four groups of SH-SY5Y cells, according to known doses where it exerts significant epigenetic effects (Sun et al., 2006a, Morimoto et al., 2008). DMSO was used as vehicle control, and each group consists of four biological replicates. Anacardic acid is a well-known HAT inhibitor that is a flavonoid extract derived from cashew nuts, and has been reported to possess anti-inflammatory properties (Sung et al., 2008). Cells were incubated with anacardic acid or vehicle for 24 hours before harvesting.

**1.2.3.3  Dose-dependent treatment with natural p300-specific HAT**

**inhibitor, curcumin (CCM)**

To explore the effect of the natural p300-specific HAT inhibitor, CCM, on $cPLA_2$ and $iPLA_2$ expression, dose-dependent treatments of 10 $\mu$M, 20 $\mu$M and 30 $\mu$M curcumin were administered to four groups of SH-SY5Y cells, according to known doses where it exerts significant epigenetic effects (Huang et al., 2014). DMSO was used as vehicle control, and each group consists of four biological replicates. CCM is a component of *Curcuma longa,* commonly known as turmeric (Reuter et al., 2011), and is a selective inhibitor of p300 HAT (Marcu et al., 2006). Cells were incubated with CCM or vehicle treatment for 24 hours before harvesting.

**1.2.3.4  Treatment with general HAT inhibitor, anacardic acid, and**

**general HDAC inhibitor, TSA**

To investigate the effect of the general HAT inhibitor anacardic acid and the general HDAC inhibitor TSA on $cPLA_2$ expression, SH-SY5Y cells were divided into four groups and treated as follows: (1) DMSO as vehicle control, (2) 0.5 $\mu$M TSA, (3) 20 $\mu$M AA, (4) 20 $\mu$M AA and 0.5 $\mu$M TSA. Each group consists of four biological replicates. Cells were co-incubated with anacardic acid and TSA or vehicle for 24 hours before harvesting.

**1.2.3.5  Treatment with natural p300-specific HAT inhibitor, CCM, and**

**general HDAC inhibitor, TSA**

To examine the effect of the natural p300-specific HAT inhibitor CCM

and the general HDAC inhibitor TSA on $cPLA_2$ expression, four groups of SH-SY5Y cells were treated as follows: (1) DMSO as vehicle control, (2) 0.5 $\mu$M TSA, (3) 20 $\mu$M CCM, (4) 20 $\mu$M CCM and 0.5 $\mu$M TSA. Each group consists of four biological replicates. Cells were co-incubated with CCM and TSA or vehicle for 24 hours before harvesting.

### 1.2.3.6    Treatment with synthetic p300-specific HAT inhibitor, C646, and general HDAC inhibitor, TSA

To study the effect of the synthetic p300-specific HAT inhibitor C646 and the general HDAC inhibitor TSA on $cPLA_2$ expression, four groups of SH-SY5Y cells were treated as follows: (1) DMSO as vehicle control, (2) 0.5 $\mu$M TSA, (3) 20 $\mu$M C646, (4) 20 $\mu$M C646 and 0.5 $\mu$M TSA. The doses were chosen according to doses of anacardic acid and curcumin used, so as to ensure consistency. Each group consists of four biological replicates. Cells were co-incubated with C646 and TSA or vehicle for 24 hours before harvesting.

### 1.2.3.7    Treatment with GCN5-specific HAT inhibitor, MB-3, and general HDAC inhibitor, TSA

To explore the effect of the GCN5-specific HAT inhibitor MB-3 and the general HDAC inhibitor TSA on $cPLA_2$ expression, SH-SY5Y cells were divided into four groups and treated as follows: (1) DMSO as vehicle control, (2) 0.5 $\mu$M TSA, (3) 20 $\mu$M MB-3, (4) 20 $\mu$M MB-3 and 0.5 $\mu$M TSA. The doses were chosen according to doses of anacardic acid and curcumin used, so as

to ensure consistency. Each group consists of four biological replicates. Cells were co-incubated with MB-3 and TSA or vehicle for 24 hours before harvesting.

### 1.2.3.8 Treatment with Tip60-specific HAT inhibitor, NU9056, and general HDAC Inhibitor, TSA

To investigate the effect of the Tip60-specific HAT inhibitor NU9056 and the general HDAC inhibitor TSA on $cPLA_2$ expression, SH-SY5Y cells were divided into four groups and treated as follows: (1) DMSO as vehicle control, (2) 0.5 $\mu$M TSA, (3) 20 $\mu$M NU9056, (4) 20 $\mu$M NU9056 and 0.5 $\mu$M TSA. The doses were chosen according to doses of anacardic acid and curcumin used, so as to ensure consistency. Each group consists of four biological replicates. Cells were co-incubated with NU9056 and TSA or vehicle for 24 hours before harvesting.

### 1.2.3.9 Treatment with Tip60-specific HAT inhibitor, NU9056, and class I-specific HDAC inhibitor, MS-275

To examine the effect of the Tip60-specific HAT inhibitor NU9056 and the class I-specific HDAC inhibitor MS-275 on $cPLA_2$ expression, SH-SY5Y cells were divided into four groups and treated as follows: (1) DMSO as vehicle control, (2) 5 $\mu$M MS-275, (3) 20 $\mu$M NU9056, (4) 20 $\mu$M NU9056 and 5 $\mu$M MS-275. Each group consists of four biological replicates. Cells were co-incubated with NU9056 and MS-275 or vehicle for 24 hours before harvesting.

### 1.2.3.10  Treatment with histone methyltransferase (HMT) inhibitor, MTA, and general HDAC inhibitor, TSA

To study the effect of the HMT inhibitor MTA and the general HDAC inhibitor TSA on $cPLA_2$ expression, four groups of SH-SY5Y cells were treated as follows: (1) DMSO as vehicle control, (2) 0.5 $\mu$M TSA, (3) 200 $\mu$M MTA, (4) 200 $\mu$M MTA and 0.5 $\mu$M TSA. MTA reduces trimethylation of H3K4 at micromolar doses via the inhibition of Set1 methyltransferases (Huang et al., 2006, El Mansouri et al., 2011). Each group consists of four biological replicates. Cells were co-incubated with MTA and TSA or vehicle for 24 hours before harvesting.

### 1.2.4  Real-time quantitative reverse transcription-polymerase chain reaction (qRT-PCR)

Total RNA extraction from SH-SY5Y cells was performed with the RNeasy Mini kit (Qiagen, Hamburg, Germany). Reverse transcription of RNA to complementary DNA (cDNA) was performed using the High-Capacity cDNA Reverse Transcription Kit (Applied Biosystems, Foster City, CA), with the thermal cycler of reaction conditions set at 25°C for 10 minutes, 37°C for 120 minutes, and 85°C for 5 seconds. The cDNA obtained was quantified by real-time RT-PCR using the TaqMan® Universal PCR Master Mix (Applied Biosystems, Foster City, CA) with TaqMan® Gene Expression Assay Probes for $cPLA_2\alpha$ (Hs00233352_m1), $iPLA_2\beta$ (Hs00185926_m1), and $\beta$-actin (#4326315E) (Applied Biosystems, Foster City, CA). Real-time RT-PCR was performed using a MicroAmp® 96-Well Optical Reaction Plate (Applied

Biosystems, Foster City, CA), and run on the Applied Biosystem 7500 Real-Time PCR system. Reaction conditions were set at an initial incubation of 50°C for 2 minutes, 95°C for 10 minutes, and 40 cycles of 95°C for 15 seconds and 60°C for 1 minute.

Relative amounts of gene transcript were estimated after normalization to β-actin, the endogenous control gene. It is a suitable endogenous control as it was shown to be unaffected by TSA treatment in a previous study (Makki et al., 2008). Using the $2^{-\Delta\Delta CT}$ method as previously described (Livak and Schmittgen, 2001), the relative fold changes were quantified. The mean and standard error were then calculated and significant differences analysed using one-way analysis of variance (ANOVA) with Bonferroni's multiple comparison *post-hoc* test, where *P < 0.05* was deemed significant.

### 1.2.5 Western blots

Protein samples were extracted by lysing cell samples in radioimmunoprecipitation assay (RIPA) buffer (Cell Signaling Techonology, Boston, MA), supplemented with Halt$^{TM}$ protein and phosphatase inhibitor cocktail and EDTA solution (#78440, Pierce, Rockford, IL). Lysed samples were incubated at 4ºC for one hour and subsequently centrifuged at 14,000 g, and 4ºC, for one hour to separate cellular protein extracts from cell debris. Protein quantification was performed using the Bio-Rad protein assay dye (Bio-Rad Laboratories, Hercules, CA). 30 *µ*g of protein were loaded and separated by molecular mass in 10% SDS-polyacrylamide gel via electrophoresis. Resolved proteins were electrotransferred to a polyvinylidene

difluoride (PVDF) membrane (Thermo Fisher Scientific, Waltham, MA) for 1 hour 10 minutes, 20V. Non-specific binding sites on the membrane was blocked with 3-5% bovine-serum albumin (BSA) in tris-buffered saline with 0.1% Tween-20 (TBST) for one hour, followed by overnight incubation with rabbit polyclonal anti-cPLA$_2$ (sc-438, 1:500 in 3% BSA, Santa Cruz Biotechnology, Santa Cruz, CA; #2832S, 1:500 in 5% BSA, Cell Signaling Technology, Beverly, MA), at 4ºC. Following overnight incubation, the membrane was subject to six washes, followed by secondary antibody incubation with horseradish peroxidase conjugated with anti-rabbit IgG (1:2000 in blocking buffer, Pierce, Rockford, IL) for 1 hour at r.t.p. Immunolabeled proteins were then visualized with the enhanced chemiluminescence reagent, Luminata$^{TM}$ Crescendo Western HRP Substrate (Millipore, Billerica, MA), according to the manufacturer's protocol. ß-actin was labelled to verify equal loading using a mouse monoclonal antibody (1:10,000 in 3-5% BSA, Sigma, St. Louis, MO) and its corresponding secondary antibody. Densitometric analyses of the bands were performed using the GelPro software (Media Cybernetics, Maryland, VA). The relative densities of target bands were normalised against those of ß-actin, and the mean and standard errors calculated. Significant differences between groups were analysed using the one-way ANOVA with Bonferroni's multiple comparison *post-hoc* test, where $P < 0.05$ was deemed significant.

**1.2.6  Immunocytochemistry**

SH-SY5Y cells were counted and 2 x 10$^5$ cells were cultured on poly-L-lysine-coated coverslips placed in 24-well plates. They were grown to 80% confluency before administration of treatment. The cells were incubated with treatment for 24 hours. The next day, cells were fixed with 4% paraformaldehyde, followed by antigen retrieval with formic acid for 30 minutes; and subsequently, permeabilization with 0.1% Triton-X for five minutes. They were then blocked in 3% BSA, and incubated overnight with cPLA$_2$ specific antibody (sc-438, 1:50 in 3% BSA, Santa Cruz Biotechnology, Santa Cruz, CA), followed by secondary antibody incubation with the anti-rabbit Alexa Fluor 488 (Applied Biosystems, Foster City, CA; diluted 1:200). Nuclei were labelled and coverslips mounted with the Prolong Gold Anti-fade Mountant DAPI (Invitrogen, Carlsbad, CA). After thorough drying, the samples were analysed and images captured using confocal microscopy (Zeiss, Jena, Germany).

**1.2.7  Quantitative image analysis**

To measure the fluorescence intensity of cells between the treatment groups, images were captured using the confocal microscope (Zeiss, Jena, Germany) at the plane with the best focus. An average of ten to fifteen images were captured per treatment group. The region around each cell was demarcated and measured with the Image J software (Burgess et al., 2010, Gavet and Pines, 2012). Background readings were obtained by obtaining values of at least three regions without fluorescence. The net fluorescent

intensity was calculated for each image according to the following formula:

*Corrected total cell fluoresence (CTCF) = Integrated Density − (Area of selected cell x Mean fluorescence of background readings)*. Net average intensity values were then normalised against vehicle-treated controls. The mean and standard errors were calculated and significant differences analysed using one-way ANOVA with Bonferroni's multiple comparison *post-hoc* test, where $P < 0.05$ was deemed significant.

### 1.2.8 Chromatin immunoprecipitation real-time polymerase chain reaction (ChIP-qPCR)

### 1.2.8.1 Determination of specific histone binding sites on cPLA$_2$ gene

In order to determine histone-rich regions on the cPLA$_2$α gene for downstream primer design, we used a database of ChIP-sequencing experiments known as the *Human Epigenome Atlas, release 9* (Zhou et al., 2011, Medicine, 2013). The Browser hosts sequencing experiment tracks from the Encyclopedia of DNA Elements (ENCODE) and Roadmap Epigenomics Project (Consortium, 2011, Epigenomics, 2015). The ENCODE Consortium is made up of research groups under international collaboration funded by the National Human Genome Research Institute (NHGRI) (Consortium, 2011). A detailed description of the precise standards and considerations for evaluating the quality of ChIP-seq data and antibodies used for ChIP-seq is available (Consortium, 2011). The Roadmap Epigenomics Project is an international collaboration and a detailed research workflow and list of participants and projects is available (Epigenomics, 2015). To locate potential histone binding

sites on the cPLA$_2$α gene, we used the University California Santa Cruz (UCSC) Genome Browser (Kent et al., 2002) to determine the loci of the cPLA$_2$α gene on the human genome. Together, both databases allowed us to determine the binding sites of specific histones of interest at the cPLA$_2$α promoter, for verification by chromatin Immunoprecipitation real-time polymerase chain reaction (ChIP-qPCR).

### 1.2.8.2    Primer design

In order to design primers for ChIP-qPCR, we chose to obtain ChIP-sequencing data of H3K4me3 and H3K9ac from the *Human Epigenome Atlas* because of their known associations with activated genes (Nightingale et al., 2007, Wu et al., 2012b). The human cell types analysed were the H1-derived neuronal progenitor cultured cells and H9-derived neuron cultured cells, chosen because of their relatively close association with SH-SY5Y human neuroblastoma cells. For each of the six samples analysed, histone-enriched regions were determined by observing the peaks present. Primers used in the ChIP experiment were designed based on these regions identified. A set of forward (5"-CCTCCTTAGCTTTTACTTGG-3") and reverse primers (5"-GGATTCCAACCCAAAGAAAC-3") (bp +143 to +349) was used for detection of the cPLA$_2$α gene region of interest, encoding a 206 base-pair long region. The amplification efficiencies of the primers were optimized by performing serial dilutions of the primers followed by multiple trials of qPCR using different temperature settings. The optimal annealing temperature was determined to be 55ºC and subsequent RT-PCR was performed. As a control,

qPCR of the glyceraldehyde 3-phosphate dehydrogenase (GAPDH) promoter was performed with the forward primer (5"-TACTAGCGGTTTTACGGGCG-3") and the reverse primer (5"-TCGAACAGGAGGAGCAGAGAGCGA-3") (provided in kit).

### 1.2.8.3    ChIP-qPCR

ChIP-qPCR was carried out to investigate the involvement of a specific region on the cPLA$_2\alpha$ gene in TSA-induced cPLA$_2\alpha$ expression. SH-SY5Y cells were cultured on 150 mm dishes and grown to 80% confluency. Cells were treated with DMSO as vehicle control or with 0.5 $\mu$M TSA, and subsequently incubated for 24 hours prior to performing the ChIP assay, according to the protocol as provided by the EZ-Magna ChIP$^{TM}$ A Chromatin Immunoprecipitation Kit (#17-408, Millipore, Billerica, MA). Cells were harvested on ice-cold phosphate-buffered saline (PBS) and crosslinked in 1% formaldehyde. Chromatin samples were sonicated with a Vibra-cell$^{TM}$ sonicator (Sonics and Materials Inc., Danbury, CT) to obtain DNA fragments ranging from 200 to 800 base pairs. The sonication conditions were 14 cycles of 10-second pulses and 30-second pauses, at 40% amplitude. The samples were then run on 1.5% agarose gel to confirm shearing efficiency. The sheared stock was then aliquoted in 50 $\mu$l amounts separated into 1.5 ml tubes for storage at -80°C. Three tubes from each treatment group were used for the antibody incubation, before which, 1% of total chromatin in each reaction tube was saved as 'input' for later analysis.

The remaining DNA from each tube was incubated with antibodies

overnight with rotation at 4°C. The antibodies used were histone Protein A

purified IgG raised in rabbit (provided in kit), ChIPAb+ Trimethyl-Histone H3

(Lys4) (#17-614, Millipore, Billerica, MA) and ChIPAb+ Acetyl-Histone H3

(Lys9) (#17-658, Millipore, Billerica, MA). After overnight incubation, the

samples were subjected to reverse crosslinking and purification. The enriched

DNA and 'input' samples were quantified by SYBR green real time RT-PCR,

using optimised primers specific for the region +143 to +349 base pairs

downstream from the transcriptional start site of the $cPLA_2\alpha$ gene.

Subsequently, the percent enrichment of immunoprecipitated DNA relative to

input chromatin was calculated. All quantitative ChIP assay results are

presented as the averages from three independent immunoprecipitations. The

mean and standard error were then calculated, and significant differences

were analysed using the Student's *t-test*, where *P* < 0.05 was deemed as

significant.


### 1.2.9  Detection of H3K9 acetylation levels

Detection of H3K9 acetylation was performed using the EpiQuik[TM] *In

Situ* Histone H3K9 Acetylation Assay Kit (#P-4004, Epigentek, Farmingdale,

NY). Cells were cultured in a 96-well microplate (provided in kit) and grown to

80% confluency. They were classified into two treatment groups (1) DMSO

vehicle control, (2) 0.5 $\mu$M TSA, and untreated controls. Each group consists

of four biological replicates. After treatment, cells were incubated overnight for

24 hours before the assay was performed according to the manufacturer's

protocol. The absorbance was read on the Tecan Infinite[®] 200 microplate

reader (Tecan Group Ltd., Maennedorf, Switzerland) at a wavelength of 450 nm within 10 minutes, and the % H3K9 acetylation was calculated according to the following formula:

$$\text{Acetylation } \% = \frac{\text{O. D. (treated sample-blank)}}{\text{O.D. (untreated control-blank)}} \times 100$$

Average values were then normalised against untreated controls and plotted on a graph. The mean and standard error were calculated, and significant differences analysed using the Student's *t-test*, where $P < 0.05$ was deemed significant.

### 1.2.10  Lactate dehydrogenase (LDH) assay

SH-SY5Y cells were counted and $2 \times 10^5$ cells were cultured in 24-well plates, and grown to 80% confluency before administration of treatment. AACOCF$_3$ was used for the selective inhibition of cPLA$_2$ enzyme activity, since it is known to be 500-fold more potent in blocking cPLA$_2$ activity at 15 $\mu$M as compared to iPLA$_2$ and sPLA$_2$ (Trimble et al., 1993, Liu et al., 2014). Cell viability was accessed after 24 hours by colorimetric determination of lactate dehydrogenase (LDH) release, using the LDH Cytotoxicity Detection Kit (Roche, Mannheim, Germany), according to manufacturer's protocol. Percentage of cell death was calculated and the average of three plate readings taken. The plate was read at an excitation wavelength of 490 nm on the Tecan Infinite$^®$ 200 microplate reader (Tecan Group Ltd., Maennedorf, Switzerland). The reference absorbance reading was subtracted from the absorbance at 490 nm. Percentage cytotoxicity was calculated according to the formula:

$$\text{Cytotoxicity (\%)} = \frac{\text{experimental value-low control}}{\text{high control-low control}} \times 100$$

The mean cytotoxicity values were then normalised against vehicle-treated controls. The mean and standard errors were calculated, and significant differences analysed using one-way ANOVA with Bonferroni's multiple comparison *post-hoc* test, where $P < 0.05$ was deemed significant.

## 1.3  Results

### 1.3.1  Effect of HDAC inhibitors on cPLA$_2$α and iPLA$_2$ß mRNA expression

#### 1.3.1.1          Trichostatin A (TSA)



**Effect of TSA on cPLA$_2$α mRNA Expression**

A

**Effect of TSA on iPLA$_2$β mRNA Expression**
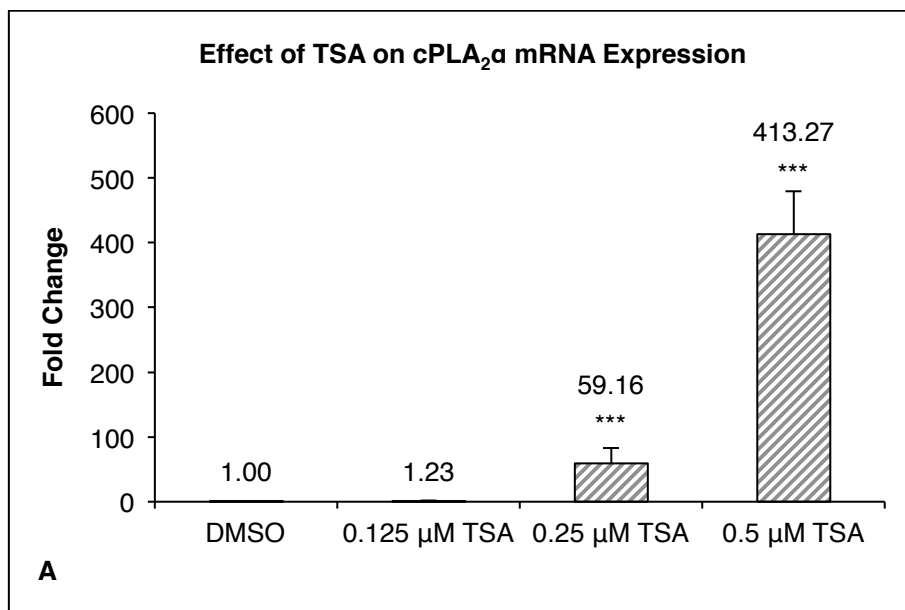
**Figure 1.3.1.1 Real-time RT-PCR analyses of (A) cPLA$_2$α and (B) iPLA$_2$ß mRNA expression after dose-dependent treatment with general HDAC inhibitor, trichostatin A (TSA).** Data represent mean and standard error of four biological replicates. Statistical analysis by one-way ANOVA with Bonferroni's multiple comparison *post-hoc* test. * Indicates significant difference compared to DMSO-treated vehicle controls. * $P < 0.05$ and *** $P < 0.001$.

Significant increases in cPLA$_2$α mRNA expression by 59.2-fold and 413.3-fold were observed after treatment with 0.25 $\mu$M and 0.5 $\mu$M TSA respectively, compared to DMSO-treated vehicle controls ($P < 0.001$) (Fig. 1.3.1.1 A). A relatively small but significant 6.4-fold increase in iPLA$_2$ß mRNA expression was observed after treatment with 0.5 $\mu$M TSA ($P < 0.001$) (Fig. 1.3.1.1 B).

### 1.3.1.2 Valproic acid (VPA)



**Figure 1.3.1.2 Real-time RT-PCR analyses of (A) cPLA$_2$α and (B) iPLA$_2$ß mRNA expression after dose-dependent treatment with class IIa HDAC inhibitor, valproic acid (VPA).** Data represent mean and standard error of four biological replicates. Statistical analysis by one-way ANOVA with Bonferroni's multiple comparison *post-hoc* test. * Indicates significant difference compared to dH$_2$O-treated vehicle controls. * $P < 0.05$, ** $P < 0.01$ and *** $P < 0.001$.

Significant increases in cPLA$_2$α mRNA expression by 15.1-fold and 25.3-fold were observed after treatment with 500 $\mu$M and 1000 $\mu$M VPA

respectively, compared to $dH_2O$-treated vehicle controls ($P < 0.001$) (Fig. 1.3.1.2 A). In contrast, a small but significant 2.0-fold decrease in $iPLA_2\beta$ expression was observed after treatment with 1000 $\mu M$ VPA, compared to $dH_2O$-treated vehicle controls ($P < 0.001$) (Fig. 1.3.1.2 B).

### 1.3.1.3 Tubacin



**Effect of Tubacin on $cPLA_2\alpha$ mRNA Expression**

**A**



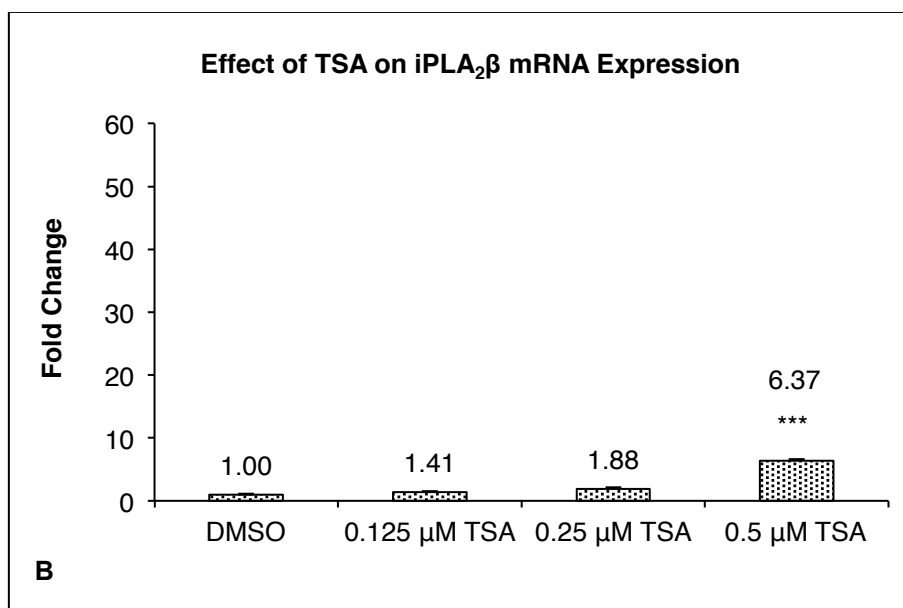**Effect of Tubacin on $iPLA_2\beta$ mRNA Expression**

**B**
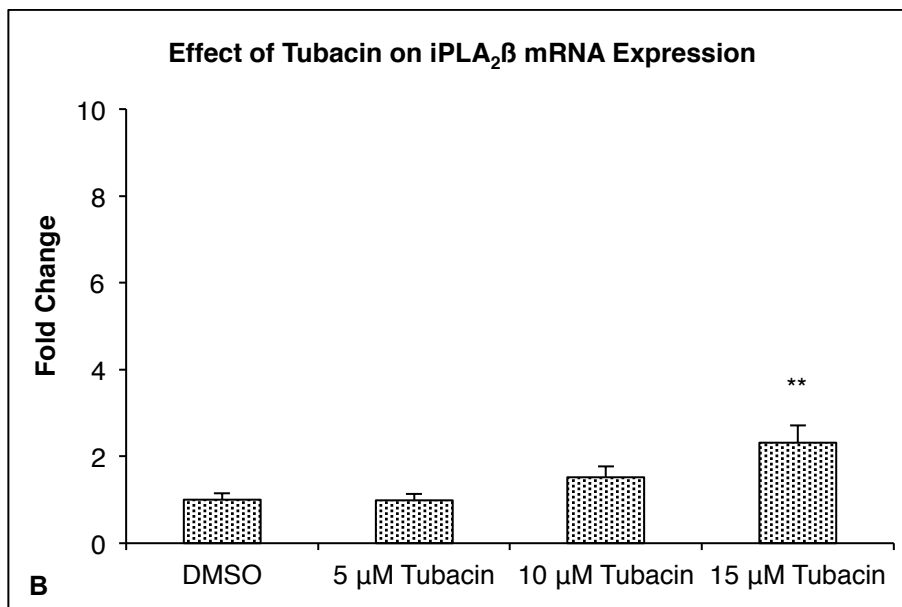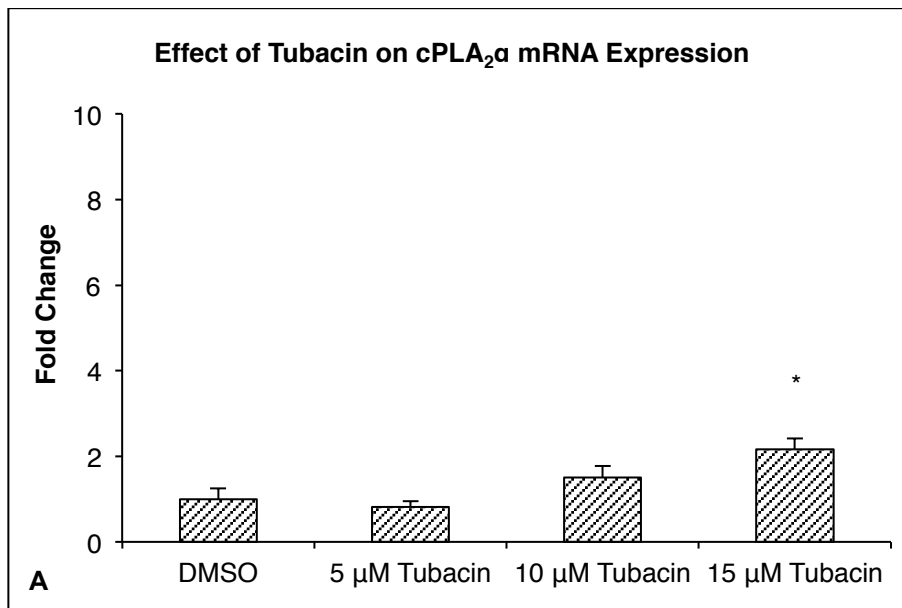
**Figure 1.3.1.3 Real-time RT-PCR analyses of (A) cPLA$_2$α, (B) iPLA$_2$ß mRNA expression after dose-dependent treatment with HDAC6-specific inhibitor, tubacin.** Data represent mean and standard error of four biological replicates. Statistical analysis by one-way ANOVA with Bonferroni's multiple comparison *post-hoc* test. * Indicates significant difference compared to DMSO-treated vehicle controls. * $P < 0.05$, ** $P < 0.01$.

A small but significant 2.2-fold increase in cPLA$_2$α mRNA expression was observed after treatment with 15 $\mu$M tubacin, compared to DMSO-treated vehicle controls ($P = 0.016$) (Fig. 1.3.1.3 A). Similarly, a significant 2.3-fold increase in iPLA$_2$ß mRNA expression was observed after treatment with 15 $\mu$M tubacin, compared to DMSO-treated vehicle controls ($P < 0.01$) (Fig 1.3.1.3 B).
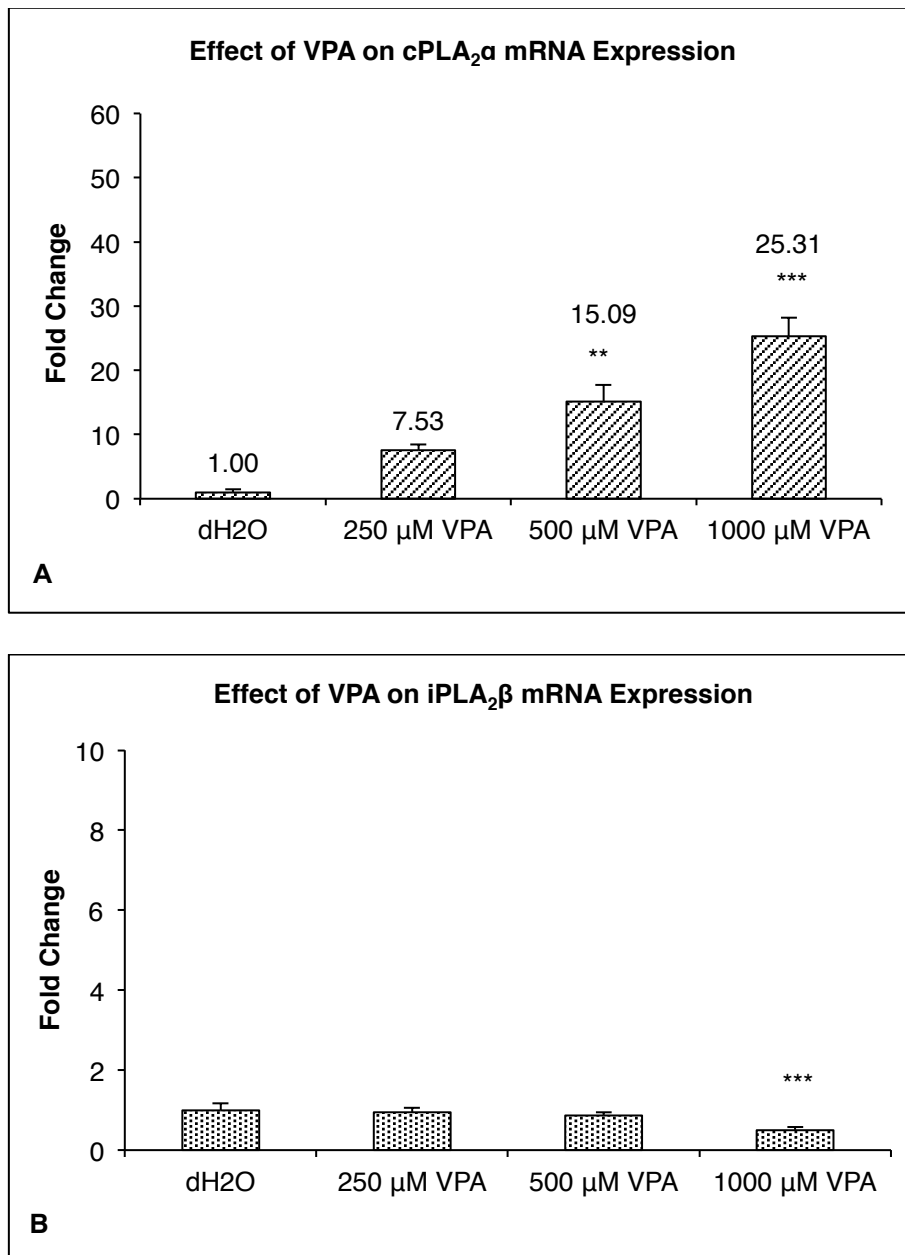
## 1.3.1.4        MS-275
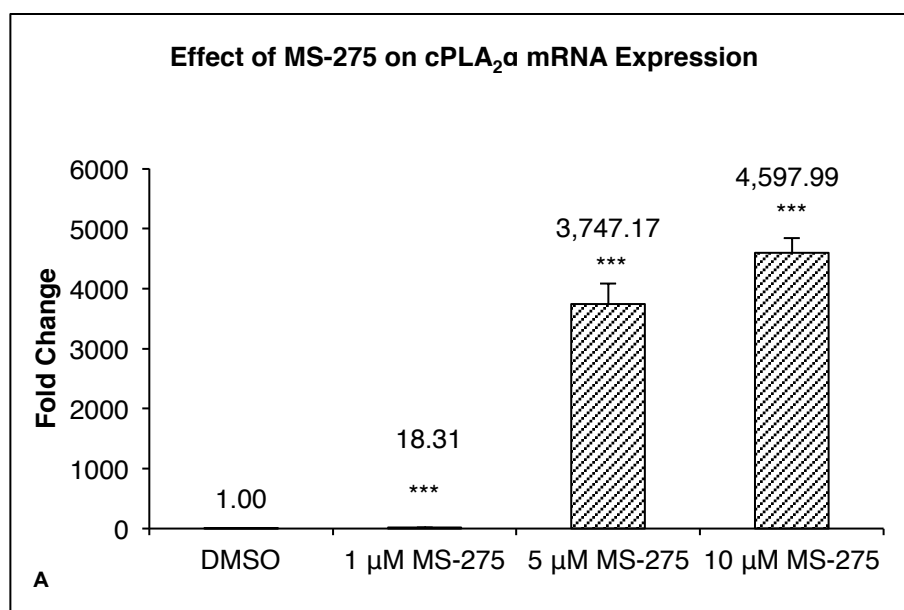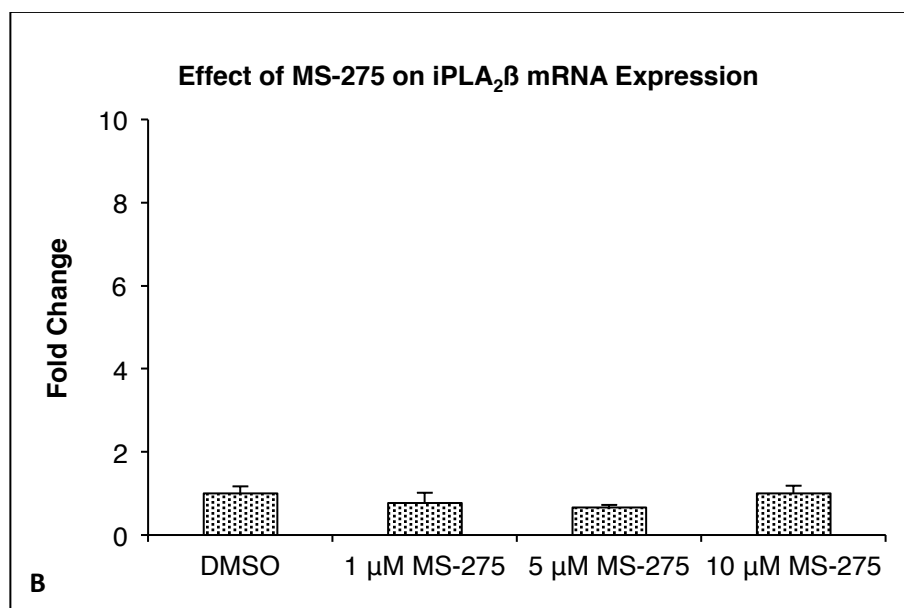
**Figure 1.3.1.4 Real-time RT-PCR analyses of (A) cPLA$_2$α, (B) iPLA$_2$ß mRNA expression after dose-dependent treatment with class I HDAC inhibitor, MS-275.** Data represent mean and standard error of four biological replicates. Statistical analysis by one-way ANOVA with Bonferroni's multiple comparison *post-hoc* test. * Indicates significant difference compared to DMSO-treated vehicle controls. * $P < 0.05$ and *** $P < 0.001$.

Significant increases in cPLA$_2$α mRNA expression by 18.3-fold, 3750-fold and 4600-fold were detected after treatments with increasing doses of 1 $\mu$M, 5 $\mu$M and 10 $\mu$M MS-275 respectively, compared to DMSO-treated vehicle controls ($P < 0.001$) (Fig. 1.3.1.4 A). In contrast, no significant changes in iPLA$_2$ß mRNA expression were observed (Fig. 1.3.1.4 B).

## 1.3.2  Effect of HAT inhibitors on cPLA₂α and iPLA₂ß mRNA expression

### 1.3.2.1          Anacardic acid (AA)
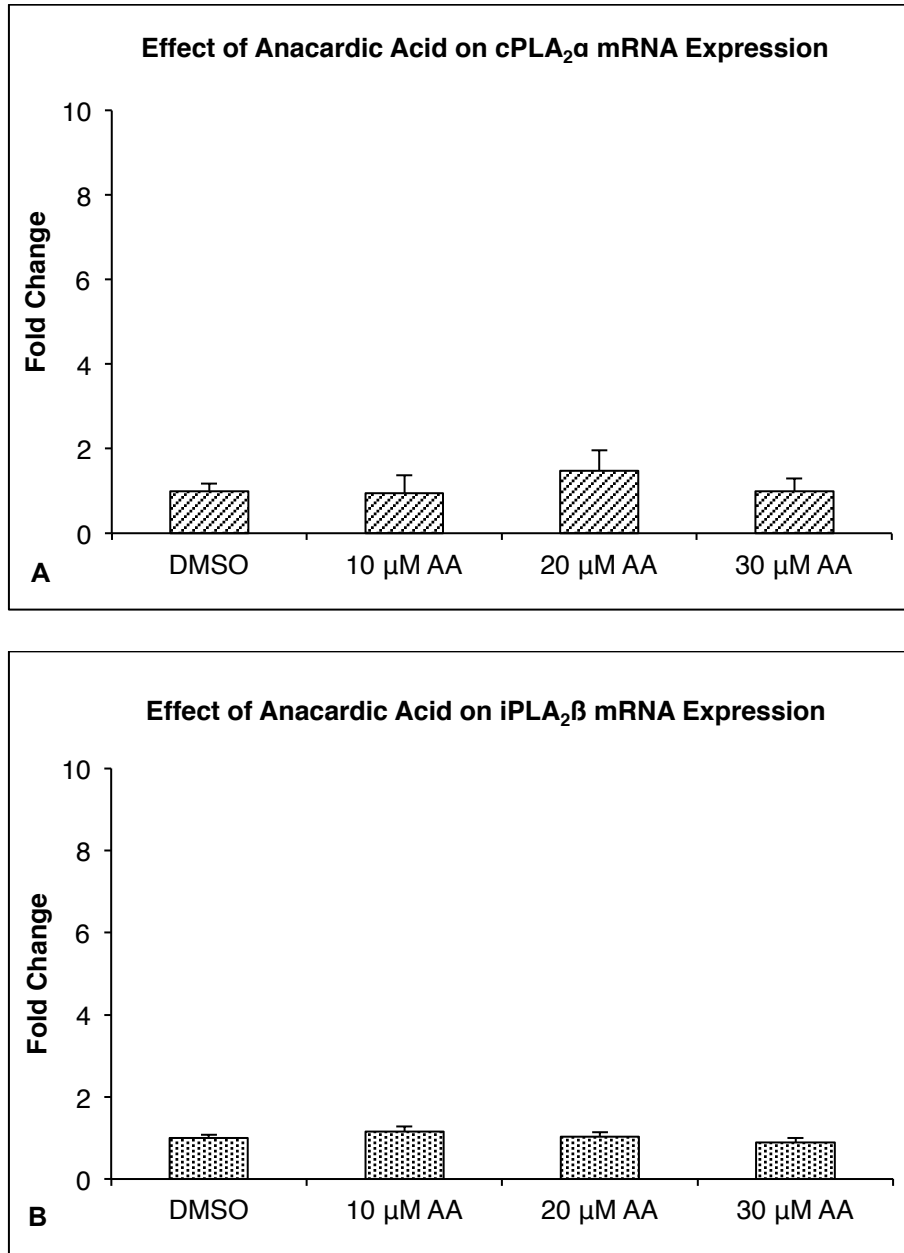


**Figure 1.3.2.1 Real-time RT-PCR analyses of (A) cPLA₂α and (B) iPLA₂ß mRNA expression after dose-dependent treatment with general HAT inhibitor, anacardic acid (AA).** Data represent mean and standard error of four biological replicates. Statistical analysis by one-way ANOVA with Bonferroni's multiple comparison *post-hoc* test.

No significant changes in $cPLA_2\alpha$ and $iPLA_2\beta$ mRNA expression were observed after dose-dependent treatment with anacardic acid, compared to DMSO-treated vehicle controls (Fig. 1.3.2.1).

## 1.3.2.2 Curcumin (CCM)



**Effect of Curcumin on $cPLA_2\alpha$ mRNA Expression**

**Effect of Curcumin on $iPLA_2\beta$ mRNA Expression**
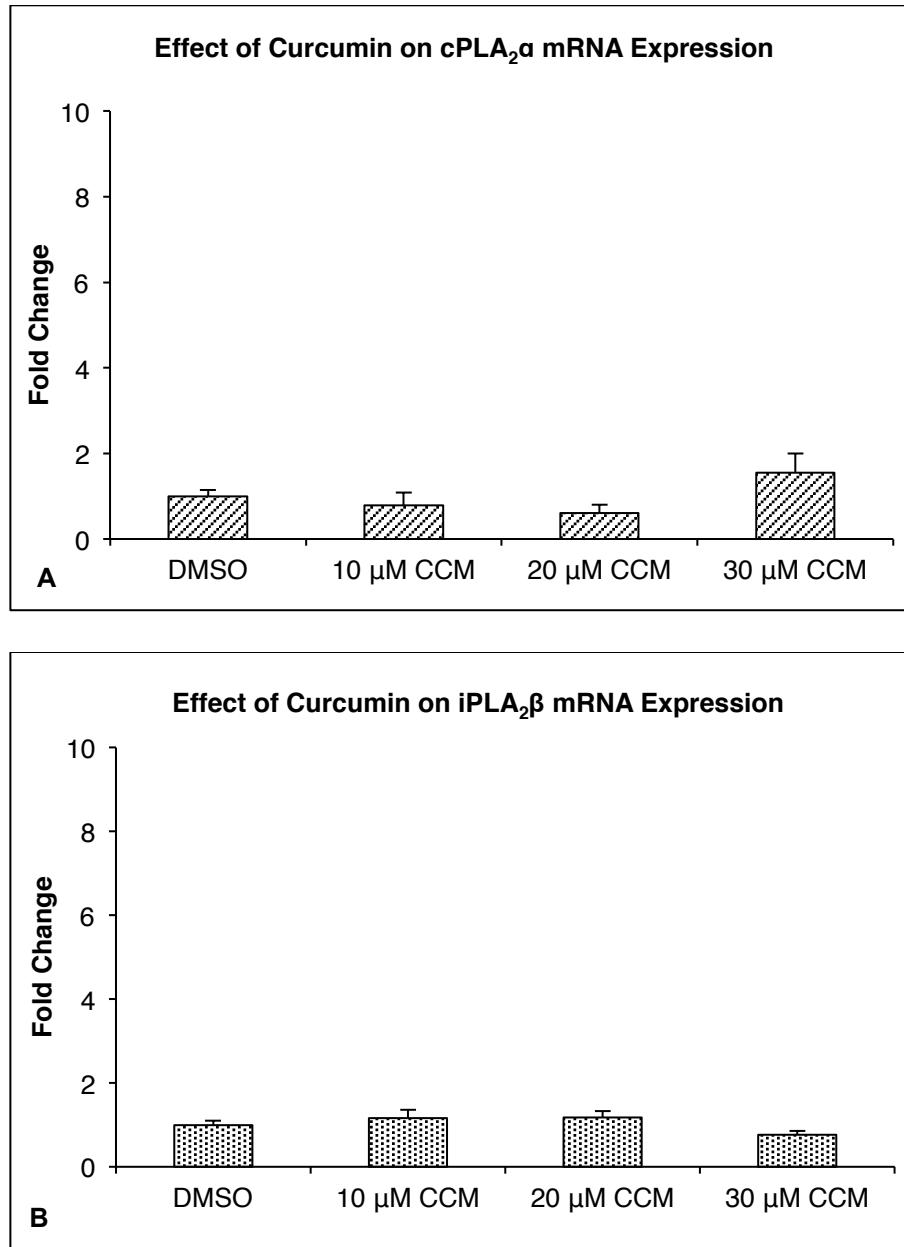
**Figure 1.3.2.2 Real-time RT-PCR analyses of (A) cPLA$_2$α, (B) iPLA$_2$ß mRNA expression after dose-dependent treatment with natural p300-specific HAT inhibitor, curcumin (CCM).** Data represent mean and standard error of four biological replicates. Statistical analysis by one-way ANOVA with Bonferroni's multiple comparison *post-hoc* test.

No significant changes in cPLA$_2$α and iPLA$_2$ß mRNA expression were observed after dose-dependent treatment with curcumin, compared to DMSO-treated vehicle controls (Fig. 1.3.2.2).

## 1.3.3 Effect of HAT and HDAC inhibitor co-treatments on cPLA$_2$ expression

### 1.3.3.1 General HAT inhibitor, anacardic acid, and general HDAC inhibitor, TSA



**Effect of Anacardic Acid and TSA on cPLA$_2$α mRNA Expression**

**B**



**C**

Quantified Fluorescence Intensity of cPLA$_2$
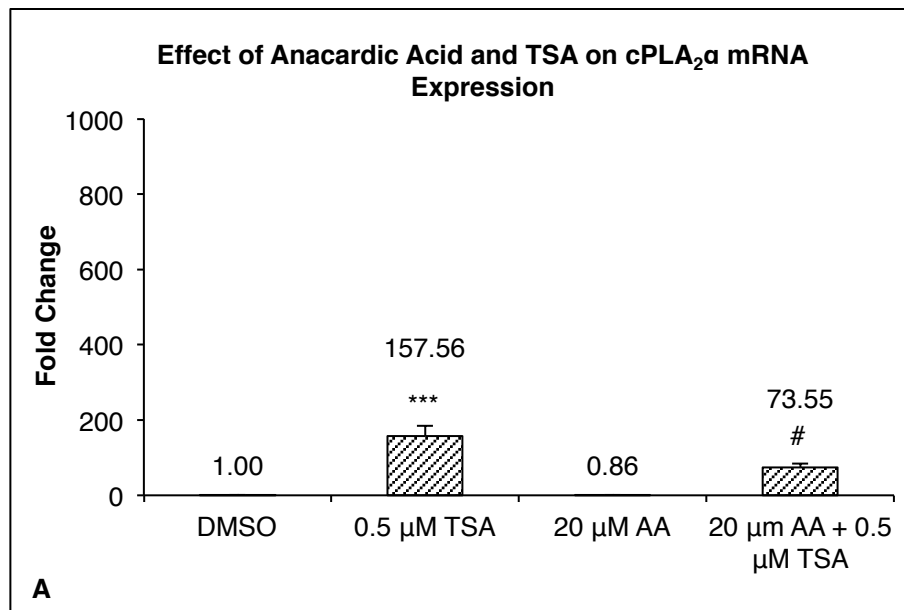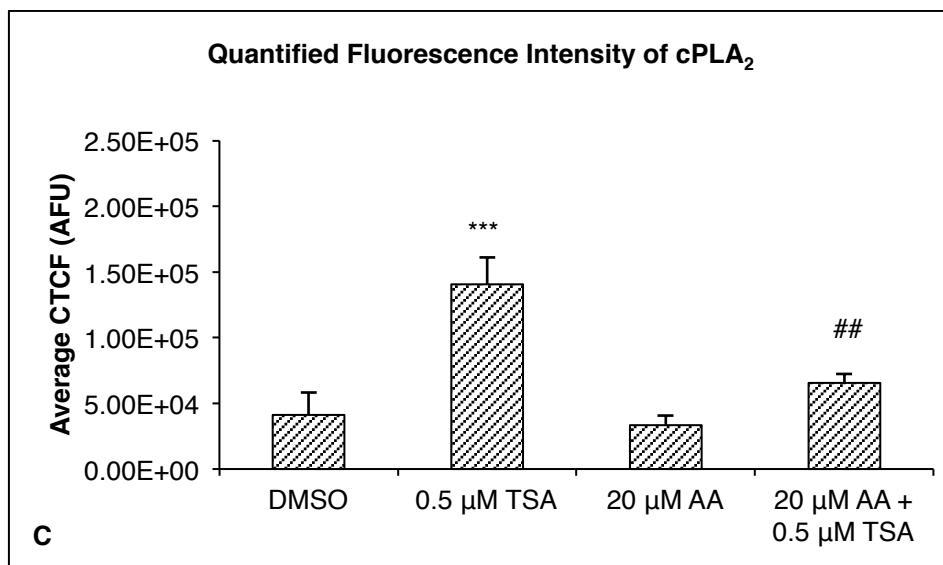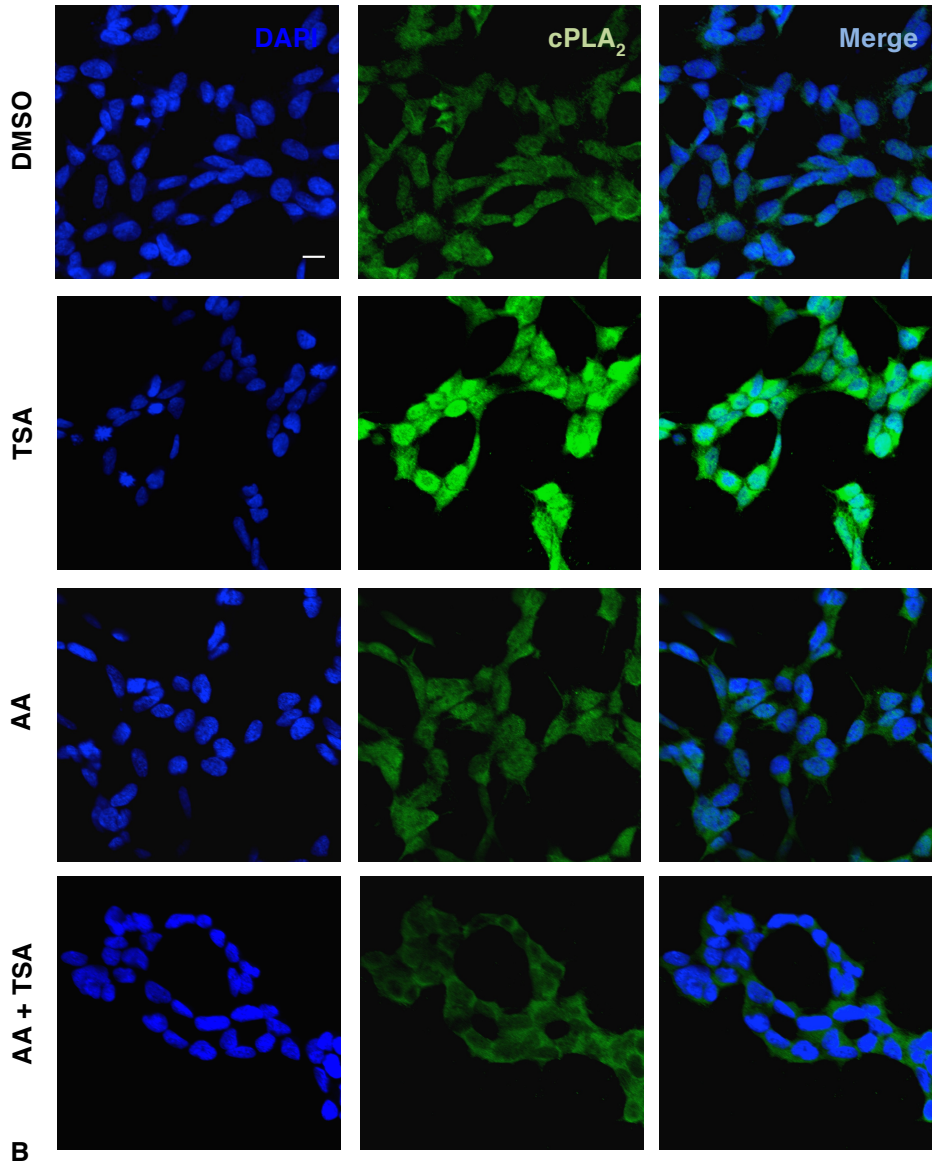
**Figure 1.3.3.1 Effect of general HAT inhibitor, anacardic acid (AA), and general HDAC inhibitor, TSA treatment. (A)** Real-time RT-PCR analyses of cPLA$_2$α mRNA expression. **(B)** Immunocytochemistry photos of cPLA$_2$ protein expression in SH-SY5Y cells after AA and TSA treatment. **(C)** Quantification of ten high-power microscopic fields from four biological replicates per group analysed and computed as average corrected total cell fluorescence (CTCF) values. Scale bar = 20 $\mu$m. AFU: arbitrary fluorescence units. Data represent mean and standard error of four biological replicates. Analysed by one-way ANOVA with Bonferroni's multiple comparison *post-hoc* test. * Indicates significant difference compared to DMSO-treated vehicle controls, *** $P < 0.001$. # indicates significant difference compared to cells treated with 0.5 $\mu$M TSA, ### $P < 0.001$.

A significant 157.6-fold increase in cPLA$_2$α mRNA expression was observed after treatment with 0.5 $\mu$M TSA, compared to DMSO-treated vehicle controls ($P < 0.001$). Interestingly, co-treatment of 20 $\mu$M anacardic acid with 0.5 $\mu$M TSA significantly suppressed the effect of TSA treatment on cPLA$_2$α mRNA expression by 53.3%, compared to cells treated with TSA only ($P = 0.0201$) (Fig. 1.3.3.1 A).

Presence of cPLA$_2$ immunoreactivity was detected in both the nucleus and cytoplasm of SH-SY5Y cells (Fig. 1.3.3.1 B). Significant increase in fluorescence intensity was detected after treatment with 0.5 $\mu$M TSA, with an average fluorescence value of (1.4 x 10$^5$ arbitrary fluorescence units (AFU)), as compared to cells in the DMSO-treated vehicle control group with average fluorescence value of (4.1 x 10$^4$ AFU) ($P < 0.001$). Fluorescence intensity remained low (3.4 x 10$^4$ AFU) after treatment with anacardic acid alone. Co-treatment of 20 $\mu$M anacardic acid with 0.5 $\mu$M TSA resulted in a significant 2-fold reduction in average fluorescence value (6.6 x 10$^4$ AFU), compared to cells treated with TSA alone ($P = 0.01$) (Fig. 1.3.3.1 B-C).

### 1.3.3.2      Specific HAT inhibitors and general HDAC inhibitor, TSA
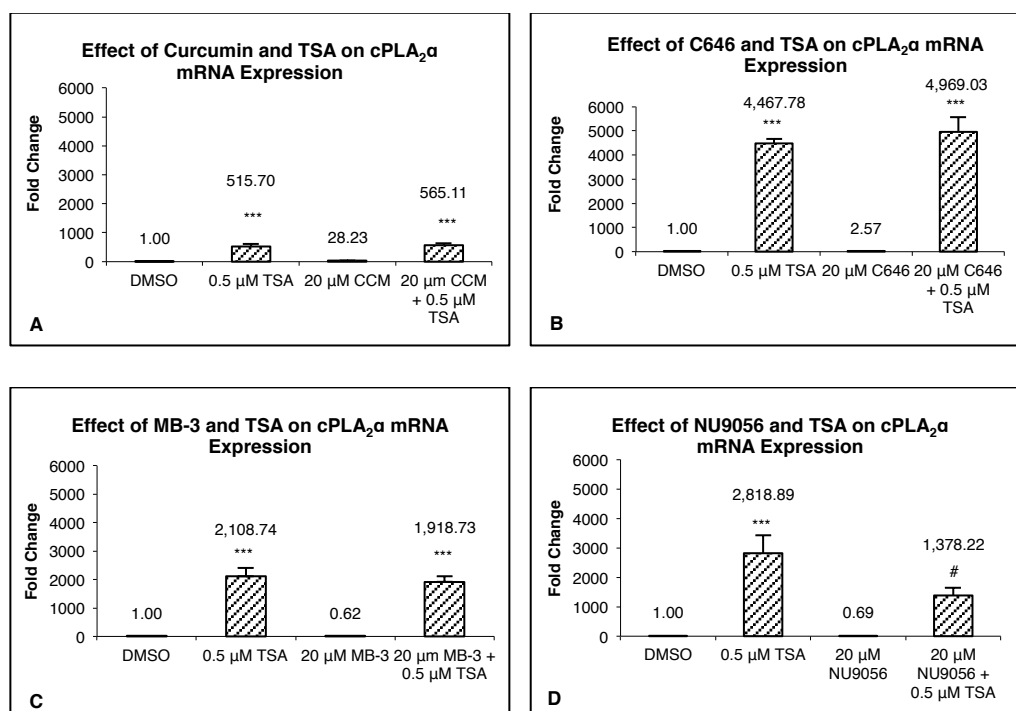


**Figure 1.3.3.2 Real-time RT-PCR analyses of cPLA$_2$α mRNA expression after treatment with specific HAT inhibitors. (A)** Natural p300-specific inhibitor CCM and TSA, **(B)** Synthetic p300-specific inhibitor C646 and TSA, **(C)** GCN5 inhibitor MB-3 and TSA, (D) Tip60 inhibitor NU9056 and TSA. Data represent mean and standard error of four biological replicates. Analysed by one-way ANOVA with Bonferroni's multiple comparison *post-hoc* test. * Indicates significant difference compared to DMSO-treated vehicle controls, *** $P < 0.001$. # Indicates significant difference compared to cells treated with 0.5 μM TSA, # $P < 0.05$.

Significant increases in cPLA$_2$α mRNA expression were observed in cells treated with 0.5 *μ*M TSA, compared to DMSO-treated vehicle controls ($P < 0.001$). However, co-treatment of 20 μM curcumin, 20 *μ*M C646, and 20 *μ*M MB-3 with 0.5 *μ*M TSA did not suppress cPLA$_2$α mRNA expression (Fig. 1.3.3.2 A-C).

For the experiment using Tip60-specific HAT inhibitor, NU9056, a significant 2820-fold increase in cPLA$_2$α expression was observed after treatment with 0.5 *μ*M TSA, compared to DMSO-treated vehicle controls ($P <$

0.001) (Fig. 1.3.3.2 D). Interestingly, co-treatment of 20 $\mu$M NU9056 with 0.5 $\mu$M TSA significantly suppressed the effect of TSA treatment on cPLA$_2$α mRNA expression by 51.1%, compared to cells treated with TSA only ($P$ = 0.043) (Fig. 1.3.3.2 D).

### 1.3.3.3      Tip60-specific HAT inhibitor NU9056 and class I-specific HDAC inhibitor, MS-275



A



B

**Effect of MS-275 and NU9056 on cPLA$_2$ Protein Expression**

C



D
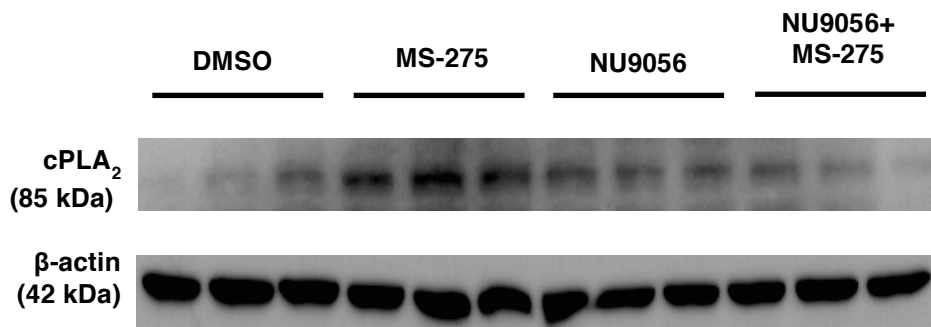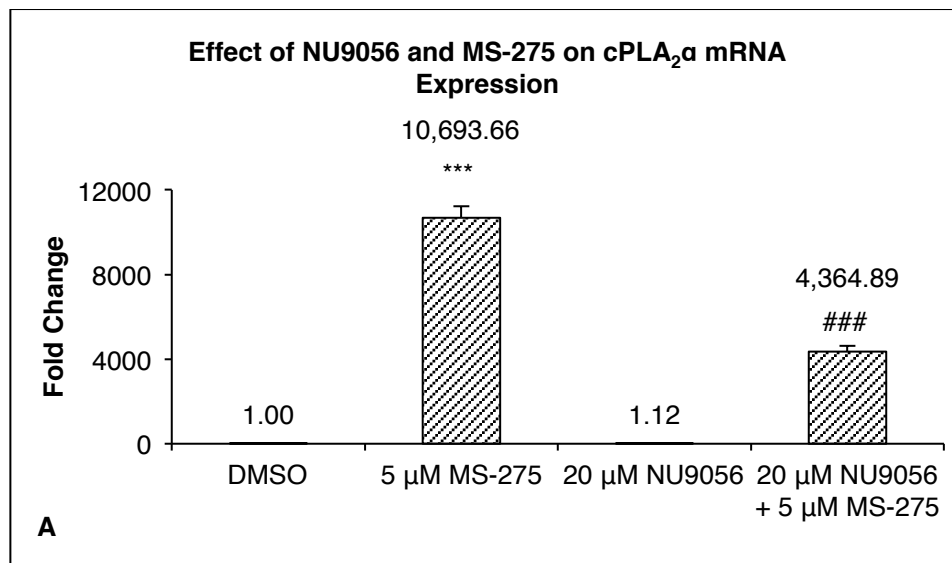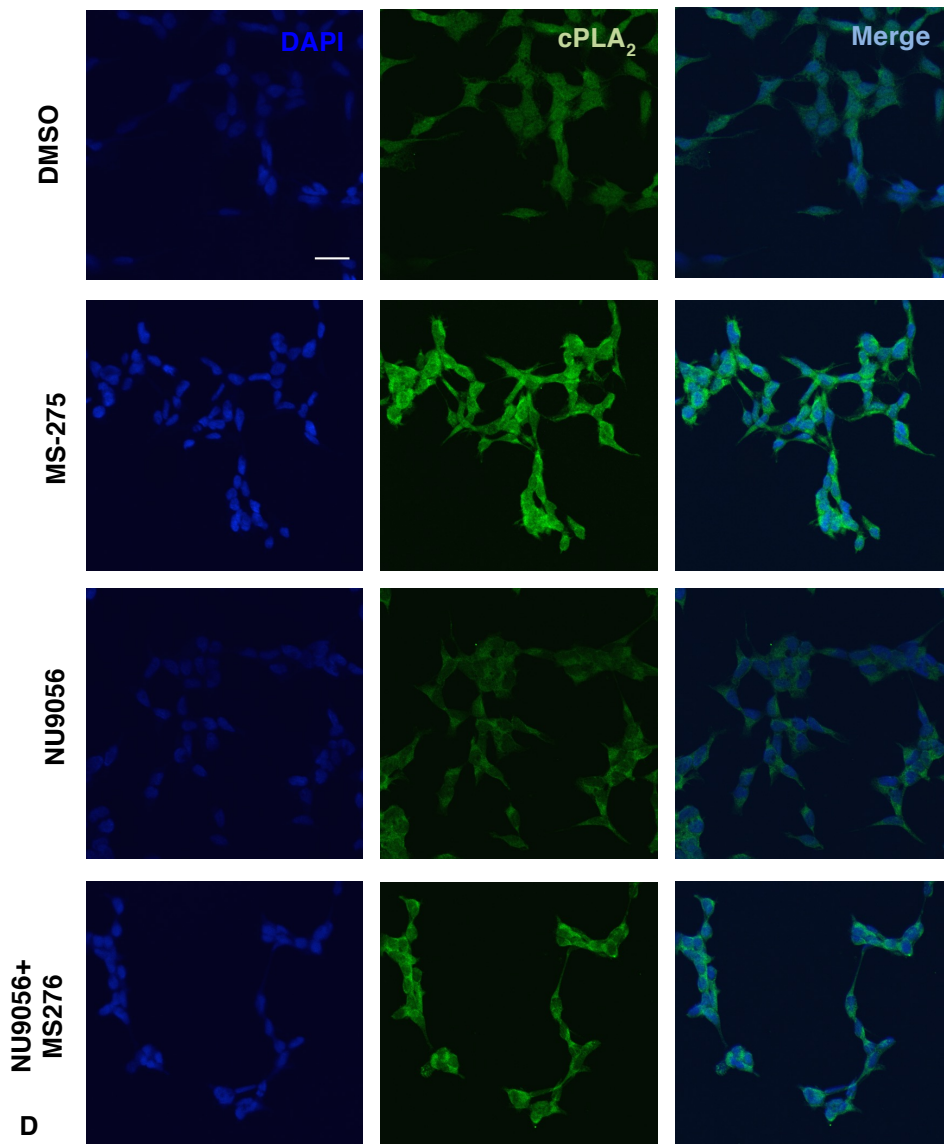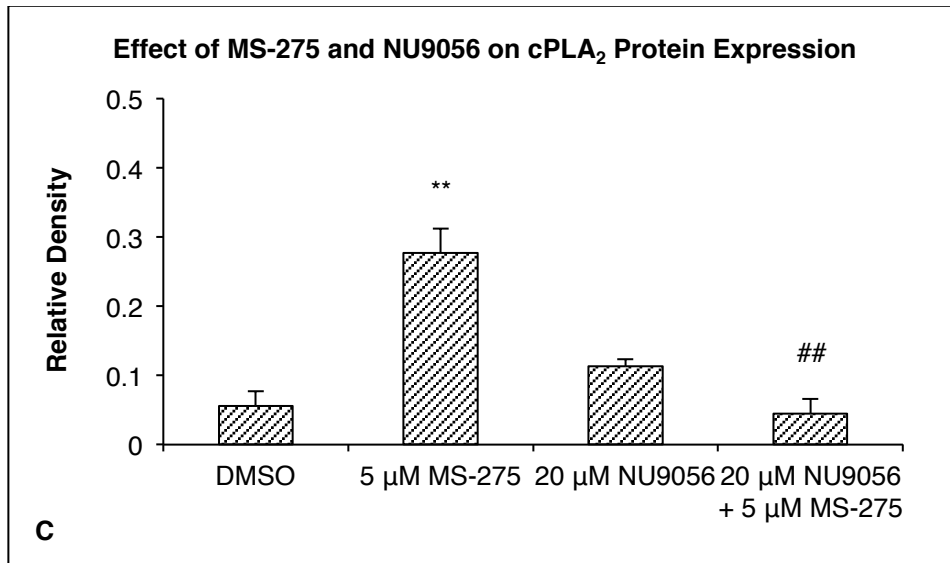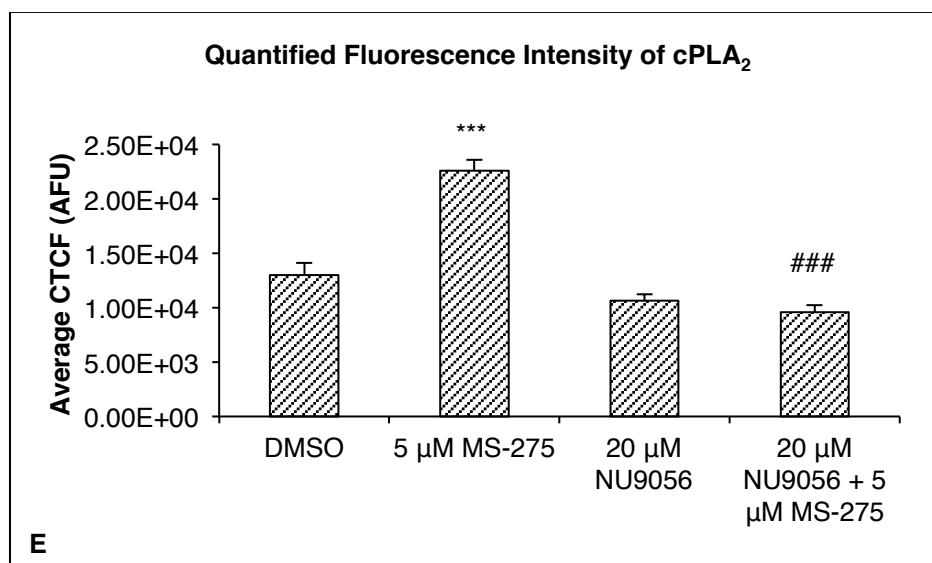
**Figure 1.3.3.3 Effect of Tip60-specific HAT inhibitor NU9056 and class I-specific HDAC inhibitor, MS-275 treatment. (A)** Real-time RT-PCR analyses of cPLA$_2$α mRNA expression. **(B)** Western blot of cPLA$_2$ protein expression after NU9056 and MS-275 treatment. **(C)** Densitometric analysis of the effect of NU9056 and MS-275 treatment on cPLA$_2$ protein expression. **(D)** Immunocytochemistry photos of cPLA$_2$ protein expression after NU9056 and MS-275 treatment. **(E)** Quantification of ten high-power microscopic fields from four biological replicates per group, analysed and computed as average corrected total cell fluorescence (CTCF) values. Scale bar = 20 $\mu$m. AFU: arbitrary fluorescence units. All data represent the mean and standard error of four biological replicates, analysed by one-way ANOVA with Bonferroni's multiple comparison *post-hoc* test. * Indicates significant difference compared to the DMSO-treated vehicle controls, ** $P < 0.01$, *** $P < 0.001$. [#] indicates significant difference compared to cells treated with 5 $\mu$M MS-275, [##] $P < 0.01$, [###] $P < 0.001$.

A significant 10,700-fold increase in cPLA$_2$α mRNA expression was observed after treatment with 5 $\mu$M MS-275, compared to DMSO-treated vehicle controls ($P < 0.001$). Co-treatment of 20 $\mu$M NU9056 with 5 $\mu$M MS-275 significantly suppressed the effect of MS-275 treatment on cPLA$_2$α mRNA expression by 59.2%, compared to cells treated with MS-275 only ($P < 0.001$) (Fig. 1.3.3.3 A).

Western blot analysis detected a single band of ~85 kDa (Fig. 1.3.3.3 B). Significant increases in relative densities were detected in the MS-275-

treated group, compared to DMSO-treated controls ($P = 0.01$) (Fig. 1.3.3.3 C).

20 $\mu$M NU9056 treatment alone did not show significant changes from the control group, while co-treatment of 20 $\mu$M NU9056 with 5 $\mu$M MS-275 showed significantly lower relative densities, compared to cells treated with MS-275 alone ($P = 0.01$) (Fig. 1.3.3.3 C).

Presence of cPLA$_2$ immunoreactivity was detected in both the nucleus and cytoplasm of SH-SY5Y cells (Fig. 1.3.3.3 D). Significant increase in fluorescence intensity was detected after treatment with 5 $\mu$M MS-275, with an average fluorescence value of ($2.3 \times 10^4$ AFU), as compared to cells in the DMSO-treated vehicle control groups with average fluorescence value of ($1.3 \times 10^4$ AFU) ($P < 0.001$). Fluorescence intensity remained low ($1.1 \times 10^4$ AFU) after treatment with NU9056 alone. Co-treatment of 20 $\mu$M NU9056 with 5 $\mu$M MS-275 resulted in a larger than 2-fold reduction in average fluorescence value ($9.6 \times 10^3$ AFU), compared to cells treated with MS-275 alone ($P < 0.001$) (Fig. 1.3.3.3 D-E).

### 1.3.4 Effect of general HMT inhibitor, MTA and general HDAC inhibitor, TSA co-treatments on cPLA$_2$ expression

**Effect of MTA and TSA on cPLA$_2$α mRNA Expression**

1,884.79
***

763.66
##

1.00

1.22

Fold Change

DMSO    0.5 µM TSA    200 µM MTA    200 µM MTA +
0.5 µM TSA

A

|  | DMSO | TSA | MTA | MTA + TSA |

cPLA$_2$
(85 kDa)

β-actin
(42 kDa)

B

**Effect of MTA and TSA on cPLA$_2$ Protein Expression**

***

##

Relative Density

DMSO    0.5 µM TSA    200 µM MTA    200 µM MTA +
0.5 µM TSA

C
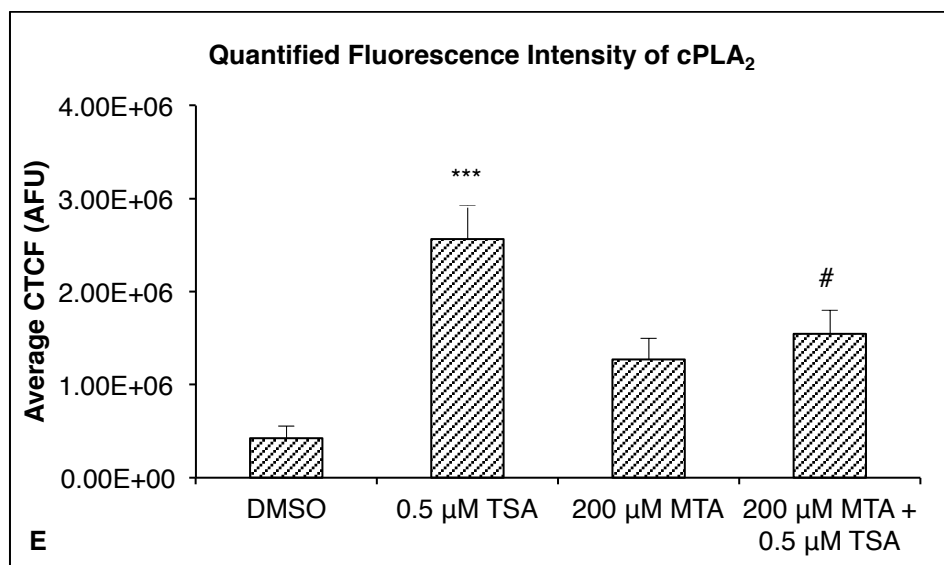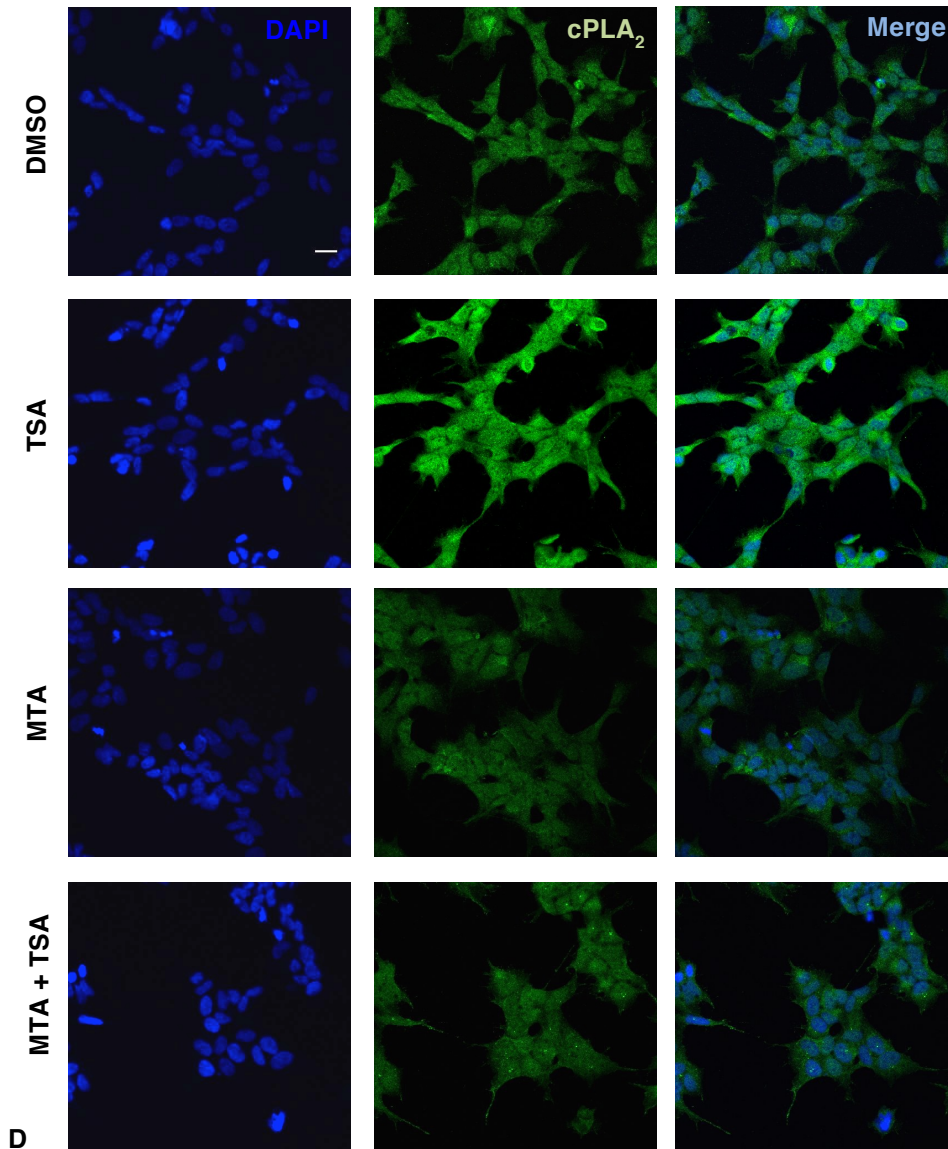
**Figure 1.3.4 Effect of HMT inhibitor MTA and general HDAC inhibitor, TSA on cPLA$_2$ expression. (A)** Real-time RT-PCR analyses of cPLA$_2$α mRNA expression. **(B)** Western blot of cPLA$_2$ protein expression after MTA and TSA treatment. **(C)** Densitometric analysis of the effect of MTA and TSA treatment on cPLA$_2$ protein expression. **(D)** Immunocytochemistry photos of cPLA$_2$ protein expression in SH-SY5Y cells after MTA and TSA treatment. **(E)** Quantification of ten high-power microscopic fields from four biological replicates per group, analysed and computed as average corrected total cell fluorescence (CTCF) values. Scale bar = 20 $\mu$m. AFU: arbitrary fluorescence units. All data represent the mean and standard error of four biological replicates, analysed by one-way ANOVA with Bonferroni's multiple comparison *post-hoc* test. * Indicates significant difference compared to the DMSO-treated vehicle controls, ** $P < 0.01$, *** $P < 0.001$. [#] indicates significant difference compared to cells treated with 0.5 µM TSA [#] $P < 0.05$, [##] $P < 0.01$, [###] $P < 0.001$.
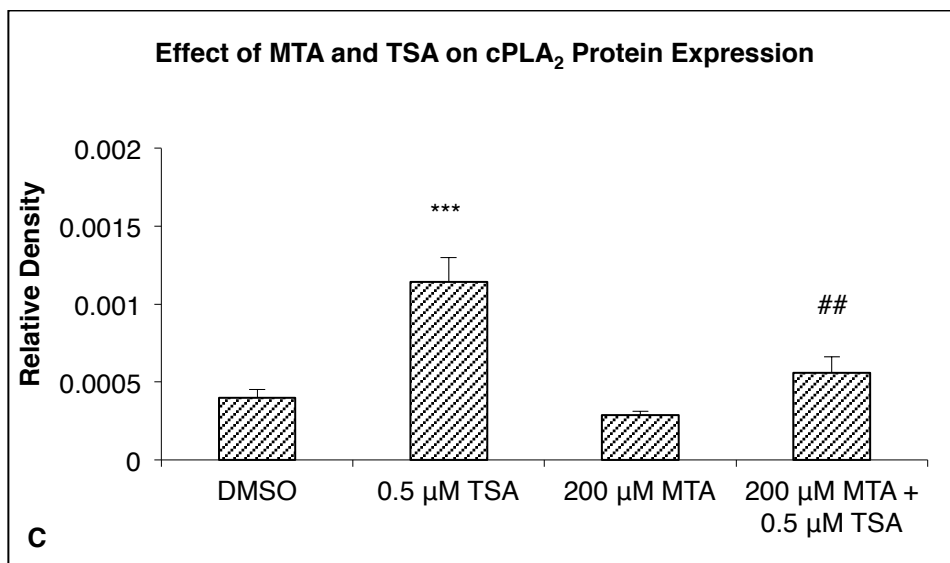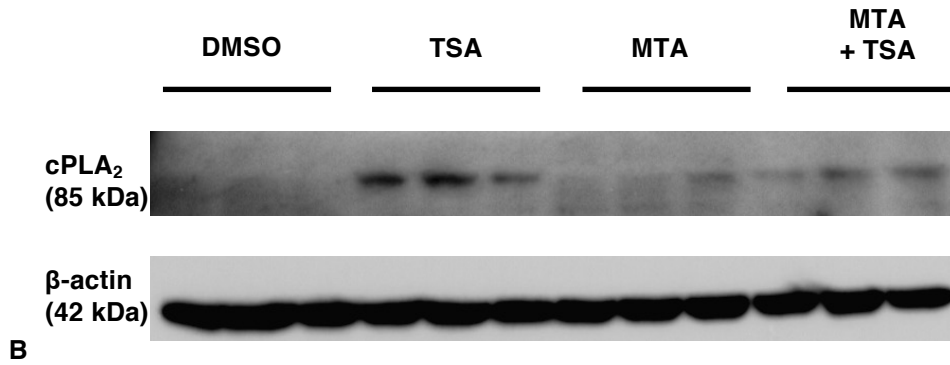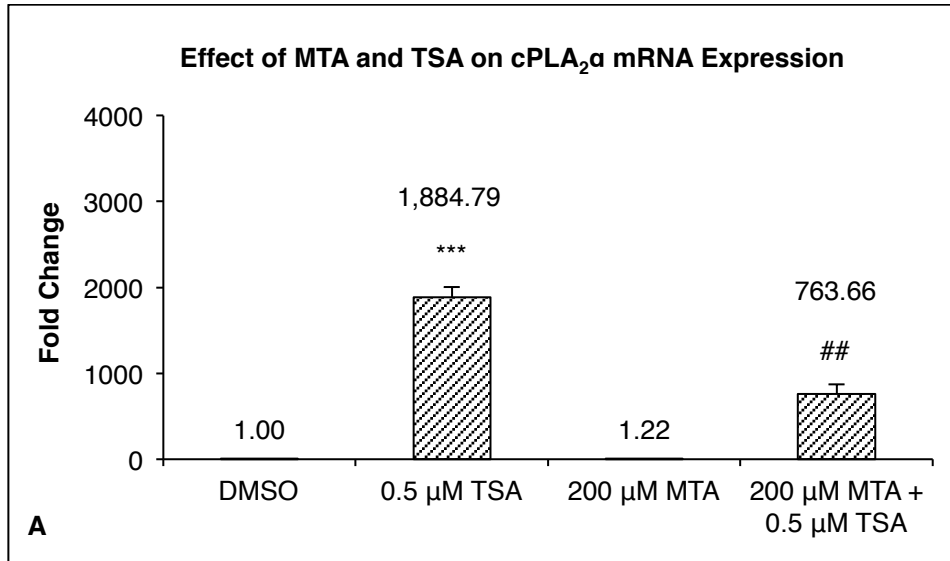
A significant 1885-fold increase in cPLA$_2$α mRNA expression was observed in TSA-only treated groups, compared to DMSO-treated vehicle controls ($P < 0.001$). Co-treatment of 200 $\mu$M MTA with 0.5 $\mu$M TSA significantly suppressed the effect of TSA treatment by 59.5%, compared to cells treated with TSA only ($P = 0.004$) (Fig. 1.3.4 A).

A single band of ~85 kDa was detected via Western blot (Fig. 1.3.4 B). Significant increases in relative densities were detected in the TSA-treated group, compared to DMSO-treated vehicle controls ($P < 0.001$) (Fig. 1.3.4 C). NU9056 treatment alone did not show significant changes from the control group, while co-treatment of 200 $\mu$M MTA with 0.5 $\mu$M TSA showed significantly lower relative densities, compared to cells treated with TSA alone ($P < 0.01$) (Fig. 1.3.4 B-C).

Presence of cPLA$_2$ immunoreactivity was detected in both the nucleus and cytoplasm of SH-SY5Y cells (Fig. 1.3.4 D). Significant increase in fluorescence intensity was detected after treatment with 0.5 $\mu$M TSA, with an average fluorescence value of (2.6 x 10$^6$ AFU), as compared to cells in the

DMSO-treated vehicle control groups with average fluorescence value of (4.3 x $10^5$ AFU) ($P < 0.001$). Fluorescence intensity remained low (1.3 x $10^6$ AFU) after treatment with MTA alone. Co-treatment of 200 $\mu$M MTA with 0.5 $\mu$M TSA resulted in a significant reduction in average fluorescence value of (1.6 x $10^6$ AFU), compared to cells treated with TSA alone ($P = 0.039$) (Fig. 1.3.4 D-E).

### 1.3.5 ChIP-qPCR

### 1.3.5.1 Analysis of shearing efficiency
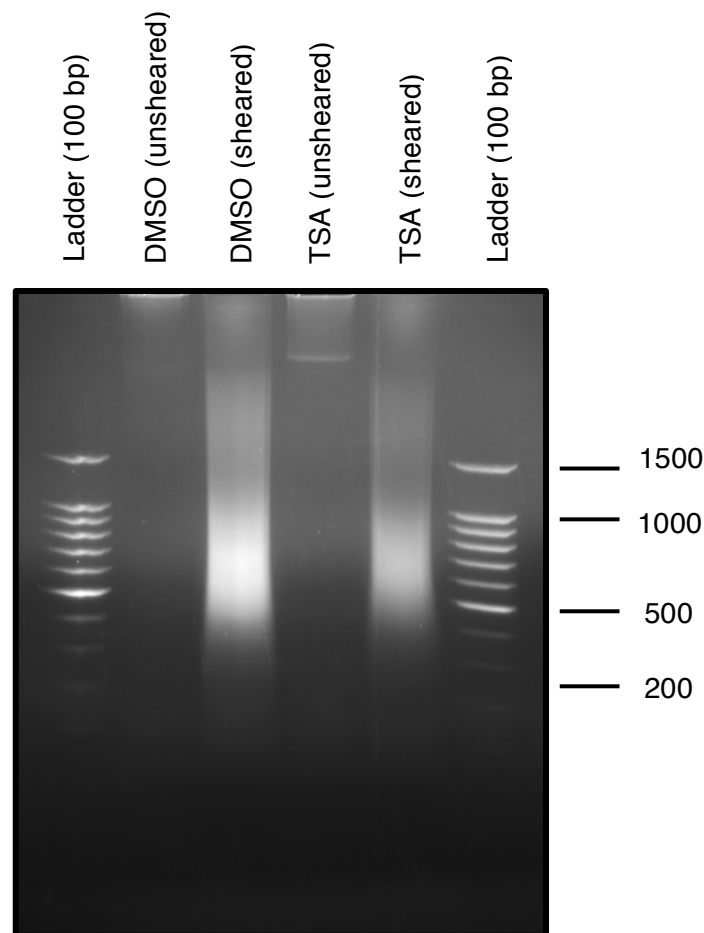


**Fig. 1.3.5.1 Shearing efficiency of DMSO control and TSA-treated chromatin analysed on 1.5% agarose gel.** Lanes (left to right; 1-6): 100 bp ladder; unsheared DMSO control sample; sheared DMSO control sample; unsheared TSA control sample; sheared TSA control sample; 100 bp ladder. Unsheared samples were analysed together as controls.

Sheared DNA obtained from SH-SY5Y cells showed smear ranging from 200-800 base pairs (lanes 3 and 5), compared to unsheared controls (lanes 2 and 4) (Fig. 1.3.5.1).

### 1.3.5.2        Primer design
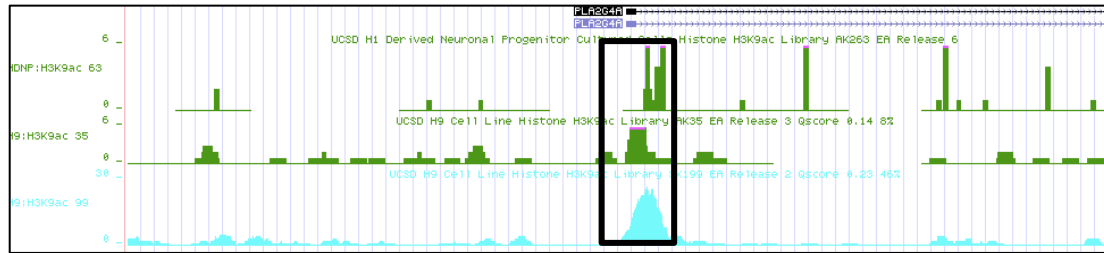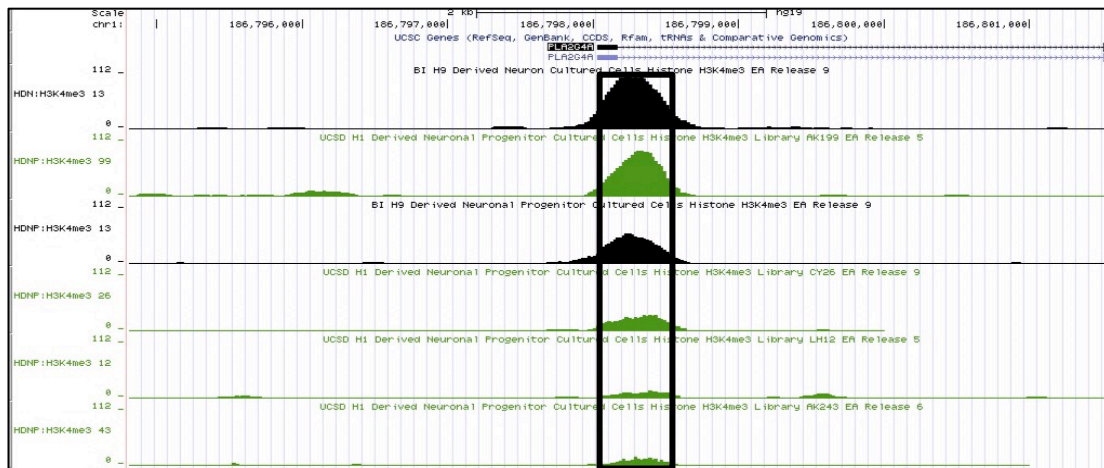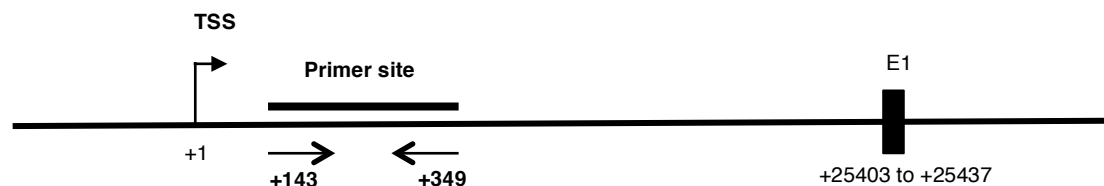


**Fig. 1.3.5.2 University of California Santa Cruz (UCSC) genome browser screenshots and loci of primer design. (A)** H3K9ac and **(B)** H3K4me3 profiles in cPLA$_2$α genome of H9 derived neuron cultured cells and H1 derived neuronal progenitor cultured cells. Box indicates histone-enriched region where primer design targeted. **(C)** Illustration showing loci where ChIP primers were designed based on alignment output: +143 to +349 downstream of the transcriptional start site of the cPLA$_2$α gene. TSS: transcriptional start site of cPLA$_2$α gene; E1: exon 1 of cPLA$_2$α gene.

Sequence alignment of histone-enriched regions in two cell types of neuronal origin showed H3K9ac-rich (Fig. 1.3.5.2 A) and H3K4me3-rich (Fig. 1.3.5.2 B) islands at the proximal promoter regions (1 kb upstream and downstream of transcriptional start site). The localisation of H3K9ac histones showed less specificity, while the localisation of H3K4me3 was found to be more distinct (boxed region, +143 to +349 from transcriptional start site). Primers were designed at +143 to +349 base pairs downstream from transcriptional start site, according to the consistent peaks detected (Fig. 1.3.5.2 C).

### 1.3.5.3    ChIP-qPCR



A
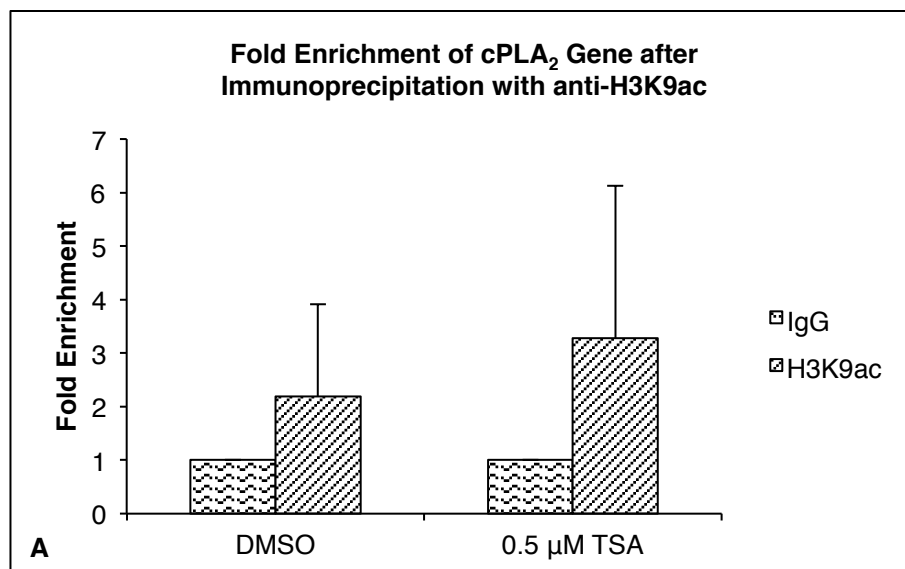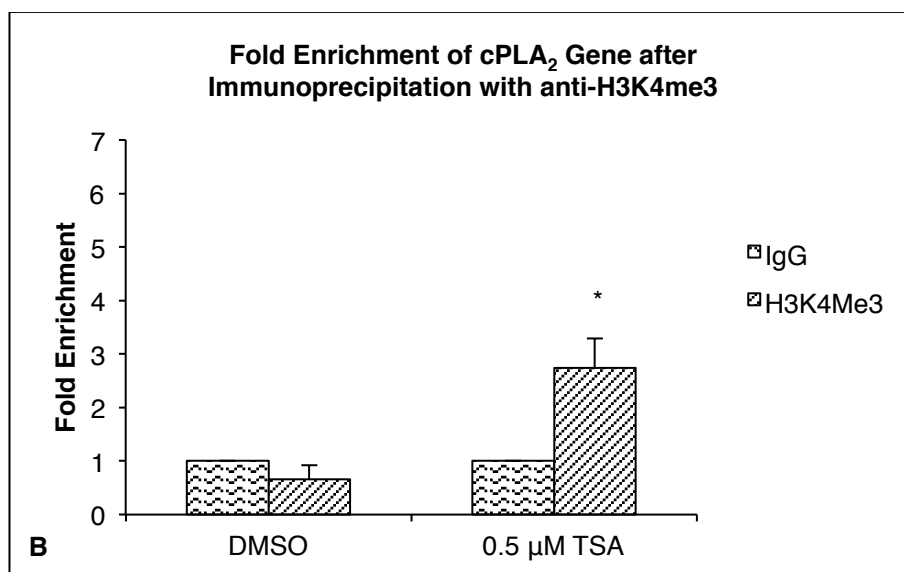
**Fig 1.3.5.3 Chromatin immunoprecipitation (ChIP) assay results. Fold enrichment of human cPLA$_2$α gene region (+143 to +349) after immunoprecipitation with (A) anti-H3K9 acetylated (H3K9ac) and (B) anti-H3K4 trimethylated (H3K4me3) antibodies.** Chromatin was immunoprecipitated using an anti-trimethyl-H3K4 and or anti-acetyl-H3K9 antibody followed by quantitative real-time PCR of the purified DNA. Immunoprecipitation with an antibody against IgG was used as a negative control. One percent of the precipitated chromatin was assayed to verify equal loading (Input). Data were normalised to IgG threshold ($C_T$) values and reported as fold enrichment of control (IgG) binding to site. Data represent the mean and standard error of three biological replicates. * Indicates significant difference compared to DMSO-vehicle controls, by Student's *t-test*, where $P < 0.05$.

No significant fold enrichment of the cPLA$_2$α promoter region was observed upon immunoprecipitation with the anti-H3K9ac antibody after TSA treatment, compared to DMSO-treated controls (Fig. 1.3.5.3 A). However, a significant 2.7-fold increase in fold enrichment of the cPLA$_2$α promoter region was observed upon immunoprecipitation with the anti-H3K4me3 antibody, compared to DMSO-treated controls ($P = 0.041$) (Fig. 1.3.5.3 B).

### 1.3.6  Detection of H3K9 acetylation
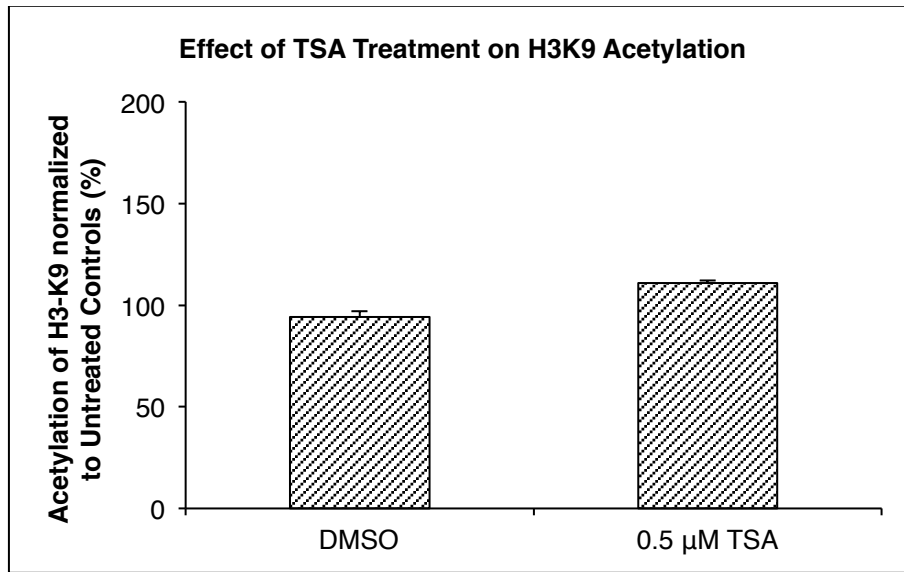


**Fig. 1.3.6 Percentage of acetylated H3K9 residues detected in cells, compared to untreated controls.** Data represent the mean and standard error of four biological replicates. Statistical significance analysed by Student's *t-test*.

No significant change in percentage acetylation of H3K9 was detected after TSA treatment (Fig. 1.3.6).

### 1.3.7  Lactate dehydrogenase assay

**Effect of MTA and TSA on LDH Release**



**Effect of AACOCF$_3$ and TSA on LDH Release**
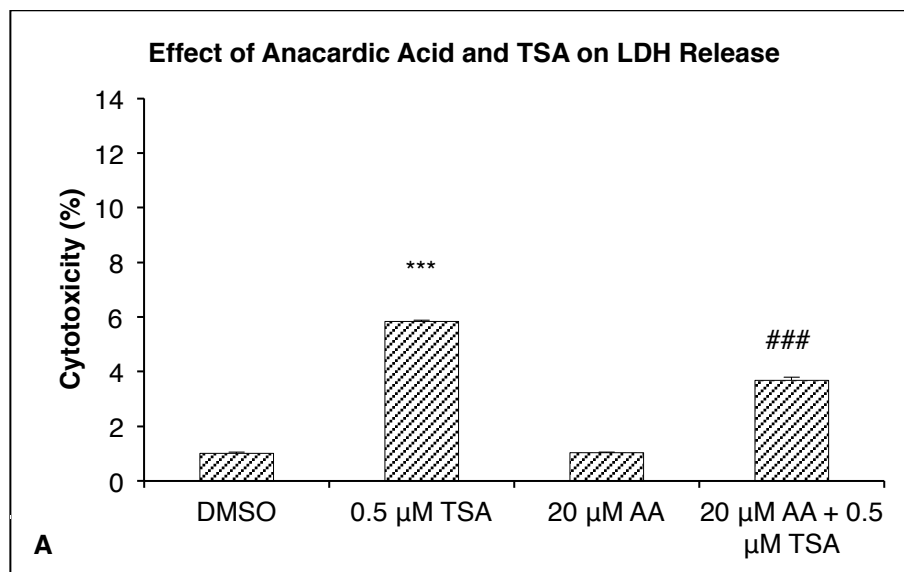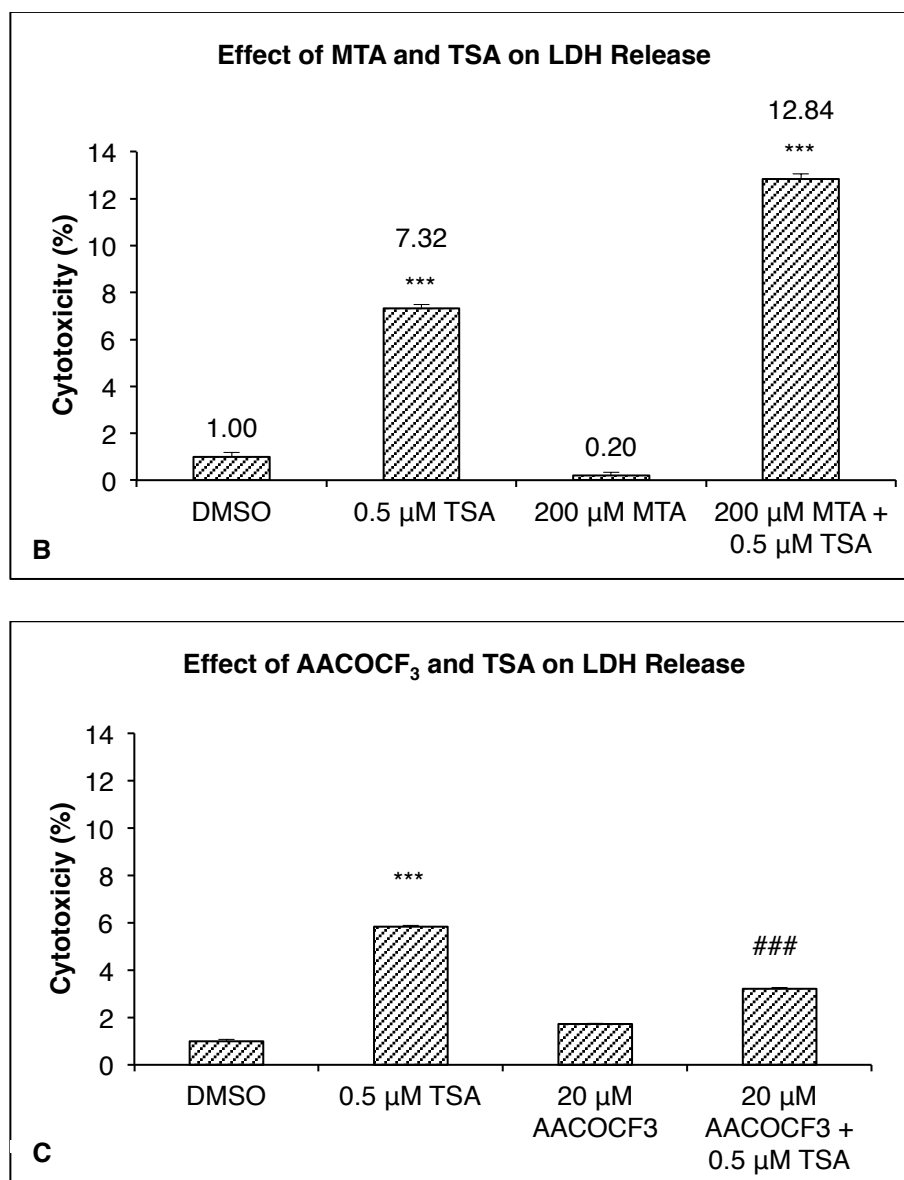
**Fig. 1.3.7 Measurement of lactate dehydrogenase (LDH) activity. (A)** Effect of anacardic acid (AA) and TSA on LDH release. **(B)** Effect of MTA and TSA on LDH release. **(C)** Effect of AACOCF$_3$ and TSA on LDH release. Analysed by one-way ANOVA with Bonferroni's multiple comparison *post-hoc* test. * Indicates significant difference compared to the vehicle-treated group, *** $P < 0.001$. [#] Indicates significant difference compared to cells treated with 0.5 $\mu$M TSA, [###] $P < 0.001$.

Significant increase in cytotoxicity by 5.8-fold was observed after 0.5 $\mu$M TSA treatment ($P < 0.001$). Co-treatment of 20 $\mu$M anacardic acid with 0.5 $\mu$M TSA caused a decrease in cytotoxicity by 36.8%, compared to cells treated with TSA only ($P = 0.001$) (Fig. 1.3.7 A). Co-treatment of 200 $\mu$M MTA

with 0.5 $\mu$M TSA exacerbated cytotoxicity, compared to cells treated with TSA only (Fig. 1.3.7 B). Co-treatment of 20 $\mu$M AACOCF$_3$ with 0.5 $\mu$M TSA significantly abrogated cell death and increased cell viability by 60%, compared to cells treated with TSA only ($p < 0.001$) (Fig. 1.3.7 C).

## 1.4    Discussion

The present study was performed to examine the epigenetic regulation of cPLA$_2$ in SH-SY5Y human neuroblastoma cells. An initial screening was performed to elucidate the effects of TSA, a general HDAC inhibitor of class I, IIa, IIb and IV HDACs (Chuang et al., 2009), on mRNA expression of PLA$_2$ isoforms. Results showed dose-dependent upregulation of cPLA$_2\alpha$ and iPLA$_2\beta$ isoforms after TSA treatment, but to a much larger extent for cPLA$_2\alpha$ compared to iPLA$_2$ß. This is consistent with current knowledge that TSA alters the expression of only ~2% of genes (Van Lint et al., 1996). In view of the large increases in cPLA$_2\alpha$ mRNA expression after TSA treatment, we investigated the effects of more specific HDAC inhibitors on cPLA$_2\alpha$ expression. Different classes of HDACs include class I, II and IV zinc-dependent enzymes and class III zinc-independent enzymes, classified based on their homology to yeast HDACs and organization of protein domains (de Ruijter et al., 2003, Chuang et al., 2009). Class I HDACs comprise HDAC1, 2, 3, and 8, due to their homology to yeast RPD3 HDACs (Chuang et al., 2009, Delcuve et al., 2012b). Class II HDACs are related to yeast HDA1 HDACs and are sub-divided into class IIa and class IIb (Chuang et al., 2009, Delcuve et al., 2012b). Class IIa includes HDAC4, 5, 7 and 9 while class IIb comprise

HDAC6 and 10 (Chuang et al., 2009, Delcuve et al., 2012b). Class I HDACs are nuclear enzymes mainly involved in cell proliferation and survival (Luo et al., 2009, Marks, 2010). In our study, we used the class I and IIa HDAC inhibitor, VPA (Gurvich et al., 2004), the HDAC6-specific inhibitor, tubacin (Haggarty et al., 2003) and the class I HDAC inhibitor, MS-275 (Khan et al., 2008, Kennedy et al., 2013, Beharry et al., 2014). As with TSA, treatment with all three inhibitors resulted in dose-dependent $cPLA_2\alpha$ mRNA upregulation. However, VPA treatment induced $iPLA_2\beta$ mRNA downregulation, possibly because VPA downregulates sterol regulatory element binding protein (SREBP) that in turn reduces $iPLA_2\beta$ expression (Lagace and Nachtigal, 2004). Tubacin induced small increases in both $cPLA_2\alpha$ and $iPLA_2\beta$ expression, indicating that HDAC6 plays a relatively small role in $cPLA_2\alpha$ and $iPLA_2\beta$ expression. MS-275 induced the largest increase in $cPLA_2\alpha$ expression, suggesting that class I HDACs play the most significant role in epigenetic regulation of $cPLA_2\alpha$. In contrast, no changes were found in $iPLA_2\beta$ expression after MS-275 treatment. Results show that $cPLA_2\alpha$ but not $iPLA_2\beta$ is differentially affected by class I HDACs.

We next explored the role of HAT inhibitors in regulation of $cPLA_2$. Treatment with the general HAT inhibitor anacardic acid and the p300-specific HAT inhibitor CCM by itself at several doses did not induce changes in $cPLA_2\alpha$ and $iPLA_2\beta$ mRNA expression. In contrast, co-treatment of cells with anacardic acid and TSA significantly reduced upregulation of $cPLA_2\alpha$ induced by TSA. The mRNA changes were reflected at the protein level as shown by immunocytochemistry, whereby increased $cPLA_2$ immunofluorescence was

observed after TSA treatment, but was suppressed in cells that were co-treated with anacardic acid and TSA. This suggests that HAT-activating processes are involved in TSA-induced cPLA$_2$α expression. Anacardic acid is a general inhibitor of 3 classes of HATs, namely, p300/CBP, GCN5/PCAF and Tip60/MYST (Roth et al., 2001, Balasubramanyam et al., 2003, Sun et al., 2006b, Cui et al., 2008). These 3 classes of HATs are classified based on sequence homology, protein structure and substrate specificity (Kuo and Allis, 1998). We next sought to investigate which HAT was selectively involved in regulation of cPLA$_2$α expression. Treatment of cells with CCM, a natural p300 HAT inhibitor (Marcu et al., 2006); C646, the pharmacological p300 inhibitor (Santer et al., 2011); and MB-3, the GCN5 inhibitor (Biel et al., 2004), did not suppress cPLA$_2$α upregulation induced by TSA. This suggests that the p300/CBP and GCN5/PCAF classes of HATs were minimally or not involved in the suppression of cPLA$_2$α upregulation. In contrast, treatment of cells with the Tip60-specific HAT inhibitor NU9056 (Coffey et al., 2012) led to significant reduction of TSA-induced upregulation of cPLA$_2$α mRNA expression, suggesting the role of Tip60 in cPLA$_2$α expression.

We further elucidated that NU9056 inhibited MS-275-induced upregulation of cPLA$_2$α mRNA, indicating that the *class I HDACs* and the *Tip60 HAT* are specific enzymes involved in epigenetic regulation of cPLA$_2$. HDAC inhibitors TSA and MS-275 induce acetylation of H3K9, H3K14, and trimethylation of H3K4 (Sike et al., Martinez-Diaz et al., 2010, Huang et al., 2011, Coffey et al., 2012, Kennedy et al., 2013) (Table I). The inhibition of the Tip60 HAT by the synthetic compound, NU9056, has been reported to cause

reduction in acetylation levels of H3K14, H4K8 and H4K16 (Coffey et al., 2012) (Table I). Therefore, one possibility by which MS-275 increase $cPLA_2\alpha$ mRNA expression may be via increased acetylation of H3K14, which is in turn suppressed by NU9056, resulting in reduced $cPLA_2\alpha$ expression. Western blots showed increased $cPLA_2$ protein expression after MS-275 treatment, and that co-treatment with the Tip60 HAT inhibitor, NU9056, reduced the increase. Immunocytochemistry also showed increased $cPLA_2$ immunofluorescence after MS-275 treatment, which was suppressed in cells that were co-treated with NU9056 and MS-275. Since Tip60 HAT inhibition suppresses $cPLA_2$ expression, it could imply that Tip60 has the potential to increase $cPLA_2\alpha$ expression at the *transcriptional* level. Our findings add to previous studies, which showed that a splice variant of Tip60, $cPLA_2$-interacting protein (PLIP) can interact with $cPLA_2$ at the *protein* level to induce apoptosis (Sheridan et al., 2001).

Although TSA is widely known to increase H3K9 *acetylation*, it is also known to induce *trimethylation* of H3K4 to cause transcriptional activation of genes (Nightingale et al., 2007, Pufahl et al., 2012, Wu et al., 2012b, a). Since trimethylated H3K4 is often associated with acetylated H3K9 histones in activated genes (Nightingale et al., 2007), we investigated the possibility of increased H3K4 trimethylation after TSA treatment. The histone methyltransferase (HMT) inhibitor MTA was used to investigate the effect of H3K4-trimethylation inhibition on TSA-induced $cPLA_2\alpha$ expression, since it effectively reduces trimethylation of H3K4 (Huang et al., 2006, El Mansouri et al., 2011). Quantitative RT-PCR analyses showed that treatment with MTA

reduced TSA-induced increase in cPLA$_2$α expression. Western blots showed that TSA treatment increased cPLA$_2$ protein expression, and this increase was modulated by the HMT inhibitor, MTA. Immunocytochemistry also showed increased cPLA$_2$ immunofluorescence after TSA treatment, which was suppressed in the cells that were co-treated with MTA and TSA. Together, results indicate that cPLA$_2$ can be regulated by histone methylation as well as histone acetylation.

We next explored the site on the cPLA$_2$α promoter, in which the above epigenetic changes might occur by chromatin immunoprecipitation (ChIP). Sheared DNA obtained from lyzed SH-SY5Y cells showed a smear ranging from 200-800 base pairs, compared to unsheared controls, indicating successful sonication of samples for downstream immuoprecipitation. ChIP-sequencing data obtained from the *Human Epigenome Atlas* on cell types most similar to SH-SY5Y cells showed no distinct genetic loci rich in H3K9ac on the cPLA$_2$α gene. In contrast, ChIP-sequencing data of H3K4me3 suggested a distinct site rich in H3K4me3 near the transcriptional start site of cPLA$_2$α, leading us to postulate that this site could be an area of active transcriptional activity. ChIP-qPCR showed absence of significant enrichment of the cPLA$_2$α promoter region after immunoprecipitation with anti-H3K9ac antibody. H3K9 acetylation assay results also showed no change in H3K9ac levels after TSA treatment. These results indicate that TSA does not increase cPLA$_2$α  expression via acetylation of H3K9. In contrast, ChIP – qPCR confirmed significant enrichment of the cPLA$_2$α promoter region in TSA-treated cells upon immunoprecipitation with anti-H3K4me3 antibody. The

findings are consistent with our observations that the HMT inhibitor MTA significantly suppresses TSA-induced $cPLA_2\alpha$ mRNA expression. Together, results suggest that TSA increases binding of H3K4me3 at this specific gene region (+143 to +349) to facilitate transcription of $cPLA_2\alpha$.

Subsequently, we investigated the role of epigenetic regulation on cell viability of SH-SY5Y cells. The neuroprotective potential of anacardic acid and MTA were first explored, followed by elucidation of the role of $cPLA_2$ in TSA-induced cell death using the specific enzymatic inhibitor, $AACOCF_3$. Recent studies highlight TSA as a potential drug candidate in the treatment of cancer (Mariadason et al., 2000), and TSA has been shown to inhibit cell viability in SH-SY5Y cells and neuron-like cells (Wang et al., 2009). In our study, treatment of cells with TSA increased LDH release into the culture media, indicating cellular injury. Conversely, treatment with anacardic acid led to significant abrogation of cytotoxicity, indicating a potentially neuroprotective role of anacardic acid. This is consistent with previous studies showing that anacardic acid protected against H3 and H4 histone acetylation and dopaminergic neuronal apoptosis in primary mesencephalic neurons (Song et al., 2010). The HMT inhibitor MTA did not protect against TSA-induced cell death. The reason for this is unknown, but possibly due to other genes that are activated by HMTs, such as inhibition of methylation of lamin B that causes solubilization of lamins and subsequent induction of apoptosis (Lee and Cho, 1998). We also sought to determine a possible role of $cPLA_2$ in TSA-induced cell death. LDH release indicating cellular injury was significantly reduced by $AACOCF_3$, a selective inhibitor of $cPLA_2$, suggesting that $cPLA_2$ is

a contributor to TSA-induced cell death. Thus, reported anti-cancer effects of TSA (Mariadason et al., 2000) may involve $cPLA_2$-related mechanisms. This could occur through release of arachidonic acid, which may be metabolised to generate free radicals and proinflammatory eicosanoids that induce cell death (Scorrano et al., 2001, Pompeia et al., 2003, Ong et al., 2010). $AACOCF_3$ was used for the selective inhibition of $cPLA_2$ enzyme activity, since it is known to be 500-fold more potent in blocking $cPLA_2$ activity at 15 $\mu$M as compared to $iPLA_2$ and $sPLA_2$ (Trimble et al., 1993, Liu et al., 2014). As a further confirmation, future studies can include the use of additional $PLA_2$ inhibitors or the specific inhibition of $cPLA_2$ using siRNA (Morris et al., 2004).

Epigenetic regulation of inflammatory genes have been proposed to give rise to chronic inflammation (Wilson, 2008). General decreases in HDAC activities have been reported in patients with chronic obstructive pulmonary disease (Mroz et al., 2007) and inflammatory lung disease treatments with corticosteroids and theophylline have been found to interfere with HAT and HDAC activities to downregulate inflammatory genes (Barnes et al., 2005). Increased HAT activity and decreased HDAC activity have also been implicated in asthma cases (Kuo et al., 2014). In the CNS, late-onset AD in humans are characterized by a phenomenon known as "age-specific epigenetic drift", where epigenetic signatures in the genome change over time, leading to changes in gene expression, pathology and behavior (Wang et al., 2008). Our findings provide novel evidence for epigenetic regulation in $cPLA_2$ expression in a neuron-like cell line, and may point to similar effects in neurons and other cells, with implications in chronic inflammation.

Nutrients and bioactive food components have also been proposed to induce epigenetic modifications and alter gene expression over time (Choi and Friso, 2010). In our study, we noted that the well-known HAT inhibitor anacardic acid, a flavonoid extract derived from cashew nuts, suppressed TSA-induced $cPLA_2$ expression. A search for South-East Asian plants with similar properties revealed that *Clinacanthus nutans* Lindau (Sabah Snake Grass) leaf extracts also suppressed TSA-induced $cPLA_2$ upregulation and cellular injury, similar to anacardic acid (Tan et al., unpublished data). Results suggest potential for phytochemicals to have significant effects on chronic neuroinflammation via epigenetic effects on $cPLA_2$.

# CHAPTER 2

# EFFECTS OF *CLINACANTHUS NUTANS* ON

# EPIGENETIC REGULATION OF CYTOSOLIC

# PHOSPHOLIPASE A$_2$

## 2.1 Introduction

*Clinacanthus nutans* Lindau (*C. nutans*) belongs to the family Acanthaceae and the genus *Clinacanthus,* along with its closely associated species, *Clinacanthus siamensis* Brem (Smitinand, 1980)*. C. nutans* was traditionally used for treatment of snake bites (Daduang et al., 2005), insect bites and herpes infections in Thailand (Sakdarat et al., 2006, Uawonggul et al., 2006). Commonly referred to as 'Sabah Snake Grass', it is now a recognised medicinal plant with anti-inflammatory and analgesic properties (Pongphasuk and Khunkitti, 1996). *C. nutans* extracts significantly inhibit carrageenan-induced paw edema in mice and rats as well as ethyl phenylpropiolate-induced ear edema in rats via suppression of neutrophil migration (Pongphasuk and Khunkitti, 1996, Wanikiat et al., 2008). It has antiviral effects against the herpes simplex virus type-2 (Wirotesangthong and Rattanakiat, 2006, Kunsorn et al., 2013), and possess antioxidant and anticancer effects on cultured human cancer cell lines (Yong et al., 2013).

The ethanol extract of *C. nutans* leaves comprise a mixture of nine cerebrosides and a monoacylmonogalactosylglycerol, as established by spectroscopic and chemical reactions (Tuntiwachwuttikul et al., 2004). The chloroform extract isolated after chromatographic separation comprise three chlorophyll derivatives (phaeophytins) related to chlorophyll a and chlorophyll b, and possesses anti-herpes simplex virus activity (Sakdarat et al., 2006). The active components, namely, lupeol, vitexin, orientin and cerebrosides, have anti-inflammatory properties, as observed by alleviation of rat paw

edema (Saleem, 2009, Loizou et al., 2010, Borghi et al., 2013, Mandal et al., 2014, Zhou et al., 2014).

Cytosolic phospholipase $A_2$ (cPLA$_2$) is a key enzyme implicated in chronic inflammatory neurodegeneration due to ischemia or excitotoxicity (Lukiw and Bazan, 2000, Bazan et al., 2002, Sun et al., 2012). It regulates the production of second messengers such as arachidonic acid and PAF in brain tissues (Farooqui et al., 1997). Arachidonic acid produces proinflammatory eicosanoids and plays a major role in signaling and inflammatory modulation in the brain (Farooqui et al., 1997).

Our previous findings (Chapter 1) elucidated that HDAC inhibition by TSA and MS-275 led to large increases in cPLA$_2$α expression, which were suppressed by HAT inhibitors, anacardic acid and NU9056. Anacardic acid is a well-known flavonoid extract derived from cashew nuts, and is a nutraceutical among several others that also possess HAT inhibitory properties (Sung et al., 2008, Ghizzoni et al., 2011). For instance, plumbagin, a compound derived from the medicinal plant *Plumbago zeylanica*, inhibits the p300/CBP HAT and downregulates NF-kB-dependent gene expression (Sandur et al., 2006, Ravindra et al., 2009). Curcumin, a component of *Curcuma longa*, commonly known as turmeric, is also an inhibitor of p300/CBP HAT that suppresses TNFα-induced p65 acetylation, which in turn downregulates NF-kB-dependent expression of many inflammatory genes (Balasubramanyam et al., 2004). Garcinol, a polyisoprenylated benzophenone derivative from Garcinia indica fruit, possess p300/CBP HAT inhibitory properties (Hong et al., 2006, Oike et al., 2012). Nutraceuticals also possess

anti-cytotoxic effects by generating neurotrophic factors essential for cell viability (Blaylock and Maroon, 2012). In this part of the study, we investigated the anti-inflammatory effects of *C. nutans* via $cPLA_2$ regulation in SH-SY5Y human neuroblastoma cells, and explored its potential mechanism of function via epigenetic means. Last but not least, the role of *C. nutans* in modulation of cell viability was investigated.

## 2.2    Materials and Methods

### 2.2.1  Plant materials and plant extracts

*Clinacanthus nutans* extracts were derived from the whole plant commonly known as Sabah Snake grass. It was provided by A/P Ong Wei Yi, and extracted with the kind assistance of A/P Benny Tan and Annie Hsu (Department of Pharmacology, National University of Singapore). The leaves (*778.65 g*) were rinsed with distilled water and soaked in 80% denatured ethanol. The leaves were homogenized (Wiggen Hauser D-500) and the mixture left to stand for one hour. The ethanol extract was then filtered under vacuum (Gast USA DOA-PIO4-BN) with 90 mm glass microfiber filter membranes (Whatman, Little Chalfont, Buckinghamshire, UK). The filtrate was concentrated in a rotary evaporator at 50°C (Buchi Labortechnik AG, Postfach, Switzerland). The resultant dark green condensate was subject to freeze-drying (Christ Gamma 1-16 LSC) for 1–2 days. After drying, appearance of the solid residue obtained (*27.02 g*) was a dark green powder. The extract yield (w/w) from 778.65 g of fresh leaves was approximately 3.47%. Prior to usage, the powder extract was dissolved in 10% DMSO. The

freeze-dried leaf extracts were obtained and stored for long-term usage at -80°C.

## 2.2.2  Materials

Treatments administered to SH-SY5Y cells were DMSO, TSA and *C. nutans*. DMSO and TSA were purchased from Sigma (St. Louis, MO). The *C. nutans* extracts were weighed and dissolved in DMSO before treatment.

## 2.2.3  Cell culture

SH-SY5Y human neuroblastoma cells were obtained from ATCC (Manassas, VA) and cultured in DMEM supplemented with 10% FBS and 1% penicillin/streptomycin (Gibco-Invitrogen, Carlsbad, CA). Cells were grown in 100 mm$^2$ cell culure dishes and incubated in 37°C, 100% humidity with 95% air and 5% $CO_2$, as previously described.

## 2.2.4  Treatment with *C. nutans* and general HDAC inhibitor, TSA

To study the effects of *C. nutans* and the general HDAC inhibitor TSA on $cPLA_2$ expression, SH-SY5Y cells were divided into four groups and treated as follows: (1) DMSO as vehicle control, (2) 0.5 $\mu$M TSA, (3) 100 $\mu$g/ml *C. nutans*, (4) 100 $\mu$g/ml *C. nutans* and 0.5 $\mu$M TSA. TSA was administered at the IC50 dose of 0.5 $\mu$M (Muhlethaler-Mottet et al., 2008). *C. nutans* was administered at a dose of 100 $\mu$g/ml, a dose known to exert a physiological effect in cells (Wanikiat et al., 2008, Yong et al., 2013). Cells were co-incubated with *C. nutans* and TSA or vehicle for 24 hours before harvesting.

## 2.2.5 Real-time quantitative reverse transcription-polymerase chain reaction (qRT-PCR)

Total RNA extraction from SH-SY5Y cells was performed with the RNeasy Mini kit (Qiagen, Hamburg, Germany). Reverse transcription of RNA to cDNA was performed using the High-Capacity cDNA Reverse Transcription Kit (Applied Biosystems, Foster City, CA), as described previously. Real-time RT-PCR was then carried out using the TaqMan® Universal PCR Master Mix (Applied Biosystems, Foster City, CA) with specific TaqMan® Gene Expression Assay Probes for cPLA$_2$α (Hs00233352_m1), and β-actin (#4326315E) (Applied Biosystems, Foster City, CA). The qRT-PCR was run on the Applied Biosystem 7500 Real-Time PCR system (Applied Biosystems, Foster City, CA), as described previously. The relative amount of gene transcript was estimated after normalization to the endogenous control gene, β-actin. Using the $2^{-\Delta\Delta CT}$ method as previously described (Livak and Schmittgen, 2001), the relative fold changes were quantified. All reactions were performed in triplicates and the mean and standard error calculated. Statistical differences were analysed using one-way ANOVA with Bonferroni's multiple comparison *post-hoc* test, where $P < 0.05$ was deemed significant.

## 2.2.6 HAT activity assay

In vitro acetylation assay was performed with the Fluorescent HAT Assay kit, according to the manufacturer's protocol (Active Motif, La Hulpe, Belgium). Test reagents were added in triplicates into a 96-well flat white plate (Greiner Bio-One, Austria, Germany) for analysis. The purified p300 catalytic

domain (0.1 mg/ml) was used as a HAT source and was incubated with acetyl-CoA and specific synthetic H3 and H4 substrate peptides (provided in kit). The. To exclude a possible disturbance by autoacetylation or autofluorescence of *C. nutans* in these assays, an additional background control was performed. 15 $\mu$M anacardic acid was used as a positive control for HAT inhibition. The plate was read at an excitation wavelength of 360 nm and an emission wavelength of 450 nm on the Tecan Infinite® 200 microplate reader (Tecan Group Ltd., Maennedorf, Switzerland). Average arbitrary fluorescence units (AFU) readings from the triplicate wells were obtained. All reactions were performed in triplicates and the mean and standard error calculated. Statistical differences were analysed using one-way ANOVA with Bonferroni's multiple comparison *post-hoc* test, where $P < 0.05$ was deemed significant.

### 2.2.7  Detection of H3K9 acetylation levels

Detection of H3K9 acetylation was performed using the EpiQuik™ In Situ Histone H3-K9 Acetylation Assay Kit (# P-4004, Epigentek, Farmingdale, NY). Cells were cultured in a 96-well microplate (provided in kit) and grown to 80% confluency. They were divided into six treatment groups (1) DMSO vehicle control, (2) 0.5 $\mu$M TSA, (3) 50 $\mu$g/ml *C. nutans*, (4) 50 $\mu$g/ml *C. nutans* and 0.5 $\mu$M TSA, (5) 100 $\mu$g/ml *C. nutans*, (6) 100 $\mu$g/ml *C. nutans* and 0.5 $\mu$M TSA. Each group consisted of four biological replicates. After treatment, cells were incubated overnight for 24 hours before performance of assay, according to manufacturer's protocol. The absorbance was read on the

Tecan Infinite® 200 microplate reader (Tecan Group Ltd., Maennedorf, Switzerland) at 450 nm within 10 minutes, and the % H3K9 acetylation was calculated according to the following formula:

$$\text{Acetylation \%} = \frac{\text{O. D. (treated sample-blank)}}{\text{O.D. (untreated control-blank)}} \times 100$$

The average values were then normalised against untreated controls. The mean and standard errors were calculated, and significant differences were analysed using one-way ANOVA with Bonferroni's multiple comparison *post-hoc* test, where $P < 0.05$ was deemed significant.

### 2.2.8  Immunocytochemistry

SH-SY5Y cells were counted and $2 \times 10^5$ cells were cultured on poly-L-lysine-coated coverslips placed in 24-well plates. They were grown to 80% confluency before administration of treatment. SH-SY5Y cells were divided into four groups and treated as follows: (1) DMSO as vehicle control, (2) 0.5 $\mu$M TSA, (3) 100 $\mu$g/ml *C. nutans*, (4) 100 $\mu$g/ml *C. nutans* and 0.5 $\mu$M TSA. After 24 hours, the LDH assay was performed as previously described, using the rabbit polyclonal cPLA$_2$ antibody (sc-438, 1:50 in 3% BSA, Santa Cruz Biotechnology, Santa Cruz, CA), followed by secondary incubation with the anti-rabbit Alexa Fluor 488 (Applied Biosystems, Foster City, CA; diluted 1:200). Nuclei were labelled and coverslips mounted with the Prolong Gold Anti-fade Mountant DAPI (Invitrogen, Carlsbad, CA). After drying overnight, the samples were analysed and images captured using the confocal microscope (Zeiss, Jena, Germany).

**2.2.9  Quantitative image analysis**

To measure the fluorescence intensity of cells between the treatment groups, images were captured using the confocal microscope (Zeiss, Jena, Germany) at the plane with the best focus. An average of ten to fifteen images were captured per treatment group. The region around each cell was demarcated and measured with the Image J software (Burgess et al., 2010, Gavet and Pines, 2012). Background readings were obtained by obtaining values of at least three regions of background fluorescence. The net fluorescent intensity was calculated for each image according to the following formula: *Corrected total cell fluoresence (CTCF) = Integrated Density – (Area of selected cell x Mean fluorescence of background readings)*. The net average intensity values were then normalised against vehicle-treated controls. The mean and standard error were calculated and significant differences analysed using one-way ANOVA with Bonferroni's multiple comparison *post-hoc* test, where $P < 0.05$ was deemed significant.

**2.2.10    Trypan blue exclusion and cell viability assay**

SH-SY5Y cells were grown on 100 mm$^2$ tissue culture dishes and grown to 80% confluency. SH-SY5Y cells were divided into four groups and treated as follows: (1) DMSO as vehicle control, (2) 0.5 $\mu$M TSA, (3) 100 $\mu$g/ml *C. nutans*, (4) 100 $\mu$g/ml *C. nutans* and 0.5 $\mu$M TSA. After 24 hours, cells were harvested and exposed to trypan blue for five minutes, before percentage cell viability was determined. Values were normalised against vehicle-treated controls. The mean and standard errors were calculated, and

significance differences were analysed using one-way ANOVA with Bonferroni's multiple comparison *post-hoc* test, where $P < 0.05$ was deemed significant.

## 2.2.11    Lactate dehydrogenase assay

SH-SY5Y cells were counted and 2 x $10^5$ were cultured in 24-well plates. They were grown to 80% confluency before administration of treatment. The cells were divided into four groups for administration of treatment as follows: (1) DMSO as vehicle control, (2) 0.5 $\mu$M TSA, (3) 100 $\mu$g/ml *C. nutans*, (4) 100 $\mu$g/ml *C. nutans* and 0.5 $\mu$M TSA. Cell viability was accessed after 24 hours by colorimetric determination of LDH release, using the LDH Cytotoxicity Detection Kit (Roche, Mannheim, Germany), according to manufacturer's protocol. Percentage of cell death was calculated and the average of three plate readings taken. The plate was read at an excitation wavelength of 490 nm on the Tecan Infinite® 200 microplate reader (Tecan Group Ltd., Maennedorf, Switzerland). The reference absorbance reading was subtracted from the absorbance at 490 nm. Percentage cytotoxicity was calculated according to the formula:

$$\text{Cytotoxicity (\%)} = \frac{\text{experimental value-low control}}{\text{high control-low control}} \times 100$$

The mean cytotoxicity values were then normalised against vehicle-treated controls. The mean and standard errors were calculated, and significant differences analysed using one-way ANOVA with Bonferroni's multiple comparison *post-hoc* test, where $P < 0.05$ was deemed significant.

## 2.3   Results

### 2.3.1   Effect of *C. nutans* and TSA on cPLA$_2$α mRNA expression
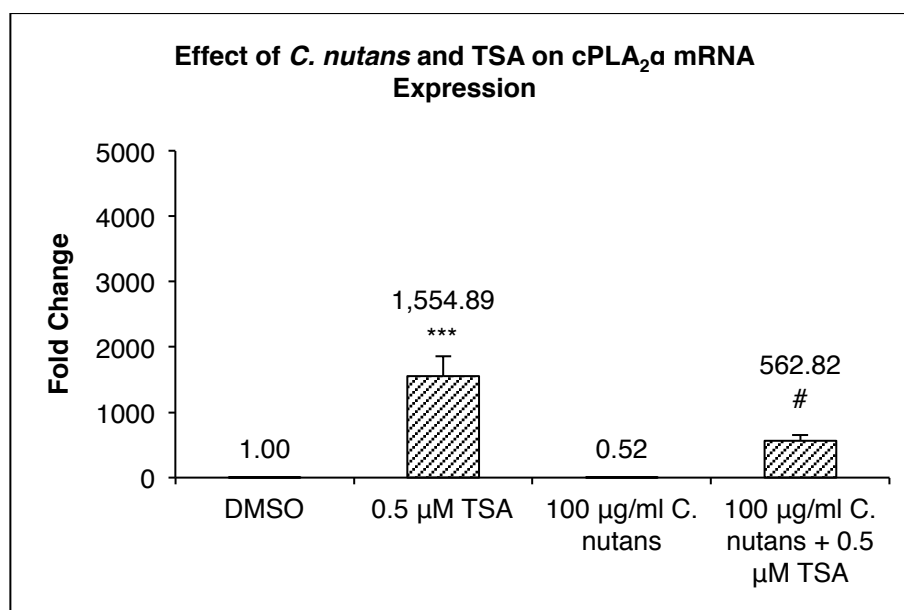


**Figure 2.3.1 Real-time RT-PCR analyses of cPLA$_2$α mRNA expression after treatment with *C. nutans* and general HDAC inhibitor, TSA**. Data represent mean and standard error of four biological replicates. Statistical analysis by one-way ANOVA with Bonferroni's multiple comparison *post-hoc* test. * Indicates significant difference compared to DMSO-treated vehicle controls, *** $P < 0.001$. # Indicates significant difference compared to cells treated with 0.5 µM TSA, # $P < 0.05$.

A significant 1554-fold increase in cPLA$_2$α mRNA expression was observed after treatment with 0.5 $\mu$M TSA, compard to DMSO-treated vehicle controls ($P < 0.001$) (Fig. 2.3.1 A). Co-treatment of 100 $\mu$g/ml *C. nutans* with 0.5 $\mu$M TSA signfically reduced the effect of TSA treatment on cPLA$_2$α mRNA expression by 36.2%, compared to cells treated with TSA only ($P = 0.041$) (Fig. 2.3.1 A).

## 2.3.2  HAT activity assay
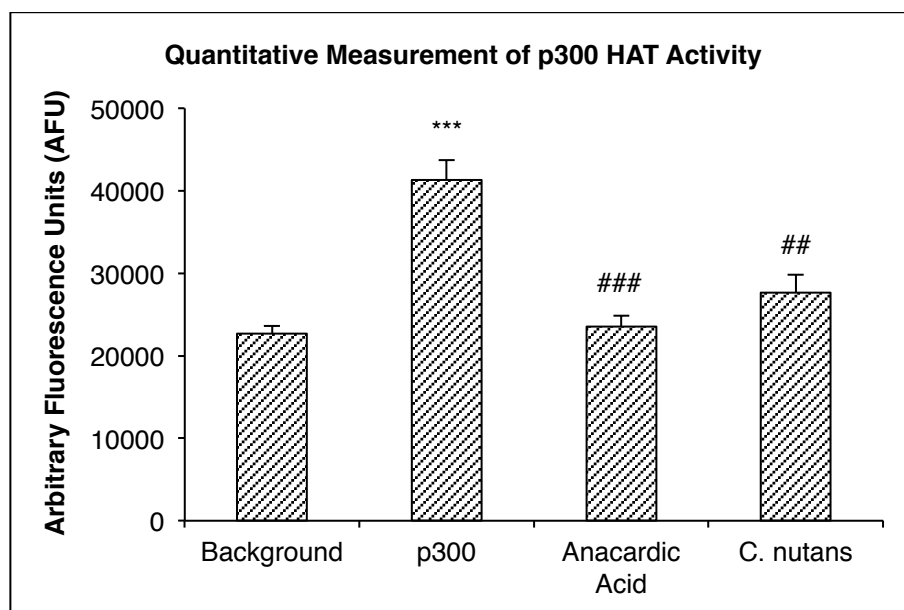


**Fig. 2.3.2 Histone acetyltransferase (HAT) activity assay results showing HAT activity in arbitrary fluorescence units (AFU).** Analysed by one-way ANOVA with Bonferroni's multiple comparison *post-hoc* test. Data represent the mean and standard error of four biological replicates. * Indicates significant difference compared background flurescence levels, *** $P < 0.001$. # Indicates significant difference compard to p300 positive control for HAT activity. ## $P < 0.01$, ### $P < 0.001$.

Background level of fluorescence indicated fluorescence reading of 22700 *AFU* ($P < 0.001$). Positive control for HAT inhibition, anacardic acid, showed similarly low fluorescence reading of 23600 *AFU* ($P = 0.001$). Significant increase in fluorescence reading of 41300 *AFU* was detected in the positive control for HAT activity, p300 HAT, compared to background controls ($P < 0.001$). Significant decrease in fluorescence reading of 27700 *AFU* was detected in *C. nutans,* compared to p300 control ($P = 0.006$) (Fig. 2.3.2).

### 2.3.3  Detection of H3K9 acetylation
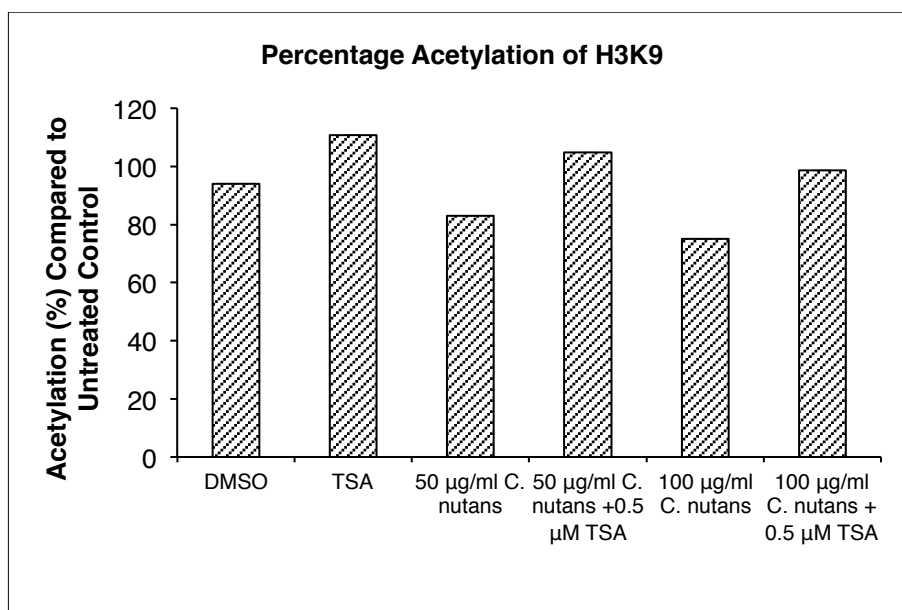


**Fig. 2.3.3 Percentage of acetylated H3K9 residues detected in cells, compared to untreated controls.** Analysed by one-way ANOVA with Bonferroni's multiple comparison *post-hoc* test. Data represent the mean and standard error of four biological replicates.

No significant change in percentage acetylation of H3K9 was detected after TSA treatment (Fig. 2.3.3).

## 2.3.4 Effect of *C. nutans* and TSA on cPLA$_2$ protein expression



A



B
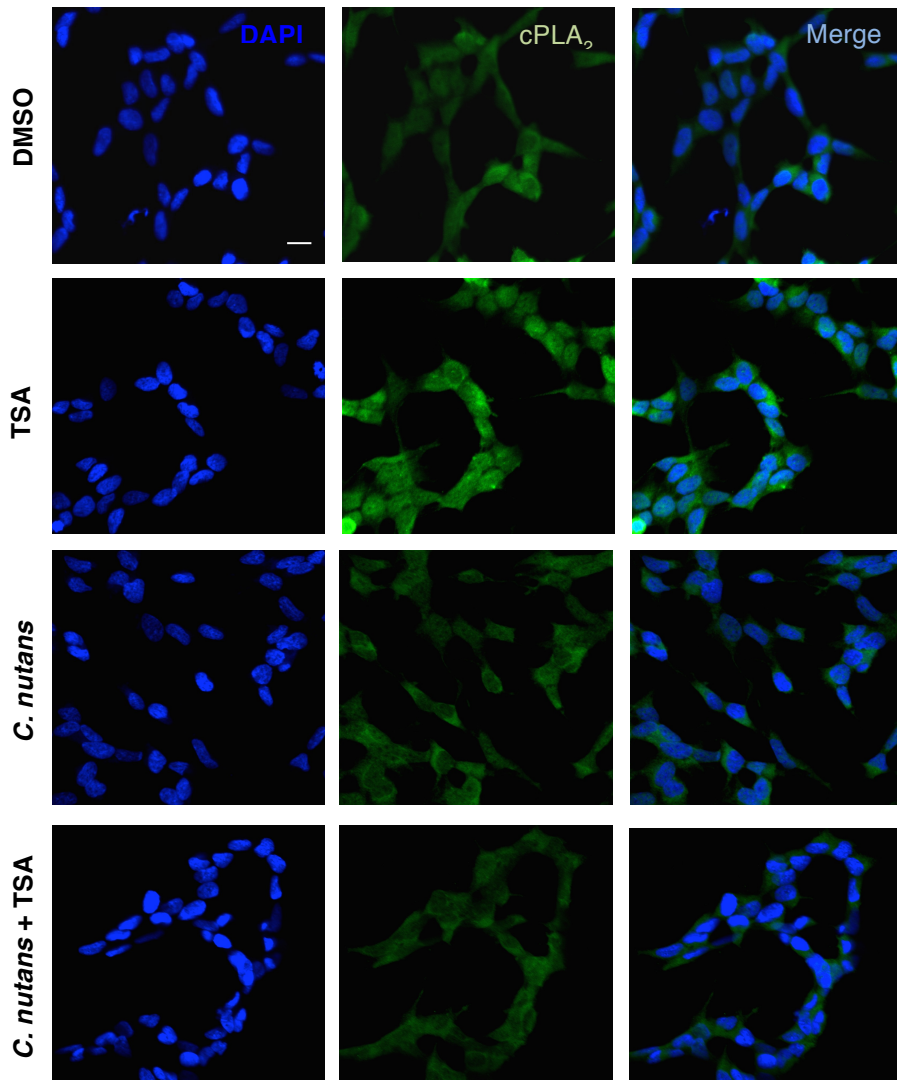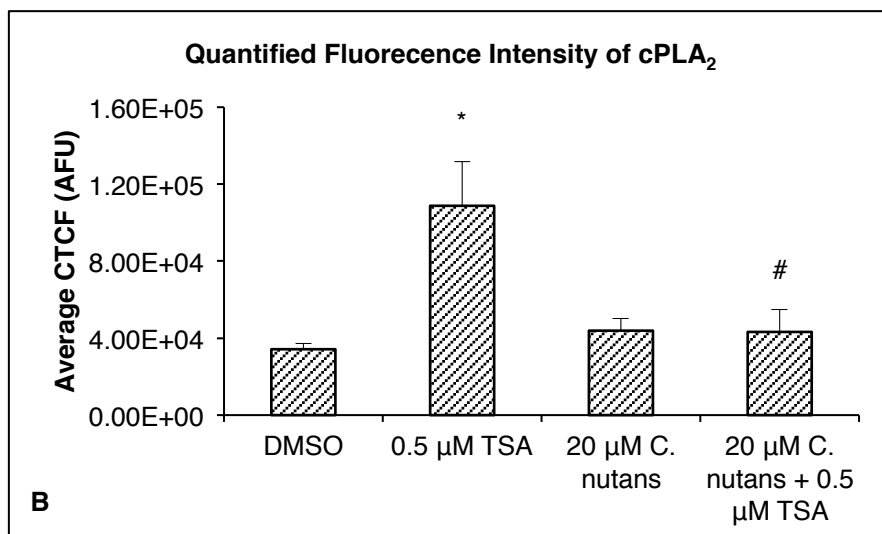
**Figure 2.3.4 Effect of *C. nutans* and general HDAC inhibitor, TSA treatment on cPLA$_2$ protein expression. (A)** Immunocytochemistry photos of cPLA$_2$ protein expression in SH-SY5Y cells after *C. nutans* and TSA treatment. **(B)** Quantification of ten high-power microscopic fields from four biological replicates per group analysed and computed as average corrected total cell fluorescence (CTCF) values. Scale bar = 20 $\mu$m. AFU: arbitrary fluorescence units. Data represent mean and standard error of four biological replicates. Analysed by one-way ANOVA with Bonferroni's multiple comparison *post-hoc* test. * Indicates significant difference compared to DMSO-treated vehicle controls, *** $P < 0.001$. [#] indicates significant difference compared to cells treated with 0.5 µM TSA, [###] $P < 0.001$.

Significant increase in fluorescence intensity was detected after treatment with 0.5 $\mu$M TSA, with an average fluorescence value of $(1.1 \times 10^5$ AFU), as compared to cells in the DMSO-treated vehicle control group with average fluorescence value of $(3.4 \times 10^4$ AFU) ($P = 0.012$). Fluorescence intensity remained low $(4.4 \times 10^4$ AFU) after treatment with *C. nutans* alone. Co-treatment of 100 $\mu$g/ml *C. nutans* with 0.5 $\mu$M TSA resulted in a significantly lowered average fluorescence value of $(4.3 \times 10^4$ AFU), compared to cells treated with TSA alone ($P = 0.027$) (Fig. 2.3.4 A-B).

## 2.3.5  Trypan blue exclusion and cell viability assay
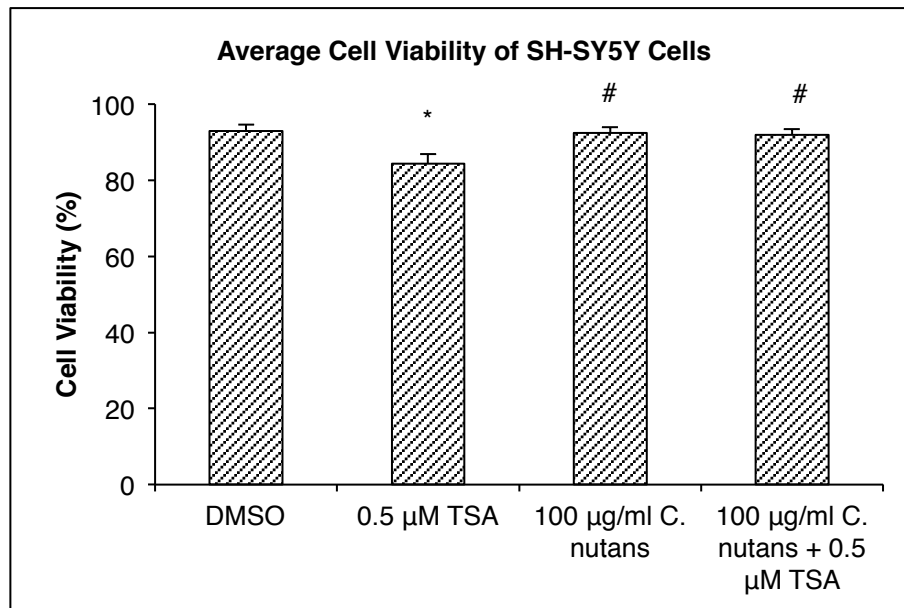


**Fig 2.3.5 Trypan blue exclusion assay results.** Measurement of cell viability after treatment with *C. nutans* and TSA. Data represent mean and standard error of six biological replicates, analysed by one-way ANOVA with Bonferroni's multiple comparison *post-hoc* test. * Indicates significant difference compared with DMSO-treated control group, * $P < 0.05$. [#] Indicates significant difference compared to cells treated with 0.5 µM TSA, [#] $P < 0.05$

Significant drop in cell viability was observed after TSA treatment ($P =$ 0.002). *C. nutans* treatment alone did not decrease cell viability, while co-treatment of 100 *µ*g/ml *C. nutans* with 0.5 *µ*M TSA significantly suppressed cell death ($P = 0.035$) (Fig. 2.3.5).

### 2.3.6  Lactate dehydrogenase assay
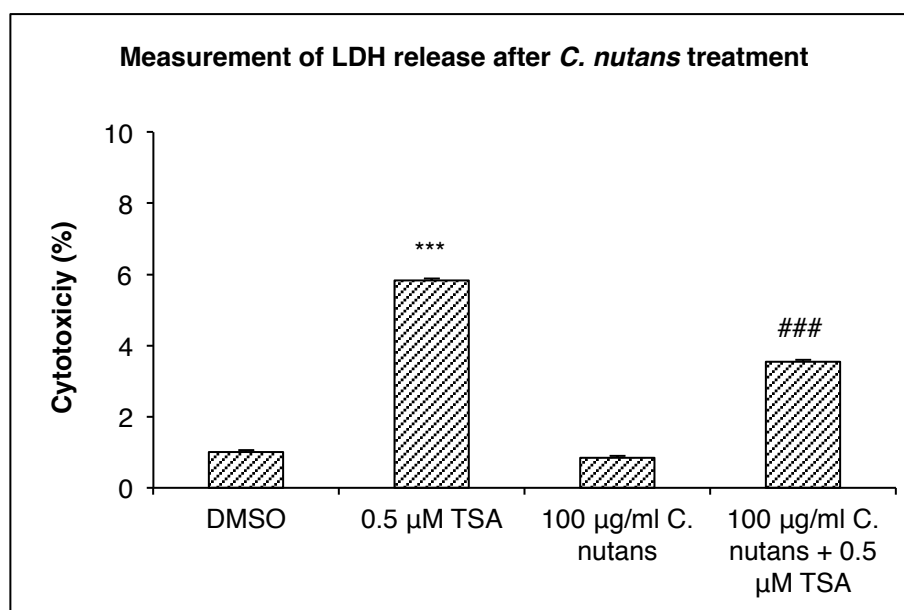


**Fig. 2.3.6 Lactate dehydrogenase (LDH) assay results.** Measurement of percentage LDH release after treatment with TSA and *C. nutans.* Data represent mean and standard error of four biological replicates, analysed by one-way ANOVA with Bonferroni's multiple comparison *post-hoc* test. * Indicates significant difference compared with DMSO-treated control group, *** $P < 0.001$. [#] Indicates significant difference compared to cells treated with 0.5 µM TSA, [###] $P < 0.001$

Significant increase in cytotoxicity by 5.8-fold was observed after 0.5 *µ*M TSA treatment ($P < 0.001$). Co-treatment of 100 *µ*g/ml *C. nutans* with 0.5 *µ*M TSA brought about significant reduction in cytotoxicity by 1.5-fold (39.2%) ($P < 0.001$), compared to cells treated with TSA only (Fig. 2.3.6).

### 2.4    Discussion

*C. nutans* is a species of medicinal plants used in Thai traditional medicine, belonging to the family Acanthaceae (Tiangburanatam, 1996). In the first part of our study (Chapter 1), we showed that the general HDAC inhibitor TSA induced significant upregulation of cPLA$_2$α expression,

indicating an important role of HDAC inhibition in the regulation of $cPLA_2$ in SH-SY5Y cells. We also found that co-treatment of cells with the general HAT inhibitor anacardic acid and TSA modulated upregulation of $cPLA_2\alpha$ induced by TSA. These changes were found to corroborate with protein expression as shown by Western blots and immunocytochemistry. Cell injury observed after TSA treatment was partially abrogated by anacardic acid. The role of $cPLA_2$ in modulating TSA-induced injury was shown after co-incubation with the $cPLA_2$ selective inhibitor, $AACOCF_3$, indicating the involvement of $cPLA_2$ in TSA-induced cell injury. In view of the positive effects of the natural compound, anacardic acid, on $cPLA_2$ expression, this part of the study was performed to investigate the effects of *C. nutans* and TSA on $cPLA_2$ expression, and thereafter to investigate its mechanism of action and possible cytoprotective effects.

In line with our previous findings, the general HDAC inhibitor TSA induced significant upregulation of $cPLA_2\alpha$ mRNA expression. Co-treatment of cells with *C. nutans* and TSA significantly reduced expression of $cPLA_2\alpha$ induced by TSA. This suppression of $cPLA_2\alpha$ mRNA expression by *C. nutans* highlights its anti-inflammatory potential, similar to the general HAT inhibitor anacardic acid and Tip60-specific HAT inhibitor NU9056, which significantly suppressed TSA-induced $cPLA_2\alpha$ upregulation (Chapter 1).

In view of the fact that many nutraceuticals have HAT inhibitory properties (Sung et al., 2008, Choi and Friso, 2010), we hypothesized that *C. nutans* may possess HAT inhibitory properties similar to that of the general HAT inhibitor, anacardic acid and the Tip60-specific HAT inhibitor, NU9056.

HAT activity assay showed significantly lowered fluorescence reading produced by *C. nutans* extracts, compared to the p300 HAT control, indicating the presence of significant inhibition of p300 HAT activity by *C. nutans*. Results indicate that *C. nutans* regulate cPLA$_2$α expression at least in part via p300 HAT inhibition.

We next explored the effects of *C. nutans* and TSA on the acetylation status of Lys-9 of histone H3 (H3K9) because it is a known substrate of the p300 HAT (Yuan et al., 2013) and is typically associated with activated genes (Karmodiya et al., 2012). H3K9 acetylation assay results showed no significant change in H3K9ac levels after TSA and *C. nutans* treatment. This supports our previous ChIP-qPCR findings showing absence of significant enrichment of the cPLA$_2$α promoter region after immunoprecipitation with anti-H3K9ac antibody (Chapter 1). Together, findings suggest that TSA does not increase cPLA$_2$α expression via acetylation of H3K9. Our findings add to previous studies on mouse embryos, which showed that the positive effect of TSA on the development of the embryo was not attributed to modifications in acetylation levels of H3K9 (Li et al., 2015). *C. nutans* might regulate cPLA$_2$α expression via altering acetylation statuses of other histone residues besides H3K9. Since TSA induces acetylation of H3K9, H3K14, and trimethylation of H3K4 (Sike et al., Martinez-Diaz et al., 2010, Huang et al., 2011, Coffey et al., 2012, Kennedy et al., 2013) (Table I), TSA might increase cPLA$_2$α mRNA expression by increasing acetylation of H3K14, which is in turn reduced by the HAT inhibitory effects of *C. nutans*.

The mRNA changes were reflected at the protein level, where Western

blots showed increased $cPLA_2$ protein expression after TSA treatment, and co-treatment with *C. nutans* reduced the increase. Immunocytochemistry also showed increased $cPLA_2$ immunofluorescence after TSA treatment, which was suppressed in cells that were co-treated with *C. nutans* and TSA. Results indicate that leaf extracts of *C. nutans* possess anti-inflammatory effects, and point to potential anti-inflammatory effects in distinct constituents of *C. nutans*.

We previously showed that cell injury observed after TSA treatment was abrogated by co-treatment with $cPLA_2$ selective inhibitor $AACOCF_3$, indicating that TSA induces cell injury via $cPLA_2$-related mechanisms (Chapter 1). We also showed presence of cytoprotective effects by anacardic acid where significant abrogation of cytotoxicity was detected after co-treatment of cells with anacardic acid and TSA (Chapter 1). Here, we further explored the cytoprotective potential of *C. nutans* in TSA-induced cell injury. Significant decrease in the number of trypan blue negative cells were observed after TSA treatment compared to DMSO-treated vehicle controls, showing that TSA reduced cell viability. Co-treatment of cells with *C. nutans* and TSA led to a significant increase in number of trypan blue negative cells compared to cells treated with TSA alone, indicating that *C. nutans* modulated the cell injury induced by TSA. The cytoprotective nature of *C. nutans* was confirmed using the LDH assay. As observed previously, treatment of cells with TSA increased LDH release into the culture media, indicating cellular injury. Co-treatment of cells with *C. nutans* and TSA significantly reduced LDH release, pointing to significant abrogation of cytotoxicity. Together, results from both assays suggest a cytoprotective role of *C. nutans* in TSA-induced cellular injury.

The suppression of cPLA$_2\alpha$ mRNA upregulation by *C. nutans* indicates presence of anti-inflammatory properties in *C. nutans* and possibly in distinct constituents within the leaf extracts. The constituents of *C. nutans* have been phytochemically and chemically studied (Sakdarat et al., 2009), and some of these such as lupeol (Saleem, 2009), β-sitosterol (Loizou et al., 2010), vitexin (Borghi et al., 2013), orientin (Zhou et al., 2014) and cerebrosides (Mandal et al., 2014) were previously shown to have anti-inflammatory properties. Lupeol is found in various other natural foods such as mangoes, grapes, white cabbage, strawberries, olives and green peppers (Saleem, 2009), and thus point to potential anti-inflammatory properties within these foods. A closely related species, *Clinacanthus siemensis* (*C. siemensis*), possess anti-inflammatory properties (Sreena et al., 2012). *Hygrophilaspinosa T. Anders*, a species of the same family Acanthaceae, also show anti-inflammatory potential via alleviation of carrageenan-induced paw oedema in rats (Arjun et al., 2009). Therefore, our findings add to previous studies that show benefits of phytochemicals in natural plant products, and point to the potential for more phytochemicals in this family to be identified for the alleviation of chronic inflammation.

Besides inhibiting *p300 HAT*, *C. nutans* could likewise inhibit the *Tip60 HAT*, since the Tip60 HAT was shown to play a significant role in cPLA$_2$ regulation (Chapter 1). *C. nutans* could also inhibit other substrates such as the transcription factor NF-kB, which is known to be affected by HATs and HDACs (Dai et al., 2005). One such example is triptolide, a diterpene triepoxide isolated from a medicinal plant *Tripterygium wilfordii* Hook. F.,

which inhibits acetylation of the p65 subunit of NF-kB and suppresses its activation (Zhu et al., 2009, Park et al., 2011). In view of such functions in other phytochemicals such as triptolide, it is possible that *C. nutans* may likewise suppress cPLA$_2$α expression via NF-kB inhibition.

Taken together, it was observed that co-treatment of SH-SY5Y cells with *C. nutans* leaf extracts suppressed TSA-induced cPLA$_2$ expression in a similar manner as known HAT inhibitors, and it possesses p300 HAT inhibitory properties. We also found that *C. nutans* also abrogated cytotoxicity induced by TSA. Therefore, results in this part of the study show anti-inflammatory and cytoprotective effects of *C. nutans*. These findings provide hope for natural dietary strategies for therapy for chronic inflammation. The constituents of *C. nutans* can also serve as potential candidates for the development of new anti-inflammatory compounds that can alleviate inflammation and cytotoxicity caused by oxidative stress and inflammation.

# SECTION IV

# CONCLUSION

In conclusion, this study shows the presence of epigenetic regulation in cPLA$_2$. In the first part of our study, we showed that the general HDAC inhibitor TSA induced significant upregulation in cPLA$_2\alpha$ expression, indicating an important role of HDAC inhibition in the regulation of cPLA$_2$ in SH-SY5Y cells. This was especially so for the class I HDAC specific inhibitor, MS-275, which induced the greatest increase in cPLA$_2\alpha$ expression, suggesting that class I HDACs play the most significant role in epigenetic regulation of cPLA$_2\alpha$. We also found that co-treatment of the general HAT inhibitor anacardic acid with TSA modulated upregulation of cPLA$_2\alpha$ induced by TSA. Specific involvement of class I HDACs and the Tip60 HAT in cPLA$_2\alpha$ regulation was further shown, where the Tip60 HAT inhibitor, NU9056, significantly reduced the upregulation of cPLA$_2\alpha$ induced by MS-275. These changes were found to corroborate with protein expression as shown by Western blots and immunocytochemistry. Co-treatment with the HMT inhibitor, MTA also suppressed TSA-induced cPLA$_2$ upregulation, showing that cPLA$_2$ expression can be influenced by histone methylation as well. ChIP results show that TSA increases expression of the cPLA$_2\alpha$ gene via increases in H3K4 trimethylation. Cell injury observed after TSA treatment was partially abrogated by anacardic acid, indicating presence of cytoprotective effects. The role of cPLA$_2$ in modulating TSA-induced cell injury was elucidated by significant abrogation of cytotoxicity after co-incubation with the cPLA$_2$ selective inhibitor, AACOCF$_3$.

In the second part of the study, we showed that co-treatment of cells with *C. nutans* and TSA suppressed TSA-induced cPLA$_2$ expression in a

similar manner as anacardic acid, and presence of p300 HAT inhibitory properties was elucidated. *C. nutans* also abrogated cytotoxicity induced by TSA, pointing to the presence of anti-inflammatory as well as cytoprotective effects.

Taken together, results in this study show presence of epigenetic regulation in cPLA$_2$, and provides promising hope for the use of phytochemicals to affect this process, for therapy for chronic inflammation.

**SECTION V**

**REFERENCES**

# REFERENCES

Agholme L, Lindstrom T, Kagedal K, Marcusson J, Hallbeck M (2010) An in vitro model for neuroscience: differentiation of SH-SY5Y cells into cells with morphological and biochemical characteristics of mature neurons. Journal of Alzheimer's disease : JAD 20:1069-1082.

Alberts B, Johnson A, Lewis J, Raff M, Roberts K, Walter P (2002) Molecular Biology of the Cell, Fourth Edition: Garland Science.

Alexandrov P, N., Cui P-G, Lukiw W, J. (2006) Hypoxia-sensitive domain in the human cytosolic phospholipase A2 promoter. Neuroreport 17:303-307.

Allan SM, Rothwell NJ (2001) Cytokines and acute neurodegeneration. Nat Rev Neurosci 2:734-744.

Allis CD, Jenuwein T, Reinberg D, Caparros M-L (2007) Epigenetics. New York: Cold Spring Harbor Laboratory Press.

Arjun P, Shivesh J, Narasimha M, Aher V, Pronobesh C, Ghanshyam P, Devdeep R (2009) Anti-Inflammatory and Antipyretic Activities of Hygrophila spinosa T. Anders Leaves (Acanthaceae). Tropical Journal of Pharmaceutical Research 8:133-137.

Balasubramanyam K, Swaminathan V, Ranganathan A, Kundu TK (2003) Small molecule modulators of histone acetyltransferase p300. The Journal of biological chemistry 19134-19140.

Balasubramanyam K, Varier RA, Altaf M, Swaminathan V, Siddappa NB, Ranga U, Kundu TK (2004) Curcumin, a novel p300/CREB-binding protein-specific inhibitor of acetyltransferase, represses the acetylation of histone/nonhistone proteins and histone acetyltransferase-dependent chromatin transcription. J Biol Chem 279:51163-51171.

Balsinde J, Bianco ID, Ackermann EJ, Conde-Frieboes K, Dennis EA (1995) Inhibition of calcium-independent phospholipase A2 prevents arachidonic acid incorporation and phospholipid remodeling in P388D1 macrophages. Proceedings of the National Academy of Sciences of the United States of America 92:8527-8531.

Barnes PJ, Adcock IM, Ito K (2005) Histone acetylation and deacetylation: importance in inflammatory lung diseases. Eur Respir J 25:552-563.

Bauer S, Kerr BJ, Patterson PH (2007) The neuropoietic cytokine family in development, plasticity, disease and injury. Nat Rev Neurosci 8:221-232.

Bayarsaihan D (2011) Epigenetic mechanisms in inflammation. Journal of dental research 90:9-17.

Bazán Jr NG (1970) Effects of ischemia and electroconvulsive shock on free fatty acid pool in the brain. Biochimica et Biophysica Acta (BBA) - Lipids and Lipid Metabolism 218:1-10.

Bazan NG (2003) Synaptic lipid signaling: significance of polyunsaturated fatty acids and platelet-activating factor. J Lipid Res 44:2221-2233.

Bazan NG, Colangelo V, Lukiw WJ (2002) Prostaglandins and other lipid mediators in Alzheimer's disease. Prostaglandins & other lipid mediators 68-69:197-210.

Beharry AW, Sandesara PB, Roberts BM, Ferreira LF, Senf SM, Judge AR (2014) HDAC1 activates FoxO and is both sufficient and required for skeletal muscle atrophy. Journal of cell science 127:1441-1453.

Beier UH, Akimova T, Liu Y, Wang L, Hancock WW (2011) Histone/protein deacetylases control Foxp3 expression and the heat shock response of T-regulatory cells. Current opinion in immunology 23:670-678.

Berger SL, Kouzarides T, Shiekhattar R, Shilatifard A (2009) An operational definition of epigenetics. Genes Dev 23:781-783.

Biel M, Kretsovali A, Karatzali E, Papamatheakis J, Giannis A (2004) Design, synthesis, and biological evaluation of a small-molecule inhibitor of the histone acetyltransferase Gcn5. Angewandte Chemie (International ed in English) 43:3974-3976.

Blaylock RL, Maroon J (2012) Natural plant products and extracts that reduce immunoexcitotoxicity-associated neurodegeneration and promote repair within the central nervous system. Surg Neurol Int 3:19.

Bonventre JV (1997) Roles of phospholipases A2 in brain cell and tissue injury associated with ischemia and excitotoxicity. J Lipid Mediat Cell Signal 17:71-79.

Borghi SM, Carvalho TT, Staurengo-Ferrari L, Hohmann MS, Pinge-Filho P, Casagrande R, Verri WA, Jr. (2013) Vitexin inhibits inflammatory pain in mice by targeting TRPV1, oxidative stress, and cytokines. J Nat Prod 76:1141-1149.

Bottomley MJ (2004) Structures of protein domains that create or recognize histone modifications. EMBO Reports 5:464-469.

Bradbury CA, Khanim FL, Hayden R, Bunce CM, White DA, Drayson MT, Craddock C, Turner BM (2005) Histone deacetylases in acute myeloid leukaemia show a distinctive pattern of expression that changes selectively in response to deacetylase inhibitors. Leukemia 19:1751-1759.

Bramham CR, Alkon DL, Lester DS (1994) Arachidonic acid and diacylglycerol ACT synergistically through protein kinase C to persistently enhance synaptic transmission in the hippocampus. Neuroscience 60:737-743.

Bravo L (1998) Polyphenols: Chemistry, dietary sources, metabolism, and nutritional significance. Nutrition Reviews 56:317-333.

Brower V (1998) Nutraceuticals: poised for a healthy slice of the healthcare market? Nat Biotechnol 16:728-731.

Burgess A, Vigneron S, Brioudes E, Labbe J-C, Lorca T, Castro A (2010) Loss of human Greatwall results in G2 arrest and multiple mitotic defects due to deregulation of the cyclin B-Cdc2/PP2A balance. Proceedings of the National Academy of Sciences of the United States of America 107:12564-12569.

Burke JE, Dennis EA (2009a) Phospholipase A2 biochemistry. Cardiovasc Drugs Ther 23:49-59.

Burke JE, Dennis EA (2009b) Phospholipase A(2) structure/function, mechanism, and signaling. Journal of Lipid Research 50:S237-S242.

Burke JE, Hsu YH, Deems RA, Li S, Woods VL, Jr., Dennis EA (2008) A phospholipid substrate molecule residing in the membrane surface mediates opening of the lid region in group IVA cytosolic phospholipase A2. J Biol Chem 283:31227-31236.

Buro LJ, Chipumuro E, Henrikson MA (2010) Menin and RNF20 recruitment is associated with dynamic histone modifications that regulate signal transducer and activator of transcription 1 (STAT1)-activated transcription of the interferon regulatory factor 1 gene (IRF1). Epigenetics & Chromatin 3:1-16.

Cagnin A, Brooks DJ, Kennedy AM, Gunn RN, Myers R, Turkheimer FE, Jones T, Banati RB (2001) In-vivo measurement of activated microglia in dementia. Lancet 358:461-467.

Cappellano G, Carecchio M, Fleetwood T, Magistrelli L, Cantello R, Dianzani U, Comi C (2013) Immunity and inflammation in neurodegenerative diseases. American Journal of Neurodegenerative Disease 2:89-107.

Chi PL, Luo SF, Hsieh HL, Lee IT, Hsiao LD, Chen YL, Yang CM (2011) Cytosolic phospholipase A2 induction and prostaglandin E2 release by interleukin-1beta via the myeloid differentiation factor 88-dependent pathway and cooperation of p300, Akt, and NF-kappaB activity in human rheumatoid arthritis synovial fibroblasts. Arthritis and rheumatism 63:2905-2917.

Choi K-C, Jung MG, Lee Y-H, Yoon JC, Kwon SH, Kang H-B, Kim M-J, Cha J-H, Kim YJ, Jun WJ (2009) Epigallocatechin-3-gallate, a histone acetyltransferase inhibitor, inhibits EBV-induced B lymphocyte transformation via suppression of RelA acetylation. Cancer research 69:583-592.

Choi SW, Friso S (2010) Epigenetics: A New Bridge between Nutrition and Health. Advances in nutrition 1:8-16.

Choi YH (2005) Induction of apoptosis by trichostatin A, a histone deacetylase inhibitor, is associated with inhibition of cyclooxygenase-2 activity in human non-small cell lung cancer cells. Int J Oncol 27:473-479.

Chuang DM, Leng Y, Marinova Z, Kim HJ, Chiu CT (2009) Multiple roles of HDAC inhibition in neurodegenerative conditions. Trends Neurosci 32:591-601.

Clark JD, Lin L-L, Kriz RW, Ramesha CS, Sultzman LA, Lin AY, Milona N, Knopf JL (1995) A novel arachidonic acid-selective cytosolic PLA2 contains a Ca2+-dependent translocation domain with homology to PKC and GAP. Cell 65:1043-1051.

Clemens JA, Stephenson DT, Smalstig EB, Roberts EF, Johnstone EM, Sharp JD, Little SP, Kramer RM (1996) Reactive glia express cytosolic phospholipase A2 after transient global forebrain ischemia in the rat. Stroke 27:527-535.

Coffey K, Blackburn TJ, Cook S, Golding BT, Griffin RJ, Hardcastle IR, Hewitt L, Huberman K, McNeill HV, Newell DR, Roche C, Ryan-Munden CA, Watson A, Robson CN (2012) Characterisation of a Tip60 specific inhibitor, NU9056, in prostate cancer. PloS one 7:e45539.

Cohen N, Betts DR, Rechavi G, Amariglio N, Trakhtenbrot L (2003) Clonal expansion and not cell interconversion is the basis for the neuroblast and nonneuronal types of the SK-N-SH neuroblastoma cell line. Cancer genetics and cytogenetics 143:80-84.

Collins HM, Abdelghany MK, Messmer M, Yue B, Deeves SE, Kindle KB, Mantelingu K, Aslam A, Winkler GS, Kundu TK (2013) Differential effects of garcinol and curcumin on histone and p53 modifications in tumour cells. BMC cancer 13:37.

Consortium EP (2011) Encyclopedia of DNA Elements at UCSC. vol. 9, p e1001046 PLoS Biol.

Constantinescu R, Constantinescu AT, Reichmann H, Janetzky B (2007) Neuronal differentiation and long-term culture of the human neuroblastoma line SH-SY5Y. Journal of neural transmission Supplementum 17-28.

Cotman CW, Berchtold NC, Christie L-A (2007) Exercise builds brain health: key roles of growth factor cascades and inflammation. Trends in Neurosciences 30:464-472.

Cowan MJ, Yao XL, Pawliczak R, Huang X, Logun C, Madara P, Alsaaty S, Wu T, Shelhamer JH (2004) The role of TFIID, the initiator element and a novel 5' TFIID binding site in the transcriptional control of the TATA-less human cytosolic phospholipase A2-alpha promoter. Biochimica et biophysica acta 1680:145-157.

Cui L, Miao J, Furuya T, Fan Q, Li X, Rathod PK, Su XZ, Cui L (2008) Histone acetyltransferase inhibitor anacardic acid causes changes in global gene expression during in vitro Plasmodium falciparum development. Eukaryotic cell 7:1200-1210.

Czerniawski J, Guzowski JF (2014) Acute neuroinflammation impairs context discrimination memory and disrupts pattern separation processes in hippocampus. J Neurosci 34:12470-12480.

Daduang S, Sattayasai N, Sattayasai J, Tophrom P, Thammathaworn A, Chaveerach A, Konkchaiyaphum M (2005) Screening of plants containing Naja naja siamensis cobra venom inhibitory activity using modified ELISA technique. Anal Biochem 341:316-325.

Dai Y, Rahmani M, Dent P, Grant S (2005) Blockade of histone deacetylase inhibitor-induced RelA/p65 acetylation and NF-kappaB activation potentiates apoptosis in leukemia cells through a process mediated by oxidative damage, XIAP downregulation, and c-Jun N-terminal kinase 1 activation. Mol Cell Biol 25:5429-5444.

Dayton CLG, Staller KP, Berkshire TL (2010) reacting a crude vegetable oil source of edible vegetable oil with an enzyme thereby cleaving fats; improves the operational characteristics, provides degummed edible oils in an efficient manner and reduces down time; provides salad oil quality edible oils while addressing a serious processing issue. Google Patents.

de Ruijter AJ, van Gennip AH, Caron HN, Kemp S, van Kuilenburg AB (2003) Histone deacetylases (HDACs): characterization of the classical HDAC family. Biochem J 370:737-749.

Delcuve GP, Khan DH, Davie JR (2012a) Roles of histone deacetylases in epigenetic regulation: emerging paradigms from studies with inhibitors. Clinical Epigenetics 4:5-5.

Delcuve GP, Khan DH, Davie JR (2012b) Roles of histone deacetylases in epigenetic regulation: emerging paradigms from studies with inhibitors. Clin Epigenetics 4:5.

Desbene C, Malaplate-Armand C, Youssef I, Garcia P, Stenger C, Sauvee M, Fischer N, Rimet D, Koziel V, Escanye MC, Oster T, Kriem B, Yen FT, Pillot T, Olivier JL (2012) Critical role of cPLA2 in Abeta oligomer-induced neurodegeneration and memory deficit. Neurobiol Aging 33:1123 e1117-1129.

Dessen A, Tang J, Schmidt H, Stahl M, Clark JD, Seehra J, Somers WS (1999) Crystal structure of human cytosolic phospholipase A2 reveals a novel topology and catalytic mechanism. Cell 97:349-360.

Dhalluin C, Carlson JE, Zeng L, He C, Aggarwal AK, Zhou MM (1999) Structure and ligand of a histone acetyltransferase bromodomain. Nature 399:491-496.

Dillard CJ, German JB (2000) Phytochemicals: nutraceuticals and human health. Journal of the Science of Food and Agriculture 80:1744-1756.

Do J, Kim I, Lee J, Choi D-K (2011) Comparison of genomic profiles in human neuroblastic SH-SY5Y and substrate-adherent SH-EP cells using array comparative genomic hybridization. BioChip J 5:165-174.

Durham B (2012) Novel histone deacetylase (HDAC) inhibitors with improved selectivity for HDAC2 and 3 protect against neural cell death. Bioscience Horizons 5.

Dutta K, Ghosh D, Basu A (2009) Curcumin protects neuronal cells from Japanese encephalitis virus-mediated cell death and also inhibits infective viral particle formation by dysregulation of ubiquitin-proteasome system. J Neuroimmune Pharmacol 4:328-337.

Economics A (2006) Dementia in the Asia Pacific Region: The Epidemic is here. In: Alzheimer's disease Report by Access Economics Pte Ltd for Asia Pacific Members of Alzheimer's Disease International.

Ekici M, Hohl M, Schuit F, Martínez-Serrano A, Thiel G (2008) Transcription of genes encoding synaptic vesicle proteins in human neural stem cells: chromatin accessibility, histone methylation pattern, and the essential role of rest. Journal of Biological Chemistry 283:9257-9268.

El Mansouri FE, Chabane N, Zayed N, Kapoor M, Benderdour M, Martel-Pelletier J, Pelletier JP, Duval N, Fahmi H (2011) Contribution of H3K4 methylation by SET-1A to interleukin-1-induced cyclooxygenase 2 and inducible nitric oxide synthase expression in human osteoarthritis chondrocytes. Arthritis and rheumatism 63:168-179.

Engelhart MJ, Geerlings MI, Meijer J, Kiliaan A, Ruitenberg A, van Swieten JC, Stijnen T, Hofman A, Witteman JC, Breteler MM (2004) Inflammatory proteins in plasma and the risk of dementia: the rotterdam study. Arch Neurol 61:668-672.

Epigenomics R (2015) Roadmap Epigenomics Project.

Farooqui AA, Horrocks LA (2006) Glycerophospholipids in the brain: phospholipases A2 in neurological disorders: Springer Science & Business Media.

Farooqui AA, Horrocks LA (2007) Glycerophospholipids in the Brain: Phospholipases A2 in Neurological Disorders: Springer.

Farooqui AA, Ong WY, Horrocks LA, Farooqui T (2000) Brain Cytosolic Phospholipase A2: Localization, Role, and Involvement in Neurological Diseases. The Neuroscientist 6:169-180.

Farooqui AA, Yang H-C, Rosenberger TA, Horrocks LA (1997) Phospholipase A2 and Its Role in Brain Tissue. Journal of Neurochemistry 69:889-901.

Fischer A, Sananbenesi F, Mungenast A, Tsai L-H (2010) Targeting the correct HDAC(s) to treat cognitive disorders. Trends in Pharmacological Sciences 31:605-617.

Formisano L, Guida N, Laudati G, Mascolo L, Di Renzo G, Canzoniero LMT (2015) MS-275 Inhibits Aroclor 1254–Induced SH-SY5Y Neuronal Cell Toxicity by Preventing the Formation of the HDAC3/REST Complex on the Synapsin-1 Promoter. Journal of Pharmacology and Experimental Therapeutics 352:236-243.

Franci G, Casalino L, Petraglia F, Miceli M, Menafra R, Radic B, Tarallo V, Vitale M, Scarfo M, Pocsfalvi G, Baldi A, Ambrosino C, Zambrano N, Patriarca E, De Falco S, Minchiotti G, Stunnenberg HG, Altucci L (2013) The class I-specific HDAC inhibitor MS-275 modulates the differentiation potential of mouse embryonic stem cells. Biol Open 2:1070-1077.

Francis YI, Fa M, Ashraf H, Zhang H, Staniszewski A, Latchman DS, Arancio O (2009) Dysregulation of histone acetylation in the APP/PS1 mouse model of Alzheimer's disease. Journal of Alzheimer's disease : JAD 18:131-139.

Frank-Cannon TC, Alto LT, McAlpine FE, Tansey MG (2009) Does neuroinflammation fan the flame in neurodegenerative diseases? Mol Neurodegener 4:47.

Gajer JM, Furdas SD, Grunder A, Gothwal M, Heinicke U, Keller K, Colland F, Fulda S, Pahl HL, Fichtner I, Sippl W, Jung M (2015) Histone acetyltransferase inhibitors block neuroblastoma cell growth in vivo. Oncogenesis 4:e137.

Galli M, Van Gool F, Leo O (2011) Sirtuins and inflammation: Friends or foes? Biochemical pharmacology 81:569-576.

Gavet O, Pines J (2012) Progressive activation of CyclinB1-Cdk1 coordinates entry to mitosis. Dev Cell 18:533-543.

Gelb MH, Valentin E, Ghomashchi F, Lazdunski M, Lambeau G (2000) Cloning and recombinant expression of a structurally novel human secreted phospholipase A2. J Biol Chem 275:39823-39826.

Ghizzoni M, Haisma HJ, Maarsingh H, Dekker FJ (2011) Histone acetyltransferases are crucial regulators in NF-kappaB mediated inflammation. Drug discovery today 16:504-511.

Ghosh M, Tucker DE, Burchett SA, Leslie CC (2006) Properties of the Group IV phospholipase A2 family. Progress in lipid research 45:487-510.

Gilany K, Van Elzen R, Mous K, Coen E, Van Dongen W, Vandamme S, Gevaert K, Timmerman E, Vandekerckhove J, Dewilde S, Van Ostade X, Moens L (2008) The proteome of the human neuroblastoma cell line SH-SY5Y: an enlarged proteome. Biochimica et biophysica acta 1784:983-985.

Glass CK, Saijo K, Winner B, Marchetto MC, Gage FH (2010a) Mechanisms underlying inflammation in neurodegeneration. Cell 140:918-934.

Glass CK, Saijo K, Winner B, Marchetto MC, Gage FH (2010b) Mechanisms Underlying Inflammation in Neurodegeneration. Cell 140:918-934.

Goate A, Chartier-Harlin MC, Mullan M, Brown J, Crawford F, Fidani L, Giuffra L, Haynes A, Irving N, James L, et al. (1991) Segregation of a missense mutation in the amyloid precursor protein gene with familial Alzheimer's disease. Nature 349:704-706.

Gomathinayagam R, Sowmyalakshmi S, Mardhatillah F, Kumar R, Akbarsha MA, Damodaran C (2008) Anticancer mechanism of plumbagin, a natural compound, on non-small cell lung cancer cells. Anticancer Res 28:785-792.

Grant WB, Campbell A, Itzhaki RF, Savory J (2002) The significance of environmental factors in the etiology of Alzheimer's disease. J Alzheimers Dis 4:179-189.

Guo C, Li J, Myatt L, Zhu X, Sun K (2010) Induction of Galphas contributes to the paradoxical stimulation of cytosolic phospholipase A2alpha expression by cortisol in human amnion fibroblasts. Molecular endocrinology (Baltimore, Md) 24:1052-1061.

Gurvich N, Tsygankova OM, Meinkoth JL, Klein PS (2004) Histone deacetylase is a target of valproic acid-mediated cellular differentiation. Cancer Res 64:1079-1086.

Haggarty SJ, Koeller KM, Wong JC, Grozinger CM, Schreiber SL (2003) Domain-selective small-molecule inhibitor of histone deacetylase 6 (HDAC6)-mediated tubulin deacetylation. Proceedings of the National Academy of Sciences 100:4389-4394.

Harikrishnan KN, Karagiannis TC, Chow MZ, El-Osta A (2008) Effect of valproic acid on radiation-induced DNA damage in euchromatic and heterochromatic compartments. Cell Cycle 7:468-476.

He S, Sun JM, Li L, Davie JR (2005) Differential intranuclear organization of transcription factors Sp1 and Sp3. Molecular biology of the cell 16:4073-4083.

Hebert LE, Scherr PA, Bienias JL, Bennett DA, Evans DA (2003) Alzheimer disease in the US population: prevalence estimates using the 2000 census. Arch Neurol 60:1119-1122.

Hensley K (2010) Neuroinflammation in Alzheimer's Disease: Mechanisms, Pathologic Consequences, and Potential for Therapeutic Manipulation. Journal of Alzheimer's disease : JAD 21:1-14.

Heo HJ, Lee CY (2004) Protective effects of quercetin and vitamin C against oxidative stress-induced neurodegeneration. Journal of agricultural and food chemistry 52:7514-7517.

Herbert MK, Eeftens JM, Aerts MB, Esselink RA, Bloem BR, Kuiperij HB, Verbeek MM (2014) CSF levels of DJ-1 and tau distinguish MSA patients from PD patients and controls. Parkinsonism Relat Disord 20:112-115.

Hernandez M, Bayon Y, Sanchez Crespo M, Nieto ML (1999) Signaling mechanisms involved in the activation of arachidonic acid metabolism in human astrocytoma cells by tumor necrosis factor-alpha: phosphorylation of cytosolic phospholipase A2 and transactivation of cyclooxygenase-2. J Neurochem 73:1641-1649.

Herranz M, Esteller M (2007) DNA methylation and histone modifications in patients with cancer: potential prognostic and therapeutic targets. Methods Mol Biol 361:25-62.

Hezroni H, Sailaja BS, Meshorer E (2011) Pluripotency-related, valproic acid (VPA)-induced genome-wide histone H3 lysine 9 (H3K9) acetylation patterns in embryonic stem cells. The Journal of biological chemistry 286:35977-35988.

Hirsch EC, Vyas S, Hunot S (2012) Neuroinflammation in Parkinson's disease. Parkinsonism Relat Disord 18 Suppl 1:S210-212.

Hong J, Sang S, Park HJ, Kwon SJ, Suh N, Huang MT, Ho CT, Yang CS (2006) Modulation of arachidonic acid metabolism and nitric oxide synthesis by garcinol and its derivatives. Carcinogenesis 27:278-286.

Hsieh H-L, Yang C-M (2013) Role of redox signaling in neuroinflammation and neurodegenerative diseases. BioMed research international 2013.

Hsu YH, Burke JE, Stephens DL, Deems RA, Li S, Asmus KM, Woods VL, Jr., Dennis EA (2008) Calcium binding rigidifies the C2 domain and the intradomain interaction of GIVA phospholipase A2 as revealed by hydrogen/deuterium exchange mass spectrometry. J Biol Chem 283:9820-9827.

Huang H-C, Tang D, Xu K, Jiang Z-F (2014) Curcumin attenuates amyloid-β-induced tau hyperphosphorylation in human neuroblastoma SH-SY5Y cells involving PTEN/Akt/GSK-3β signaling pathway. Journal of Receptors and Signal Transduction 34:26-37.

Huang J, Kent JR, Placek B, Whelan KA, Hollow CM, Zeng PY, Fraser NW, Berger SL (2006) Trimethylation of histone H3 lysine 4 by Set1 in the lytic infection of human herpes simplex virus 1. Journal of virology 80:5740-5746.

Huang PH, Plass C, Chen CS (2011) Effects of Histone Deacetylase Inhibitors on Modulating H3K4 Methylation Marks - A Novel Cross-Talk Mechanism between Histone-Modifying Enzymes. Molecular and cellular pharmacology 3:39-43.

International AsD (2010) World Alzheimer Report 2010: The Global Economic Impact of Dementia. p 2.

Ishizawa K, Dickson DW (2001) Microglial activation parallels system degeneration in progressive supranuclear palsy and corticobasal degeneration. J Neuropathol Exp Neurol 60:647-657.

Iyer NG, Ozdag H, Caldas C (2004) p300/CBP and cancer. Oncogene 23:4225-4231.

Jafarian-Tehrani M (2009) Neuroinflammation – LPS-induced Acute Neuroinflammation, Rat Model. In: Encyclopedia of Neuroscience (Binder, M. et al., eds), pp 2720-2722: Springer Berlin Heidelberg.

Jämsä A, Hasslund K, Cowburn RF, Bäckström A, Vasänge M (2004) The retinoic acid and brain-derived neurotrophic factor differentiated SH-SY5Y cell line as a model for Alzheimer's disease-like tau phosphorylation. Biochemical and Biophysical Research Communications 319:993-1000.

Jenuwein T, Allis CD (2001) Translating the histone code. Science 293:1074-1080.

Jeong MR, Hashimoto R, Senatorov VV, Fujimaki K, Ren M, Lee MS, Chuang DM (2003) Valproic acid, a mood stabilizer and anticonvulsant, protects rat cerebral cortical neurons from spontaneous cell death: a role of histone deacetylase inhibition. FEBS letters 542:74-78.

Kalaria RN, Maestre GE, Arizaga R, Friedland RP, Galasko D, Hall K, Luchsinger JA, Ogunniyi A, Perry EK, Potocnik F, Prince M, Stewart R, Wimo A, Zhang ZX, Antuono P (2008) Alzheimer's disease and vascular dementia in developing countries: prevalence, management, and risk factors. Lancet Neurol 7:812-826.

Kalra EK (2003) Nutraceutical--definition and introduction. AAPS PharmSci 5:E25.

Kang JH, Irwin DJ, Chen-Plotkin AS, Siderowf A, Caspell C, Coffey CS, Waligorska T, Taylor P, Pan S, Frasier M, Marek K, Kieburtz K, Jennings D, Simuni T, Tanner CM, Singleton A, Toga AW, Chowdhury S, Mollenhauer B, Trojanowski JQ, Shaw LM (2013) Association of cerebrospinal fluid beta-amyloid 1-42, T-tau, P-tau181, and alpha-synuclein levels with clinical features of drug-naive patients with early Parkinson disease. JAMA Neurol 70:1277-1287.

Karmodiya K, Krebs A, Oulad-Abdelghani M, Kimura H, Tora L (2012) H3K9 and H3K14 acetylation co-occur at many gene regulatory elements, while H3K14ac marks a subset of inactive inducible promoters in mouse embryonic stem cells. BMC Genomics 13:1-18.

Kelsey NA, Wilkins HM, Linseman DA (2010) Nutraceutical antioxidants as novel neuroprotective agents. Molecules 15:7792-7814.

Kennedy PJ, Feng J, Robison AJ, Maze I, Badimon A, Mouzon E, Chaudhury D, Damez-Werno DM, Haggarty SJ, Han MH, Bassel-Duby R, Olson EN, Nestler EJ (2013) Class I HDAC inhibition blocks cocaine-induced plasticity by targeted changes in histone methylation. Nat Neurosci 16:434-440.

Kent WJ, Sugnet CW, Furey TS, Roskin KM, Pringle TH, Zahler AM, Haussler D (2002) The human genome browser at UCSC. Genome research 12:996-1006.

Khan N, Jeffers M, Kumar S, Hackett C, Boldog F, Khramtsov N, Qian X, Mills E, Berghs SC, Carey N, Finn PW, Collins LS, Tumber A, Ritchie JW, Jensen PB, Lichenstein HS, Sehested M (2008) Determination of the class and isoform selectivity of small-molecule histone deacetylase inhibitors. The Biochemical journal 409:581-589.

Khansari N, Shakiba Y, Mahmoudi M (2009) Chronic inflammation and oxidative stress as a major cause of age-related diseases and cancer. Recent Pat Inflamm Allergy Drug Discov 3:73-80.

Kigerl KA, Gensel JC, Ankeny DP, Alexander JK, Donnelly DJ, Popovich PG (2009) Identification of two distinct macrophage subsets with divergent effects causing either neurotoxicity or regeneration in the injured mouse spinal cord. J Neurosci 29:13435-13444.

Kitazawa M, Yamasaki TR, LaFerla FM (2004) Microglia as a potential bridge between the amyloid beta-peptide and tau. Ann N Y Acad Sci 1035:85-103.

Koehler NK, Stransky E, Shing M, Gaertner S, Meyer M, Schreitmuller B, Leyhe T, Laske C, Maetzler W, Kahle P, Celej MS, Jovin TM, Fallgatter AJ, Batra A, Buchkremer G, Schott K, Richartz-Salzburger E (2013) Altered serum IgG levels to alpha-synuclein in dementia with Lewy bodies and Alzheimer's disease. PLoS One 8:e64649.

Koh SH, Kwon H, Kim KS, Kim J, Kim MH, Yu HJ, Kim M, Lee KW, Do BR, Jung HK, Yang KW, Appel SH, Kim SH (2004) Epigallocatechin gallate prevents oxidative-stress-induced death of mutant Cu/Zn-superoxide dismutase (G93A) motoneuron cells by alteration of cell survival and death signals. Toxicology 202:213-225.

Kontopoulos E, Parvin JD, Feany MB (2006) Alpha-synuclein acts in the nucleus to inhibit histone acetylation and promote neurotoxicity. Human molecular genetics 15:3012-3023.

Kornberg RD (1974) Chromatin structure: a repeating unit of histones and DNA. Science 184:868-871.

Kramer RM, Sharp JD (1997) Structure, function and regulation of Ca2+-sensitive cytosolic phospholipase A2 (cPLA2). FEBS Lett 410:49-53.

Kriem B, Sponne I, Fifre A, Malaplate-Armand C, Lozac'h-Pillot K, Koziel V, Yen-Potin FT, Bihain B, Oster T, Olivier J-L, Pillot T (2005) Cytosolic phospholipase A2 mediates neuronal apoptosis induced by soluble oligomers of the amyloid-β peptide. The FASEB Journal 19:85-87.

Kunsorn P, Ruangrungsi N, Lipipun V, Khanboon A, Rungsihirunrat K, Chaijaroenkul W (2013) The identities and anti-herpes simplex virus activity of Clinacanthus nutans and Clinacanthus siamensis. Asian Pac J Trop Biomed 3:284-290.

Kuo C-H, Hsieh C-C, Lee M-S, Chang K-T, Kuo H-F, Hung C-H (2014) Epigenetic regulation in allergic diseases and related studies. Asia Pacific Allergy 4:14-18.

Kuo MH, Allis CD (1998) Roles of histone acetyltransferases and deacetylases in gene regulation. Bioessays 20:615-626.

Lagace DC, Nachtigal MW (2004) Inhibition of histone deacetylase activity by valproic acid blocks adipogenesis. Journal of Biological Chemistry 279:18851-18860.

Lambeau G, Gelb MH (2008) Biochemistry and physiology of mammalian secreted phospholipases A2. Annu Rev Biochem 77:495-520.

Larsson Forsell PK, Kennedy BP, Claesson HE (1999) The human calcium-independent phospholipase A2 gene multiple enzymes with distinct properties from a single gene. Eur J Biochem 262:575-585.

Larsson PK, Claesson HE, Kennedy BP (1998) Multiple splice variants of the human calcium-independent phospholipase A2 and their effect on enzyme activity. J Biol Chem 273:207-214.

Lau OD, Kundu TK, Soccio RE, Ait-Si-Ali S, Khalil EM, Vassilev A, Wolffe AP, Nakatani Y, Roeder RG, Cole PA (2000) HATs off: selective synthetic inhibitors of the histone acetyltransferases p300 and PCAF. Mol Cell 5:589-595.

Lautens LL, Chiou XG, Sharp JD, Young WS, 3rd, Sprague DL, Ross LS, Felder CC (1998) Cytosolic phospholipase A2 (cPLA2) distribution in murine brain and functional studies indicate that cPLA2 does not participate in muscarinic receptor-mediated signaling in neurons. Brain Res 809:18-30.

Lee AC (2009) Global burden of neurological disorders. Global Health Education Consortium.

Lee SH, Cho YD (1998) Induction of Apoptosis in Leukemia U937 Cells by 5′-Deoxy-5′-methylthioadenosine, a Potent Inhibitor of Protein Carboxylmethyltransferase. Experimental Cell Research 240:282-292.

Leslie CC (1997) Properties and regulation of cytosolic phospholipase A2. The Journal of biological chemistry 272:16709-16712.

Li C, Fang D, Yong L, Fengrui W, Biao D, Rong W, Wenyong L (2015) Comparative analysis of H3K9 acetylation level in parthenogenetic, and in vitro and in vivo developed mouse embryos. Yi chuan = Hereditas / Zhongguo yi chuan xue hui bian ji 37:77-83.

Lin L-L, Wartmann M, Lin AY, Knopf JL, Seth A, Davis RJ (1993) cPLA2 is phosphorylated and activated by MAP kinase. Cell 72:269-278.

Liscovitch M (1994) Signal-activated phospholipases.

Liu L, Scolnick DM, Trievel RC, Zhang HB, Marmorstein R, Halazonetis TD, Berger SL (1999) p53 Sites Acetylated In Vitro by PCAF and p300 Are Acetylated In Vivo in Response to DNA Damage. Molecular and Cellular Biology 19:1202-1209.

Liu NK, Deng LX, Zhang YP, Lu QB, Wang XF, Hu JG, Oakes E, Bonventre JV, Shields CB, Xu XM (2014) Cytosolic phospholipase A2 protein as a novel therapeutic target for spinal cord injury. Annals of neurology 75:644-658.

Livak KJ, Schmittgen TD (2001) Analysis of relative gene expression data using real-time quantitative PCR and the 2(-Delta Delta C(T)) Method. Methods 25:402-408.

Lohse B, Kristensen JL, Kristensen LH, Agger K, Helin K, Gajhede M, Clausen RP (2011) Inhibitors of histone demethylases. Bioorganic & Medicinal Chemistry 19:3625-3636.

Loizou S, Lekakis I, Chrousos GP, Moutsatsou P (2010) Beta-sitosterol exhibits anti-inflammatory activity in human aortic endothelial cells. Mol Nutr Food Res 54:551-558.

Lopes FM, Schroder R, da Frota ML, Jr., Zanotto-Filho A, Muller CB, Pires AS, Meurer RT, Colpo GD, Gelain DP, Kapczinski F, Moreira JC, Fernandes Mda C, Klamt F (2010) Comparison between proliferative and neuron-like SH-SY5Y cells as an in vitro model for Parkinson disease studies. Brain Res 1337:85-94.

Loring JF, Wen X, Lee JM, Seilhamer J, Somogyi R (2001) A gene expression profile of Alzheimer's disease. DNA Cell Biol 20:683-695.

Lozano D, Gonzales-Portillo GS, Acosta S, de la Pena I, Tajiri N, Kaneko Y, Borlongan CV (2015) Neuroinflammatory responses to traumatic brain injury: etiology, clinical consequences, and therapeutic opportunities. Neuropsychiatric Disease and Treatment 11:97-106.

Lu XR, Ong WY, Halliwell B, Horrocks LA, Farooqui AA (2001) Differential effects of calcium-dependent and calcium-independent phospholipase A(2) inhibitors on kainate-induced neuronal injury in rat hippocampal slices. Free radical biology & medicine 30:1263-1273.

Lucas T, Waisman A, Ranjan R, Roes J, Krieg T, Muller W, Roers A, Eming SA (2010) Differential roles of macrophages in diverse phases of skin repair. J Immunol 184:3964-3977.

Lukiw W, Bazan N (2000) Neuroinflammatory Signaling Upregulation in Alzheimer's Disease. Neurochem Res 25:1173-1184.

Lukiw WJ, Cui JG, Marcheselli VL, Bodker M, Botkjaer A, Gotlinger K, Serhan CN, Bazan NG (2005) A role for docosahexaenoic acid-derived neuroprotectin D1 in neural cell survival and Alzheimer disease. J Clin Invest 115:2774-2783.

Lull ME, Block ML (2010) Microglial Activation & Chronic Neurodegeneration. Neurotherapeutics : the journal of the American Society for Experimental NeuroTherapeutics 7:354-365.

Luo Y, Jian W, Stavreva D, Fu X, Hager G, Bungert J, Huang S, Qiu Y (2009) Trans-regulation of histone deacetylase activities through acetylation. The Journal of biological chemistry 284:34901-34910.

Makki MS, Heinzel T, Englert C (2008) TSA downregulates Wilms tumor gene 1 (Wt1) expression at multiple levels. Nucleic Acids Res 36:4067-4078.

Malapeira J, Khaitova LC, Mas P (2012) Ordered changes in histone modifications at the core of the Arabidopsis circadian clock. Proceedings of the National Academy of Sciences of the United States of America 109:21540-21545.

Malmberg NJ, Van Buskirk DR, Falke JJ (2003) Membrane-docking loops of the cPLA2 C2 domain: detailed structural analysis of the protein-membrane interface via site-directed spin-labeling. Biochemistry 42:13227-13240.

Mancuso DJ, Jenkins CM, Gross RW (2000) The genomic organization, complete mRNA sequence, cloning, and expression of a novel human intracellular membrane-associated calcium-independent phospholipase A(2). J Biol Chem 275:9937-9945.

Mandal A, Ojha D, Lalee A, Kaity S, Das M, Chattopadhyay D, Samanta A (2014) Bioassay directed isolation of a novel anti-inflammatory cerebroside from the leaves of Aerva sanguinolenta. Medicinal Chemistry Research 1-12.

Marcheselli VL, Hong S, Lukiw WJ, Tian XH, Gronert K, Musto A, Hardy M, Gimenez JM, Chiang N, Serhan CN, Bazan NG (2003) Novel docosanoids inhibit brain ischemia-reperfusion-mediated leukocyte infiltration and pro-inflammatory gene expression. J Biol Chem 278:43807-43817.

Marcu MG, Jung YJ, Lee S, Chung EJ, Lee MJ, Trepel J, Neckers L (2006) Curcumin is an inhibitor of p300 histone acetylatransferase. Medicinal chemistry (Shariqah (United Arab Emirates)) 2:169-174.

Mariadason JM, Corner GA, Augenlicht LH (2000) Genetic reprogramming in pathways of colonic cell maturation induced by short chain fatty acids: comparison with trichostatin A, sulindac, and curcumin and implications for chemoprevention of colon cancer. Cancer research 60:4561-4572.

Marks PA (2010) Histone deacetylase inhibitors: a chemical genetics approach to understanding cellular functions. Biochimica et biophysica acta 1799:717-725.

Marmorstein R (2001) Structure and function of histone acetyltransferases. Cell Mol Life Sci 58:693-703.

Martinez-Diaz MA, Che L, Albornoz M, Seneda MM, Collis D, Coutinho AR, El-Beirouthi N, Laurin D, Zhao X, Bordignon V (2010) Pre- and postimplantation development of swine-cloned embryos derived from fibroblasts and bone marrow cells after inhibition of histone deacetylases. Cellular reprogramming 12:85-94.

Mattson MP (2000) Apoptosis in neurodegenerative disorders. Nat Rev Mol Cell Biol 1:120-130.

McLean LR, Hagaman KA, Davidson WS (1993) Role of lipid structure in the activation of phospholipase A2 by peroxidized phospholipids. Lipids 28:505-509.

Medicine BCo (2013) Human Epigenome Atlas. vol. 9.

Meeran SM, Patel SN, Chan TH, Tollefsbol TO (2011) A novel prodrug of epigallocatechin-3-gallate: differential epigenetic hTERT repression in human breast cancer cells. Cancer Prev Res (Phila) 4:1243-1254.

Migliore L, Coppedè F (2009) Genetics, environmental factors and the emerging role of epigenetics in neurodegenerative diseases. Mutation Research/Fundamental and Molecular Mechanisms of Mutagenesis 667:82-97.

Miller AA, Spencer SJ (2014) Obesity and neuroinflammation: A pathway to cognitive impairment. Brain, Behavior, and Immunity 42:10-21.

Moller T (2010) Neuroinflammation in Huntington's disease. J Neural Transm 117:1001-1008.

Molloy GY, Rattray M, Williams RJ (1998) Genes encoding multiple forms of phospholipase A2 are expressed in rat brain. Neurosci Lett 258:139-142.

Monti B, Polazzi E, Contestabile A (2009) Biochemical, molecular and epigenetic mechanisms of valproic acid neuroprotection. Curr Mol Pharmacol 2:95-109.

Morii H, Ozaki M, Watanabe Y (1994a) 5'-flanking region surrounding a human cytosolic phospholipase a2 gene. Biochemical and Biophysical Research Communications 205:6-11.

Morii H, Ozaki M, Watanabe Y (1994b) 5′-Flanking Region Surrounding a Human Cytosolic Phospholipase A2 Gene. Biochemical and Biophysical Research Communications 205:6-11.

Morimoto T, Sunagawa Y, Kawamura T, Takaya T, Wada H, Nagasawa A, Komeda M, Fujita M, Shimatsu A, Kita T, Hasegawa K (2008) The dietary compound curcumin inhibits p300 histone acetyltransferase activity and prevents heart failure in rats. The Journal of clinical investigation 118:868-878.

Morris JC, Roe CM, Xiong C, Fagan AM, Goate AM, Holtzman DM, Mintun MA (2010) APOE predicts amyloid-beta but not tau Alzheimer pathology in cognitively normal aging. Ann Neurol 67:122-131.

Morris KV, Chan SW-L, Jacobsen SE, Looney DJ (2004) Small interfering RNA-induced transcriptional gene silencing in human cells. Science 305:1289-1292.

Morris MC (2009) The role of nutrition in Alzheimer's disease: epidemiological evidence. European Journal of Neurology 16:1-7.

Mroz RM, Noparlik J, Chyczewska E, Braszko JJ, Holownia A (2007) Molecular basis of chronic inflammation in lung diseases: new therapeutic approach. J Physiol Pharmacol 58 Suppl 5:453-460.

Muhlethaler-Mottet A, Meier R, Flahaut M, Bourloud KB, Nardou K, Joseph JM, Gross N (2008) Complex molecular mechanisms cooperate to mediate histone deacetylase inhibitors anti-tumour activity in neuroblastoma cells. Molecular cancer 7:55.

Murakami M, Kudo I (2002) Phospholipase A2. J Biochem 131:285-292.

Murakami M, Nakatani Y, Atsumi G, Inoue K, Kudo I (1997) Regulatory functions of phospholipase A2. Crit Rev Immunol 17:225-283.

Murakami M, Taketomi Y, Sato H, Yamamoto K (2011) Secreted phospholipase A2 revisited. J Biochem 150:233-255.

Nelson PT, Alafuzoff I, Bigio EH, Bouras C, Braak H, Cairns NJ, Castellani RJ, Crain BJ, Davies P, Del Tredici K, Duyckaerts C, Frosch MP, Haroutunian V, Hof PR, Hulette CM, Hyman BT, Iwatsubo T, Jellinger KA, Jicha GA, Kövari E, Kukull WA, Leverenz JB, Love S, Mackenzie IR, Mann DM, Masliah E, McKee AC, Montine TJ, Morris JC, Schneider JA, Sonnen JA, Thal DR, Trojanowski JQ, Troncoso JC, Wisniewski T, Woltjer RL, Beach TG (2012) Correlation of Alzheimer Disease Neuropathologic Changes With Cognitive Status: A Review of the Literature. Journal of neuropathology and experimental neurology 71:362-381.

Newman SP, Croxtall JD, Choudhury Q, Flower RJ (1997) The co-ordinate regulation of lipocortin 1, COX 2 and CPLA, by IL-1 beta in A549 cells. In: Eicosanoids and Other Bioactive Lipids in Cancer, Inflammation, and Radiation Injury 3, vol. 407 (Honn, K. V. et al., eds), pp 249-253.

Nightingale KP, Gendreizig S, White DA, Bradbury C, Hollfelder F, Turner BM (2007) Cross-talk between histone modifications in response to histone deacetylase inhibitors: MLL4 links histone H3 acetylation and histone H3K4 methylation. J Biol Chem 282:4408-4416.

O'Callaghan JP, Sriram K, Miller DB (2008) Defining "neuroinflammation". Ann N Y Acad Sci 1139:318-330.

Oike T, Ogiwara H, Torikai K, Nakano T, Yokota J, Kohno T (2012) Garcinol, a histone acetyltransferase inhibitor, radiosensitizes cancer cells by inhibiting non-homologous end joining. Int J Radiat Oncol Biol Phys 84:815-821.

Ong W-Y, Farooqui T, Farooqui A (2010) Involvement of cytosolic phospholipase A2, calcium independent phospholipase A2 and plasmalogen selective phospholipase A2 in neurodegenerative and neuropsychiatric conditions. Current medicinal chemistry 17:2746-2763.

Ong WY, Sandhya TL, Horrocks LA, Farooqui AA (1999) Distribution of cytoplasmic phospholipase A2 in the normal rat brain. J Hirnforsch 39:391-400.

Ong WY, Yeo JF, Ling SF, Farooqui AA (2005) Distribution of calcium-independent phospholipase A2 (iPLA 2) in monkey brain. J Neurocytol 34:447-458.

Owada Y, Tominaga T, Yoshimoto T, Kondo H (1994) Molecular cloning of rat cDNA for cytosolic phospholipase A2 and the increased gene expression in the dentate gyrus following transient forebrain ischemia. Brain research Molecular brain research 25:364-368.

Park B, Sung B, Yadav VR, Chaturvedi MM, Aggarwal BB (2011) Triptolide, histone acetyltransferase inhibitor, suppresses growth and chemosensitizes leukemic cells through inhibition of gene expression regulated by TNF-TNFR1-TRADD-TRAF2-NIK-TAK1-IKK pathway. Biochem Pharmacol 82:1134-1144.

Patel HC, Boutin H, Allan SM (2003) Interleukin-1 in the brain: mechanisms of action in acute neurodegeneration. Ann N Y Acad Sci 992:39-47.

Pavicevic Z, Leslie CC, Malik KU (2008) cPLA2 phosphorylation at serine-515 and serine-505 is required for arachidonic acid release in vascular smooth muscle cells. Journal of lipid research 49:724-737.

Philips T, Robberecht W (2011) Neuroinflammation in amyotrophic lateral sclerosis: role of glial activation in motor neuron disease. Lancet Neurol 10:253-263.

Piomelli D (1993) Arachidonic acid in cell signaling. Curr Opin Cell Biol 5:274-280.

Pompeia C, Lima T, Curi R (2003) Arachidonic acid cytotoxicity: can arachidonic acid be a physiological mediator of cell death? Cell Biochemistry and Function 21:97-104.

Pongphasuk N, Khunkitti W (1996) Anti-inflammatory and Analgesic Activities of the Extract from Garcinia mangostana Linn. Traditional Medicine and Nutraceuticals 6:125-130.

Portela A, Esteller M (2010) Epigenetic modifications and human disease. Nat Biotech 28:1057-1068.

Przedborski S, Vila M, Jackson-Lewis V (2003) Series Introduction: Neurodegeneration: What is it and where are we? The Journal of Clinical Investigation 111:3-10.

Pu F, Mishima K, Irie K, Motohashi K, Tanaka Y, Orito K, Egawa T, Kitamura Y, Egashira N, Iwasaki K, Fujiwara M (2007) Neuroprotective effects of quercetin and rutin on spatial memory impairment in an 8-arm radial maze task and neuronal death induced by repeated cerebral ischemia in rats. J Pharmacol Sci 104:329-334.

Pufahl L, Katryniok C, Schnur N, Sorg BL, Metzner J, Grez M, Steinhilber D (2012) Trichostatin A induces 5-lipoxygenase promoter activity and mRNA expression via inhibition of histone deacetylase 2 and 3. Journal of cellular and molecular medicine 16:1461-1473.

Rapoport M, Dawson HN, Binder LI, Vitek MP, Ferreira A (2002) Tau is essential to β-amyloid-induced neurotoxicity. Proceedings of the National Academy of Sciences 99:6364-6369.

Raven EP, Lu PH, Tishler TA, Heydari P, Bartzokis G (2013) Increased Iron Levels and Decreased Tissue Integrity in Hippocampus of Alzheimer's Disease Detected in vivo with Magnetic Resonance Imaging. Journal of Alzheimer's Disease 37:127-136.

Ravindra KC, Selvi BR, Arif M, Reddy BAA, Thanuja GR, Agrawal S, Pradhan SK, Nagashayana N, Dasgupta D, Kundu TK (2009) Inhibition of lysine acetyltransferase KAT3B/ p300 activity by a naturally occurring, hydroxynaphthoquinone, plumbagin. Journal of Biological Chemistry.

Reuter S, Gupta SC, Park B, Goel A, Aggarwal BB (2011) Epigenetic changes induced by curcumin and other natural compounds. Genes & Nutrition 6:93-108.

Rice JC, Allis CD (2001) Histone methylation versus histone acetylation: new insights into epigenetic regulation. Curr Opin Cell Biol 13:263-273.

Ridet JL, Privat A, Malhotra SK, Gage FH (1997) Reactive astrocytes: cellular and molecular cues to biological function. Trends in Neurosciences 20:570-577.

Ritchie K, Kildea D (1995) Is senile dementia "age-related" or "ageing-related"? —evidence from meta-analysis of dementia prevalence in the oldest old. The Lancet 346:931-934.

Rogaev EI, Sherrington R, Rogaeva EA, Levesque G, Ikeda M, Liang Y, Chi H, Lin C, Holman K, Tsuda T, et al. (1995) Familial Alzheimer's disease in kindreds with missense mutations in a gene on chromosome 1 related to the Alzheimer's disease type 3 gene. Nature 376:775-778.

Ross BM, Moszczynska A, Erlich J, Kish SJ (1998) Low activity of key phospholipid catabolic and anabolic enzymes in human substantia nigra: possible implications for Parkinson's disease. Neuroscience 83:791-798.

Roth SY, Denu JM, Allis CD (2001) HISTONE ACETYLTRANSFERASES. Annual Review of Biochemistry 70:81-120.

Russo VE, Martienssen RA, Riggs AD (1996) Epigenetic mechanisms of gene regulation: Cold Spring Harbor Laboratory Press.

Sakdarat S, Shuyprom A, Ayudhya T, Waterman PG, Karagianis G (2006) Chemical composition investigation of the Clinacanthus nutans Lindau leaves. Thai Journal of Phytopharmacy 13:14-24.

Sakdarat S, Shuyprom A, Pientong C, Ekalaksananan T, Thongchai S (2009) Bioactive constituents from the leaves of Clinacanthus nutans Lindau. Bioorganic & Medicinal Chemistry 17:1857-1860.

Saleem M (2009) Lupeol, a novel anti-inflammatory and anti-cancer dietary triterpene. Cancer Lett 285:109-115.

Sandhya TL, Ong WY, Horrocks LA, Farooqui AA (1998) A light and electron microscopic study of cytoplasmic phospholipase A2 and cyclooxygenase-2 in the hippocampus after kainate lesions. Brain Res 788:223-231.

Sandur SK, Ichikawa H, Sethi G, Ahn KS, Aggarwal BB (2006) Plumbagin (5-hydroxy-2-methyl-1,4-naphthoquinone) suppresses NF-kappaB activation and NF-kappaB-regulated gene products through modulation of p65 and IkappaBalpha kinase activation, leading to potentiation of apoptosis induced by cytokine and chemotherapeutic agents. J Biol Chem 281:17023-17033.

Santer FR, Hoschele PP, Oh SJ, Erb HH, Bouchal J, Cavarretta IT, Parson W, Meyers DJ, Cole PA, Culig Z (2011) Inhibition of the acetyltransferases p300 and CBP reveals a targetable function for p300 in the survival and

invasion pathways of prostate cancer cell lines. Molecular cancer therapeutics 10:1644-1655.

Schaeffer EL, Forlenza OV, Gattaz WF (2009) Phospholipase A2 activation as a therapeutic approach for cognitive enhancement in early-stage Alzheimer disease. Psychopharmacology (Berl) 202:37-51.

Schiltz RL, Mizzen CA, Vassilev A, Cook RG, Allis CD, Nakatani Y (1999) Overlapping but distinct patterns of histone acetylation by the human coactivators p300 and PCAF within nucleosomal substrates. J Biol Chem 274:1189-1192.

Schroeder EK, Kelsey NA, Doyle J, Breed E, Bouchard RJ, Loucks FA, Harbison RA, Linseman DA (2009) Green tea epigallocatechin 3-gallate accumulates in mitochondria and displays a selective antiapoptotic effect against inducers of mitochondrial oxidative stress in neurons. Antioxid Redox Signal 11:469-480.

Schwab JM, Chiang N, Arita M, Serhan CN (2007) Resolvin E1 and protectin D1 activate inflammation-resolution programmes. Nature 447:869-874.

Scorrano L, Penzo D, Petronilli V, Pagano F, Bernardi P (2001) Arachidonic Acid Causes Cell Death through the Mitochondrial Permeability Transition: Implications for tumor necrosis factor-α apoptotic signaling. Journal of Biological Chemistry 276:12035-12040.

Seashols SJ, del Castillo Olivares A, Gil G, Barbour SE (2004) Regulation of group VIA phospholipase A2 expression by sterol availability. Biochim Biophys Acta 1684:29-37.

Serhan CN (2004) A search for endogenous mechanisms of anti-inflammation uncovers novel chemical mediators: missing links to resolution. Histochem Cell Biol 122:305-321.

Serhan CN, Haeggstrom JZ, Leslie CC (1996) Lipid mediator networks in cell signaling: update and impact of cytokines. Faseb j 10:1147-1158.

Shalini SM, Chew WS, Rajkumar R, Dawe GS, Ong WY (2014) Role of constitutive calcium-independent phospholipase A2 beta in hippocampo-prefrontal cortical long term potentiation and spatial working memory. Neurochem Int 78:96-104.

Sheridan AM, Force T, Yoon HJ, O'Leary E, Choukroun G, Taheri MR, Bonventre JV (2001) PLIP, a novel splice variant of Tip60, interacts with group IV cytosolic phospholipase A(2), induces apoptosis, and potentiates prostaglandin production. Molecular and cellular biology 21:4470-4481.

Sherrington R, Rogaev EI, Liang Y, Rogaeva EA, Levesque G, Ikeda M, Chi H, Lin C, Li G, Holman K, Tsuda T, Mar L, Foncin JF, Bruni AC,

Montesi MP, Sorbi S, Rainero I, Pinessi L, Nee L, Chumakov I, Pollen D, Brookes A, Sanseau P, Polinsky RJ, Wasco W, Da Silva HA, Haines JL, Perkicak-Vance MA, Tanzi RE, Roses AD, Fraser PE, Rommens JM, St George-Hyslop PH (1995) Cloning of a gene bearing missense mutations in early-onset familial Alzheimer's disease. Nature 375:754-760.

Shivika R, K. PK, N. C, S. R (2014) Glial Activation and Synaptic Neurotoxicity in Alzheimer's disease: A Focus on Neuroinflammation. . Pharmacologia 5:286-297.

Sike Á, Nagy E, Vedelek B, Pusztai D, Szerémy P, Venetianer A, Boros IM TSA treatment increases H3K9ac levels at the 5′ region of both rat Abcb1 genes.

Skaper SD (2012) Alzheimer's disease and amyloid: culprit or coincidence? Int Rev Neurobiol 102:277-316.

Smitinand T (1980) Thai Plant Names (Botanical Names - Vernacular Names). Royal Forest Department, Phahonyothin, Bangkhen, Bangkok, Thailand.

Soderberg M, Edlund C, Kristensson K, Dallner G (1991) Fatty acid composition of brain phospholipids in aging and in Alzheimer's disease. Lipids 26:421-425.

Soehnlein O, Lindbom L (2010) Phagocyte partnership during the onset and resolution of inflammation. Nat Rev Immunol 10:427-439.

Song C, Kanthasamy A, Anantharam V, Sun F, Kanthasamy AG (2010) Environmental neurotoxic pesticide increases histone acetylation to promote apoptosis in dopaminergic neuronal cells: relevance to epigenetic mechanisms of neurodegeneration. Molecular pharmacology 77:621-632.

Soto C (2003) Unfolding the role of protein misfolding in neurodegenerative diseases. Nat Rev Neurosci 4:49-60.

Sreena K, Molly M, Sujith SN (2012) Isolation of constituent from Clinacanthus siamensis and its anti-inflammatory studies. International Journal of Research in Pharmacy and Chemistry 2:1099-1103.

Stephenson DT, Lemere CA, Selkoe DJ, Clemens JA (1996) Cytosolic phospholipase A2 (cPLA2) immunoreactivity is elevated in Alzheimer's disease brain. Neurobiol Dis 3:51-63.

Stephenson DT, Manetta JV, White DL, Chiou XG, Cox L, Gitter B, May PC, Sharp JD, Kramer RM, Clemens JA (1994) Calcium-sensitive cytosolic phospholipase A2 (cPLA2) is expressed in human brain astrocytes. Brain Res 637:97-105.

Strahl BD, Allis CD (2000) The language of covalent histone modifications. Nature 403:41-45.

Streit WJ, Mrak RE, Griffin WST (2004) Microglia and neuroinflammation: a pathological perspective. Journal of Neuroinflammation 1:14-14.

Strokin M, Chechneva O, Reymann KG, Reiser G (2006) Neuroprotection of rat hippocampal slices exposed to oxygen-glucose deprivation by enrichment with docosahexaenoic acid and by inhibition of hydrolysis of docosahexaenoic acid-containing phospholipids by calcium independent phospholipase A2. Neuroscience 140:547-553.

Strokin M, Sergeeva M, Reiser G (2003) Docosahexaenoic acid and arachidonic acid release in rat brain astrocytes is mediated by two separate isoforms of phospholipase A(2) and is differently regulated by cyclic AMP and Ca(2+). British Journal of Pharmacology 139:1014-1022.

Sullivan KE, Reddy ABM, Dietzmann K, Suriano AR, Kocieda VP, Stewart M, Bhatia M (2007) Epigenetic Regulation of Tumor Necrosis Factor Alpha. Molecular and cellular biology 27:5147-5160.

Sun GY, He Y, Chuang DY, Lee JC, Gu Z, Simonyi A, Sun AY (2012) Integrating cytosolic phospholipase A(2) with oxidative/nitrosative signaling pathways in neurons: a novel therapeutic strategy for AD. Mol Neurobiol 46:85-95.

Sun GY, Xu J, Jensen MD, Simonyi A (2004) Phospholipase A2 in the central nervous system implications for neurodegenerative diseases. Journal of lipid research 45:205-213.

Sun Y, Jiang X, Chen S, Price BD (2006a) Inhibition of histone acetyltransferase activity by anacardic acid sensitizes tumor cells to ionizing radiation. FEBS letters 580:4353-4356.

Sun Y, Jiang X, Chen S, Price BD (2006b) Inhibition of histone acetyltransferase activity by anacardic acid sensitizes tumor cells to ionizing radiation. FEBS letters 580:4353-4356.

Sung B, Pandey MK, Ahn KS, Yi T, Chaturvedi MM, Liu M, Aggarwal BB (2008) Anacardic acid (6-nonadecyl salicylic acid), an inhibitor of histone acetyltransferase, suppresses expression of nuclear factor-kappaB-regulated gene products involved in cell survival, proliferation, invasion, and inflammation through inhibition of the inhibitory subunit of nuclear factor-kappaBalpha kinase, leading to potentiation of apoptosis. Blood 111:4880-4891.

Tanaka K, Siddiqi NJ, Alhomida AS, Farooqui AA, Ong W-Y (2012) Differential regulation of cPLA2 and iPLA2 expression in the brain. Frontiers in Biology 7:514-521.

Tang J, Kriz RW, Wolfman N, Shaffer M, Seehra J, Jones SS (1997) A Novel Cytosolic Calcium-independent Phospholipase A2 Contains Eight Ankyrin Motifs. Journal of Biological Chemistry 272:8567-8575.

Tanner CM, Ottman R, Goldman SM, Ellenberg J, Chan P, Mayeux R, Langston JW (1999) Parkinson disease in twins: an etiologic study. Jama 281:341-346.

Taubert S, Gorrini C, Frank SR, Parisi T, Fuchs M, Chan HM, Livingston DM, Amati B (2004) E2F-dependent histone acetylation and recruitment of the Tip60 acetyltransferase complex to chromatin in late G1. Mol Cell Biol 24:4546-4556.

Tay A, Maxwell P, Li Z, Goldberg H, Skorecki K (1994) Isolation of promoter for cytosolic phospholipase A2 (cPLA2). Biochim Biophys Acta 1217:345-347.

Tiangburanatam W (1996) Dictionary of Thai Medicinal Plants. fourth ed.:788-789.

Titsworth WL, Liu NK, Xu XM (2008) Role of secretory phospholipase a(2) in CNS inflammation: implications in traumatic spinal cord injury. CNS Neurol Disord Drug Targets 7:254-269.

Tornquist K, Ekokoski E, Forss L, Matsson M (1994) Importance of arachidonic acid metabolites in regulating ATP-induced calcium fluxes in thyroid FRTL-5 cells. Cell Calcium 15:153-161.

Trewick SC, McLaughlin PJ, Allshire RC (2005) Methylation: lost in hydroxylation? EMBO Reports 6:315-320.

Trimble LA, Street IP, Perrier H, Tremblay NM, Weech PK, Bernstein MA (1993) NMR Structural Studies of the Tight Complex between a Trifluoromethyl Ketone
Inhibitor and the 85-kDa Human Phospholipase A2. Biochemistry 32:12560-12565.

Trinchese F, Liu S, Battaglia F, Walter S, Mathews PM, Arancio O (2004) Progressive age-related development of Alzheimer-like pathology in APP/PS1 mice. Annals of Neurology 55:801-814.

Tsou JH, Chang KY, Wang WC, Tseng JT, Su WC, Hung LY, Chang WC, Chen BK (2007) Nucleolin regulates c-Jun/Sp1-dependent transcriptional activation of cPLA2 in phorbol ester-treated non-small cell lung cancer A549 cells. Nucleic Acids Research 36:217-227.

Tsukada Y, Fang J, Erdjument-Bromage H, Warren ME, Borchers CH, Tempst P, Zhang Y (2006) Histone demethylation by a family of JmjC domain-containing proteins. Nature 439:811-816.

Tuntiwachwuttikul P, Pootaeng-on Y, Phansa P, Taylor WC (2004) Cerebrosides and a Monoacylmonogalactosylglycerol from *Clinacanthus nutans*. Chemical and Pharmaceutical Bulletin 52:27-32.

Uawonggul N, Chaveerach A, Thammasirirak S, Arkaravichien T, Chuachan C, Daduang S (2006) Screening of plants acting against Heterometrus laoticus scorpion venom activity on fibroblast cell lysis. J Ethnopharmacol 103:201-207.

Valentin E, Lambeau G (2000) Increasing molecular diversity of secreted phospholipases A(2) and their receptors and binding proteins. Biochim Biophys Acta 1488:59-70.

Van Lint C, Emiliani S, Verdin E (1996) The expression of a small fraction of cellular genes is changed in response to histone hyperacetylation. Gene expression 5:245-253.

Varin A, Gordon S (2009) Alternative activation of macrophages: immune function and cellular biology. Immunobiology 214:630-641.

Vlad SC, Miller DR, Kowall NW, Felson DT (2008) Protective effects of NSAIDs on the development of Alzheimer disease. Neurology 70:1672-1677.

Voelter-Mahlknecht S, Ho AD, Mahlknecht U (2005) Chromosomal organization and localization of the novel class IV human histone deacetylase 11 gene. Int J Mol Med 16:589-598.

Vrba J, Trtkova K, Ulrichova J (2011) HDAC inhibitors sodium butyrate and sodium valproate do not affect human ncor1 and ncor2 gene expression in HL-60 cells. Biomed Pap Med Fac Univ Palacky Olomouc Czech Repub 155:259-262.

Wang SC, Oelze B, Schumacher A (2008) Age-specific epigenetic drift in late-onset Alzheimer's disease. PloS one 3:e2698.

Wang WY, Zhang J, Wu WY, Li J, Ma YL, Chen WH, Yan H, Wang K, Xu WW, Shen JH, Wang YP (2011) Inhibition of lipoprotein-associated phospholipase A2 ameliorates inflammation and decreases atherosclerotic plaque formation in ApoE-deficient mice. PloS one 6:e23425.

Wang X, Zhu WG (2008) [Advances in histone methyltransferases and histone demethylases]. Ai Zheng 27:1018-1025.

Wang Y, Wang X, Liu L, Wang X (2009) HDAC inhibitor trichostatin A-inhibited survival of dopaminergic neuronal cells. Neuroscience Letters 467:212-216.

Wanikiat P, Panthong A, Sujayanon P, Yoosook C, Rossi AG, Reutrakul V (2008) The anti-inflammatory effects and the inhibition of neutrophil responsiveness by Barleria lupulina and Clinacanthus nutans extracts. J Ethnopharmacol 116:234-244.

WHO (2006) Neurological disorders: public health challenges.   Geneva, Switzerland.

WHO (2012) Global health estimates (GHE) 2014: DALYs by age, sex and cause.

Wilensky RL, Shi Y, Mohler ER, 3rd, Hamamdzic D, Burgert ME, Li J, Postle A, Fenning RS, Bollinger JG, Hoffman BE, Pelchovitz DJ, Yang J, Mirabile RC, Webb CL, Zhang L, Zhang P, Gelb MH, Walker MC, Zalewski A, Macphee CH (2008) Inhibition of lipoprotein-associated phospholipase A2 reduces complex coronary atherosclerotic plaque development. Nature medicine 14:1059-1066.

Williams JH, Errington ML, Lynch MA, Bliss TV (1989) Arachidonic acid induces a long-term activity-dependent enhancement of synaptic transmission in the hippocampus. Nature 341:739-742.

Wilson AG (2008) Epigenetic regulation of gene expression in the inflammatory response and relevance to common diseases. Journal of periodontology 79:1514-1519.

Winstead MV, Balsinde J, Dennis EA (2000) Calcium-independent phospholipase A2: structure and function. Biochimica et Biophysica Acta (BBA) - Molecular and Cell Biology of Lipids 1488:28-39.

Winston F, Allis CD (1999) The bromodomain: a chromatin-targeting module? Nat Struct Biol 6:601-604.

Wirotesangthong M, Rattanakiat S (2006) Anti-herpes simplex virus type 2 activities of some Thai medicinal plants. Thai Journal of Pharm Sci 30:19-27.

Wu FR, Liu Y, Shang MB, Yang XX, Ding B, Gao JG, Wang R, Li WY (2012a) Differences in H3K4 trimethylation in in vivo and in vitro fertilization mouse preimplantation embryos. Genetics and molecular research : GMR 11:1099-1108.

Wu FR, Liu Y, Shang MB, Yang XX, Ding B, Gao JG, Wang R, Li WY (2012b) Differences in H3K4 trimethylation in in vivo and in vitro fertilization mouse preimplantation embryos. Genet Mol Res 11:1099-1108.

Wu T, Ikezono T, Angus CW, H.Shelhamer J (1999) Characterization of the promoter for the human 85 kDa cytosolic phospholipase A2 gene. Nucleic Acids Research 22:5093-5098.

Xu J, Chalimoniuk M, Shu Y, Simonyi A, Sun AY, Gonzalez FA, Weisman GA, Wood WG, Sun GY (2003) Prostaglandin E2 production in astrocytes: regulation by cytokines, extracellular ATP, and oxidative agents. Prostaglandins, Leukotrienes and Essential Fatty Acids 69:437-448.

Yamaguchi T, Cubizolles F, Zhang Y, Reichert N, Kohler H, Seiser C, Matthias P (2010) Histone deacetylases 1 and 2 act in concert to promote the G1-to-S progression. Genes & development 24:455-469.

Yamane K, Toumazou C, Tsukada Y, Erdjument-Bromage H, Tempst P, Wong J, Zhang Y (2006) JHDM2A, a JmjC-containing H3K9 demethylase, facilitates transcription activation by androgen receptor. Cell 125:483-495.

Yang C, Zhang X, Fan H, Liu Y (2009) Curcumin upregulates transcription factor Nrf2, HO-1 expression and protects rat brains against focal ischemia. Brain Res 1282:133-141.

Yang H, Siddiqi NJ, Alhomida AS, Ong WY (2013) Expression and localization of sPLA2-III in the rat CNS. Neurochem Res 38:753-760.

Yang I, Han SJ, Kaur G, Crane C, Parsa AT (2010) The role of microglia in central nervous system immunity and glioma immunology. J Clin Neurosci 17:6-10.

Yasutake T, Wada H, Higaki M, Nakamura M, Honda K, Watanabe M, Ishii H, Kamiya S, Takizawa H, Goto H (2013) Anacardic acid, a histone acetyltransferase inhibitor, modulates LPS-induced IL-8 expression in a human alveolar epithelial cell line A549. F1000Res 2:78.

Yong YK, Tan JJ, Teh SS, Mah SH, Ee GC, Chiong HS, Ahmad Z (2013) Clinacanthus nutans Extracts Are Antioxidant with Antiproliferative Effect on Cultured Human Cancer Cell Lines. Evid Based Complement Alternat Med 2013:462751.

Yoshizaki T, Schenk S, Imamura T, Babendure JL, Sonoda N, Bae EJ, Oh DY, Lu M, Milne JC, Westphal C, Bandyopadhyay G, Olefsky JM (2010) SIRT1 inhibits inflammatory pathways in macrophages and modulates insulin sensitivity. American journal of physiology Endocrinology and metabolism 298:E419-428.

Yuan H, Reddy MA, Sun G, Lanting L, Wang M, Kato M, Natarajan R (2013) Involvement of p300/CBP and epigenetic histone acetylation in TGF-beta1-mediated gene transcription in mesangial cells. Am J Physiol Renal Physiol 304:F601-613.

Zhou X, Gan P, Hao L, Tao L, Jia J, Gao B, Liu JY, Zheng LT, Zhen X (2014) Antiinflammatory effects of orientin-2"-O-galactopyranoside on lipopolysaccharide-stimulated microglia. Biol Pharm Bull 37:1282-1294.

Zhou X, Maricque B, Xie M, Li D, Sundaram V, Martin EA, Koebbe BC, Nielsen C, Hirst M, Farnham P, Kuhn RM, Zhu J, Smirnov I, Kent WJ, Haussler D, Madden PAF, Costello JF, Wang T (2011) The Human Epigenome Browser at Washington University. Nat Meth 8:989-990.

Zhu W, Ou Y, Li Y, Xiao R, Shu M, Zhou Y, Xie J, He S, Qiu P, Yan G (2009) A small-molecule triptolide suppresses angiogenesis and invasion of human anaplastic thyroid carcinoma cells via down-regulation of the nuclear factor-kappa B pathway. Mol Pharmacol 75:812-819.

Zilberman Y, Ballestrem C, Carramusa L, Mazitschek R, Khochbin S, Bershadsky A (2009) Regulation of microtubule dynamics by inhibition of the tubulin deacetylase HDAC6. Journal of cell science 122:3531-3541.